



TECHNISCHE
UNIVERSITÄT
WIEN

Vienna University of Technology

DIPLOMARBEIT

**The impact of external metal mesh screen shading devices on the
thermal and energy performance of buildings: a case study for
different European climate zones**

unter der Leitung von

Univ.-Prof. Ardeshir Mahdavi

E 259-3 Abteilung für Bauphysik und Bauökologie

Institut für Architekturwissenschaften

eingereicht an der

Technischen Universität Wien

Fakultät für Architektur und Raumplanung

von

Georgios Gourlis

1225611

Wimmergasse 22/3, 1050 Wien

Wien, Jänner 2016

.....
Georgios Gourlis

ACKNOWLEDGEMENT

First I would like to express my gratitude to my supervisor Univ. Prof. Dr. Ardeshir Mahdavi for the knowledge I acquired from his numerous lectures, enabling me as an architect to explore new scientific fields. Furthermore, I convey my thanks to Univ. Ass. M.Sc. Farhang Tahmasebi for introducing me to the world of building simulation, as well as for the constructive discussions and suggestions on this work.

I would also like to thank my parents for their support throughout the years and those friends who stood by me, when I needed a helping hand.

Last but not least, my warmest gratitude and love goes to Sofia, for being who she is.

ABSTRACT

Early design decisions with regard to building facade characteristics play a significant role in the resulting building's thermal performance. In this context, external metal mesh screens - used as a permanent second facade skin - represent a rather new shading alternative, particularly in non-residential buildings. It has been suggested that products of this kind can filter excessive incident solar radiation while maintaining the transparent quality of façade. Given the multifaceted implications of this shading device for building energy performance, a detailed simulation-based study was undertaken to evaluate the impact of metal mesh screens on annual energy demand for heating, cooling, and electric lighting in different European climate zones. To examine this shading technology in a comprehensive manner, possible design variations were considered in terms of mesh screen translucency, window to wall ratio, and facade orientation. In addition, the thesis explored the feasibility of using such a shading strategy, along with suitable ventilation scenarios, to provide passive cooling during summer. Toward this end, a number of existing approaches to simulate metal shade screens were examined, identifying their capabilities and limitations. Subsequently, a typical office space was modelled in three European locations, taking local building construction standards into account. The results of this study can help planners in their choice of the appropriate shading strategy and provide recommendations for the application of metal mesh screens according to the climatic and architectural criteria.

Keywords

Solar shading; Building performance simulation; Modeling approach; Energy demand; Adaptive thermal comfort

ZUSAMMENFASSUNG

Frühe Designentscheidungen im Hinblick auf die Eigenschaften der Gebäudefassade spielen eine bedeutende Rolle bei der thermischen Leistung der resultierenden Gebäude. In diesem Zusammenhang stellen externe Metallgewebe, verwendet als dauerhafte zweite Fassadenhaut, eine relativ neue Verschattungsalternative, vor allem in Nicht-Wohngebäuden. Es ist vorgeschlagen worden, dass Produkte dieser Art können übermäßige Sonneneinstrahlung filtern, ohne die transparente Qualität der Fassade und den Blick nach außen zu Frage zu stellen. Angesichts der vielfältigen Auswirkungen von diesem Sonnenschutzelement auf die Gebäudeenergieeffizienz, wurde eine detaillierte, simulationsbasierte Studie durchgeführt, um die Auswirkungen der Metallgewebe auf dem jährlichen Energiebedarf für Heizung, Kühlung und elektrische Beleuchtung in verschiedenen europäischen Klimazonen zu bewerten. Um diese Verschattungstechnologie in einer umfassenden Weise zu untersuchen, wurden mögliche Gestaltungsvarianten in Bezug auf Gewebe-Transluzenz, Fenster- zu Wandfläche -Verhältnis und Fassadenorientierung berücksichtigt. Darüber hinaus untersucht diese Arbeit die Machbarkeit der Verwendung eines solchen Verschattungskonzeptes, zusammen mit geeigneten Lüftungsszenarien, um die passive Kühlung im Sommer zu gewährleisten.

Zu diesem Zweck wurde eine Reihe von vorhandenen Ansätzen zur Simulation von Metallgewebe untersucht. Dadurch wurden deren Fähigkeiten und Einschränkungen identifiziert. Anschließend wurde ein typischer Büroraum in drei europäischen Standorten modelliert, mit Berücksichtigung der lokalen Hochbau-Standards. Diese Studie könnte Planer bei der Auswahl des geeigneten Verschattungskonzeptes helfen und Empfehlungen für die Anwendung von Metallgewebe mit Hinsicht auf die klimatischen und architektonischen Kriterien zusammenstellen.

CONTENTS

ACKNOWLEDGEMENT	I
ABSTRACT	II
ZUSAMMENFASSUNG	III
CONTENTS	IV
1 INTRODUCTION	1
1.1 Overview.....	1
1.2 Motivation.....	2
1.3 Objective	3
1.4 Background.....	3
1.4.1 Literature review	3
1.4.2 Types and application of metal mesh screens	4
2 METHOD	8
2.1 Overview.....	8
2.2 Hypothesis.....	10
2.2.1 Research questions.....	10
2.3 Software tools	10
2.4 Statistical Analysis	11
2.4.1 Climate data	11
2.4.2 Shade material properties.....	12
2.4.3 Characteristics of the thermal simulation model.....	12
2.5 Analysis of mesh screen modelling - calculation method	14
2.5.1 Methods overview.....	15
2.5.2 Uncertainty analysis	17
2.5.3 Comprehensive test and statistical comparison	21
2.5.4 Remarks, barriers and selection of method.....	23
2.6 Results evaluation criteria.....	25
2.6.1 Adaptive comfort model of EN 15251.....	25

2.6.2	Summer overheating.....	27
3	RESULTS.....	28
3.1	Overview	28
3.2	Predicted annual energy demand.....	28
3.2.1	Location: Athens, Greece	28
3.2.2	Location: Vienna, Austria	30
3.2.3	Location: London, United Kingdom.....	32
3.3	Feasibility study on summer thermal performance.....	34
3.3.1	Summer overheating and thermal comfort.....	35
3.3.2	Thermal comfort for selected night ventilation scenarios.....	38
4	DISCUSSION.....	42
4.1	Overview	42
4.2	Energy performance	42
4.2.1	Location - Climate	42
4.2.2	Facade orientation	43
4.2.3	Window to wall ratio (WWR).....	44
4.2.4	Type of metal mesh screen	46
4.3	Summer thermal comfort	48
5	CONCLUSION.....	51
6	INDEX	53
6.1	List of Abbreviations	53
6.2	List of Figures	54
6.3	List of Tables.....	57
6.4	List of Formulas.....	57
7	LITERATURE.....	58
	APPENDIX.....	63
A.	Metal mesh screen technical characteristics.....	63
B.	Climate data	64

C. EnergyPlus simulation parameters.....	68
D. Uncertainty analysis of modelling methods.....	70
E. Energy performance results for WINscr and EPscr methods	75

1 INTRODUCTION

1.1 Overview

The building sector is a large consumer of energy, ranging from 32% of final energy demand on global scale to 40% and 41% in the E.U. and the U.S. respectively (Ürge-Vorsatz et al. 2015, European Commission 2015, U.S. Energy Information Administration 2015). Heating and cooling are dominant contributors to the consumed energy in both residential and non-residential buildings; with heating rating first in households and cooling being one of the largest together with lighting in commercial buildings. Studies assessing the impact of climate change on building energy demand in Europe state that in the next 20 years, electricity requirement for cooling will rapidly increase by even more than 100%, while in the long term heating loads could be decreasing up to 20%, especially in Northern Europe (Aebischer et al. 2007, Eskeland and Mideksa 2010). In this sense, achieving reduction in building energy consumption is nowadays an a priori set target for planners and engineers working in the architecture, engineering and construction (AEC) industry.

Architectural decisions considering facade character and form, often made during the initial design stage, play a significant role in the final building's performance as well as thermal and visual comfort of future users. Facade design should enhance internal comfort and contribute to an energy efficient building, thus various designs and materials are being used as facade elements, trying to achieve these goals. Regarding solar shading, one of the functions that a facade should serve, a relative new method is increasingly used among architects all over the world in varying locations and climates, incorporating the use of external metal mesh screen large-scale tensioned elements as a partial or total facade second skin. Such screens usually have a permanent character as static facade elements and are mainly applied on non-residential buildings such as offices and commercial buildings. Here, it should be noted that external static shading devices affect solar heat gains throughout the year. They normally result in a reduction of cooling loads during summer months but may also increase the heating demand during the winter.

The aim of this work is to investigate the impact of external metal mesh screens used for shading, on thermal performance and energy demand of office spaces in different climate zones in Europe. It also intends to answer the question whether the application of such devices is beneficial or not in terms of net energy consumption depending on different climate conditions. In order to do so the study focuses on a hypothetical office space and by defining various parameters such as climate, geometry and materiality performs a parametric simulation research with the EnergyPlus software. This choice is made due to the

need for studying different scenarios and various geographical locations and also because through computer modelling there can be a simplification of the large variety of shading meshes. At first, a detailed research and uncertainty analysis is performed for defining the modelling method. Difficulties met when approaching the problem led to an analysis of tools capabilities and limitations. Further on the parametric study is conducted producing information about energy demand for heating, cooling and lighting. The best performing mesh screen is then identified and a feasibility analysis is conducted concerning summer overheating and thermal comfort under free running mode, without active cooling and studying different night ventilation scenarios. Based on the outcome, the possibility of providing planners with guidelines for using mesh screen shading devices is also discussed.

1.2 Motivation

Glazed areas and shading devices have an impact on building thermal performance and energy demand for heating, cooling and lighting. Highly glazed facades are increasingly used in commercial, office and other public buildings, providing daylight to the interior and view out. Normally a solar control strategy is also considered in order to prevent visual discomfort and raised cooling demands due to overheating. Studies of the shading impact on annual energy use have demonstrated that shading devices reduce the cooling demand in buildings while increasing the heating loads due to loss of beneficial solar gains (Dubois 1997). Net energy savings only occur if the reduction in cooling energy use exceeds the increase in heating energy use (Treado et al. 1984). Furthermore exterior shading devices and adsorbing glass are net energy losers in heating-dominated climates and interior devices perform better because they shade the entire window while providing additional insulation to the windowpanes (Hunn et al. 1993).

Numerous shading systems, varying in type and function are being applied on buildings facades according to orientation, performance and last but not least design criteria. As already stated, the use of metal mesh screens as solar radiation filters is increasing. However there has been no extended research on their impact on building performance. Designers argue that perforated and woven metal screens are an effective means of optimizing views while limiting radiant energy gain (Ballard Bell and Rand 2006). Manufactures claim that their products can be utilized to break and filter sunrays, performing as an effective sun protection screen. A comfortable internal climate is created with the mesh appearing almost transparent whilst at the same time offering a degree of privacy (Haver and Boecker 2014). The above statements however derive from professional experience and are mostly case oriented. Given the considerable number of projects, in

different locations globally, where such building skins are used for solar protection, a structured research on the application of metal mesh screen shading would produce information about the effects on building performance and would improve their usage.

1.3 Objective

The goal of this study is to quantify the influence of such devices on buildings energy demand and provide architects and engineers information about their performance as external facade shading elements. Knowing the potential effect on final building performance, architects during the design stage could judge whether metal mesh screens or another shading strategy should be used, considering also the climate conditions of a project. An approach that satisfies both the aesthetic characteristics and the functional role of the facade in a building's concept would be the desirable solution.

1.4 Background

1.4.1 Literature review

Extended research has been realized over the last decades on the area of building shading systems. Baruch Givoni (1998) performed studies on the thermal effect and efficiency of various shading devices. Furthermore rigorous research investigations have been carried out concerning the energy performance of external shading strategies such as overhangs (Lee and Tavit 2007), venetian blinds (Lee et al. 1998; Simmler and Binder 2008), external roller shades (Tzempelikos and Athienitis 2007), louvers (Palmero-Marrero and Oliveira 2010) and external wooden perforated window solar screens (Sherif et al. 2012). However, only few studies about metal mesh screens have been published, focusing mostly on the daylight performance of perforated metal sheets (Tsangrassoulis et al. 1996).

In terms of climate conditions, most of the aforementioned research papers study the performance of a shading device in a particular climate zone ranging from cold climates, Montreal, Quebec (Tzempelikos and Athienitis 2007), to extreme desert conditions (Sherif et al. 2012). Marked as an exception, the research by Palermo-Marrero and Oliveira (2010) concentrated on the impact of louver shading devices on indoor thermal conditions and energy demand, regarding different climates such as Mexico, Cairo, Lisbon, Madrid and London. Another study also addresses the importance of climate parameters, considering the effects of overhangs and louvers on energy requirements of office buildings in three different Italian climates - Palermo, Rome and Milan (Bellia et al. 2013). Targeting at northern parts of Europe, a simulation on solar control shading of offices in the UK, showed that benefits of shading are latitude dependent. External shading, which results in energy

savings for offices in southern England, can prove to have an energy penalty in Scotland (Littlefair et al. 2010).

Literature review showed that although a significant amount of research have been purchased on the field of external solar shading, there are not concentrated studies about metal mesh screens. The reason may be that solar shading with such devices and especially with woven steel meshes is a new approach applied on building facades. However, there is a considerable number of cases, in different locations globally, where external metal mesh screens are used for solar protection. For this reason the thesis is planning to examine their effect on buildings performance.

Considering the many variations of metal mesh screens that are available, the study is focusing on the impact of static external stainless steel mesh screens which as a single category has a wide range of types as well. At this point, it can be argued that metal mesh screens perform in terms of shading similar to perforated metal panels. Perforated sheets, usually made from aluminum or steel, are manufactured with perforations of different shapes and percentages and are able to have a closely controlled percentage of perforation by varying both the size of the holes and their proximity. However, although perforated metal panels have a significant role nowadays as solar shading devices, they are usually applied on kinetic facade systems and their impact can be controlled by automation systems. Such solar shading design strategies are not addressed in this work, as this could be another field for further investigation.

1.4.2 Types and application of metal mesh screens

Stainless steel mesh screens have been introduced into mainstream building construction only in the last 10 to 15 years. They are durable and weather resistant, making them easy for outdoor use and provide a textile-like surface across a wall, acting as a second skin that conceals a variety of facade elements behind it. The first architectural project though to implement metal meshes in various ways inside and outside the building was the French National Library designed by Dominique Perrault, completed in 1995 (Brownell 2006).

In this project mesh screens were used for shading the extensive glass facades of the staircases at the narrow edges of the buildings (Figure 1). In the next decade the use of metal meshes found favor in car park design, through which facades of open deck buildings are given architectural homogeneity. Mesh screens have been used also at non-residential buildings usually in front of glazed facades. Their varying levels of translucency can be exploited both in daylight by providing depth to a facade that gives some privacy to building

users, and from a night time glow across its surface generated by electrical light within the building (Watts 2011).

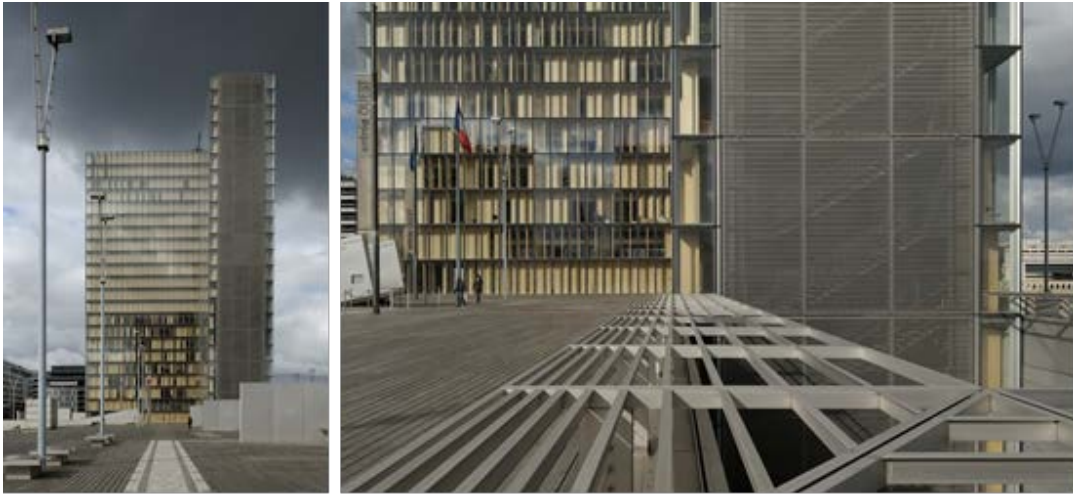


Figure 1. National Library of France, Dominique Perrault (1989-1995)

©Yuri Palmin source: <http://www.archdaily.com/103592/ad-classics-national-library-of-france-dominique-perrault-2>

Meshes are of three essential types: rigid mesh made from rod, mesh flexible in one direction made as woven wire with rods in one direction and wire in the opposite direction, and mesh that is flexible in two directions which is made from woven wire only (Watts 2011). The second type is the one usually used on facades (Figure 2). It is made in long lengths and can be tensioned at both edges to provide a large continuous semi-transparent flat surface, running from top to bottom of floors or of the entire facade without joints. By increasing the thickness and frequency of wires and by different weave patterns the level of transparency can vary, making the mesh very dense or very “open”.

Figures 3 to 6 show examples of metal mesh screen application on various building types and climatic locations in Europe. Figure 3 shows an office building in Austria with 57% open area mesh screen on a glass facade. Figure 4 shows an application of a 52% open area mesh on a wall with windows at a hospital in Spain. An educational building in England with mesh screens of 52% open area is shown in Figure 5. Figure 6 shows an office building with 68% open area screen in northwest France near the Atlantic coast.

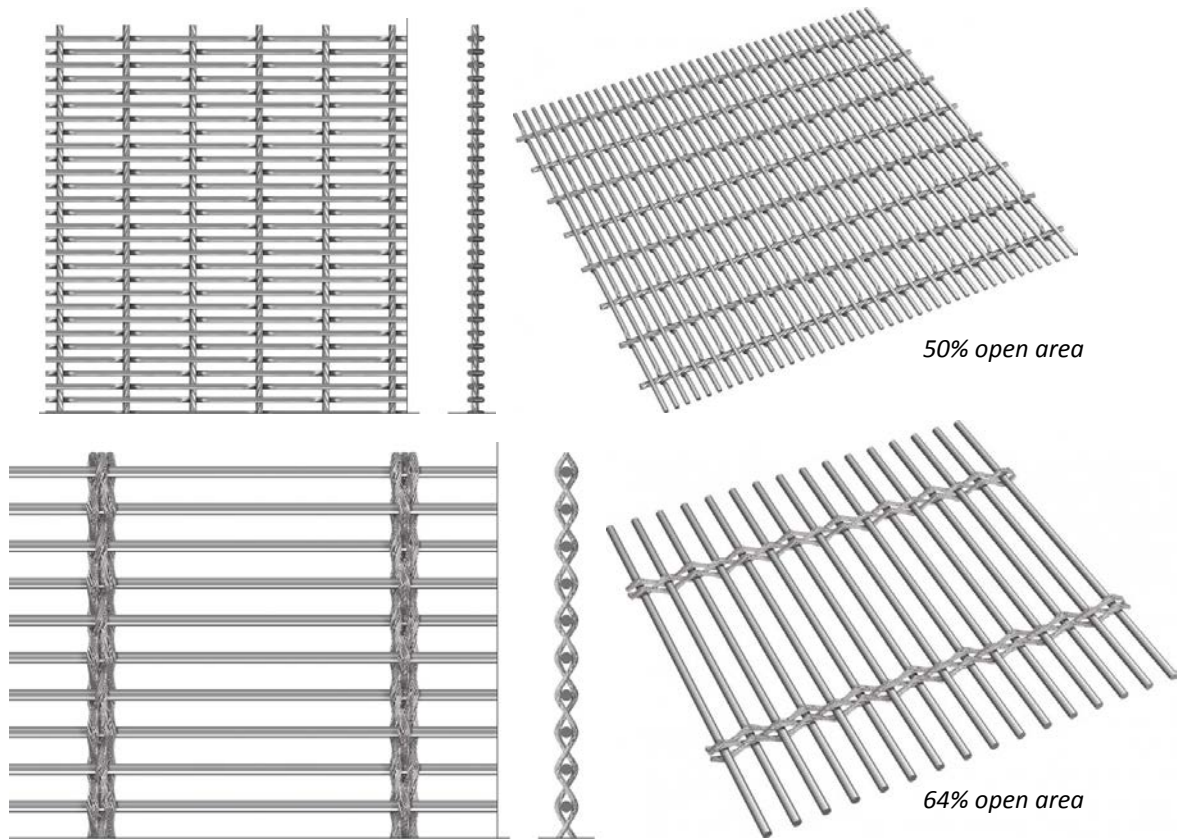


Figure 2. Stainless steel shading mesh screen made of woven wire and rods, Scale 1:2
©GKD METALFABRICS source: <http://www.gkdmetalfabrics.com/metalfabrics.html?>



Figure 3. Alpenland office building, St. Pölten – Austria
source: http://www.metallvorhang.de/index.php?article_id=32



Figure 4. Hospital, Seville – Spain

source: <http://www.weavingarchitecture.com/en/project-gallery/reference-detailseite/show/Reference/222/?cHash=abd096f60dea7a243fc538547f1b789a>



Figure 5. Aedas Holland Park School, London – U.K.

source: <http://www.weavingarchitecture.com/en/project-gallery/reference-detailseite/show/Reference/256/?cHash=364c8d77d03667a68246d714787699ad>



Figure 6. Office building, Brest – Northwest France

source: <http://www.weavingarchitecture.com/en/project-gallery/reference-detailseite/show/Reference/362/?cHash=b11b08c3862f7cf3c0393519ab16d9a9>

2 METHOD

2.1 Overview

The study employs building thermal simulations on a base model of a typical office space in EnergyPlus v8.1, an accurate whole building simulation software developed by the U.S. Department of Energy. Parametric analysis for different case scenarios is performed in order to examine the impact of four key-design parameters on the energy and thermal performance of the typical office space. For all cases initial models are simulated, when no shading is applied, so that the metal mesh screen shading impact can be compared and evaluated.

The first parameter to be addressed is that of climate conditions. Taking into account that sunshine hours and air temperatures vary from the southern parts of Europe to the central and northern regions, three locations in different climates zones are selected, Athens (Greece), Vienna (Austria) and London (UK). Athens has a Hot-Summer Mediterranean Climate (Csa – Köppen-Geiger climate classification) with 2.778 mean yearly sunshine hours. Vienna has a Humid Continental Climate (Dfb) with warm summers and 1.804 mean yearly sunshine hours. London lies in the Temperate Oceanic Climate zone (Cfb) with 1.480 mean yearly sunshine hours and warm summers (Peel et al. 20007). The aforementioned typical office space is modeled according to building codes and regulations of its location, taking into account common practice utilized in new office building constructions, regarding materials and insulation levels.

The second parameter considers the orientation of the facade. Solar shading strategies on the North Hemisphere are applied preliminary on south exposures as well as east and west orientations. Metal mesh screens, when applied as a static external second skin on the facade, function in the same way for all orientations unlike other shading devices that should be designed according to the orientation of a building. There is however the choice of using mesh screens with different density, thus different light transmittance on each side, but that would be the third parameter, as it is discussed below. The model of the office space is calculated in all three orientations of solar incidence on a facade.

The third parameter taken into account is that of the window to wall ratio (WWR). As quality daylight working spaces are requested in new offices buildings, the WWR is crucial in order to reach the desired level of 500 lx illuminance on the workplane (Zumtobel 2013). Therefore the case scenarios are examined under three variations of WWR. These are a typical 30% WWR, a higher ratio of glazing at 60% WWR and a glass facade of 90% WWR.

The fourth and last parameter is that of the actual shading device, the stainless steel mesh screen. Depending on the weave, the open area of a mesh varies from 5% to 75%. Meshes, that are used as shading devices, usually have an open area from 35% to 65% and a visible light transmittance varying from 0.15 to 0.65 according to manufacturer's characteristics (GKD Metafabrics 2015). Three degrees of mesh density are tested in this work in order to simplify the variety of materials available on the market (GKD Creativeweave 2015). These are mesh screens of 35%, 50% and 64% open area respectively. The distance from the glazing surface is defined after reviewing practices that are used for mounting such meshes and an analysis of the modelling method for the simulations. However, a general rule implies that the mesh is placed at a significant greater distance from the building facade when compared to other shading system devices, ranging from 20 cm to more than 100 cm. Modelling approach and analysis of the capabilities and limitations of the tools selected are presented in the following sub-chapters.

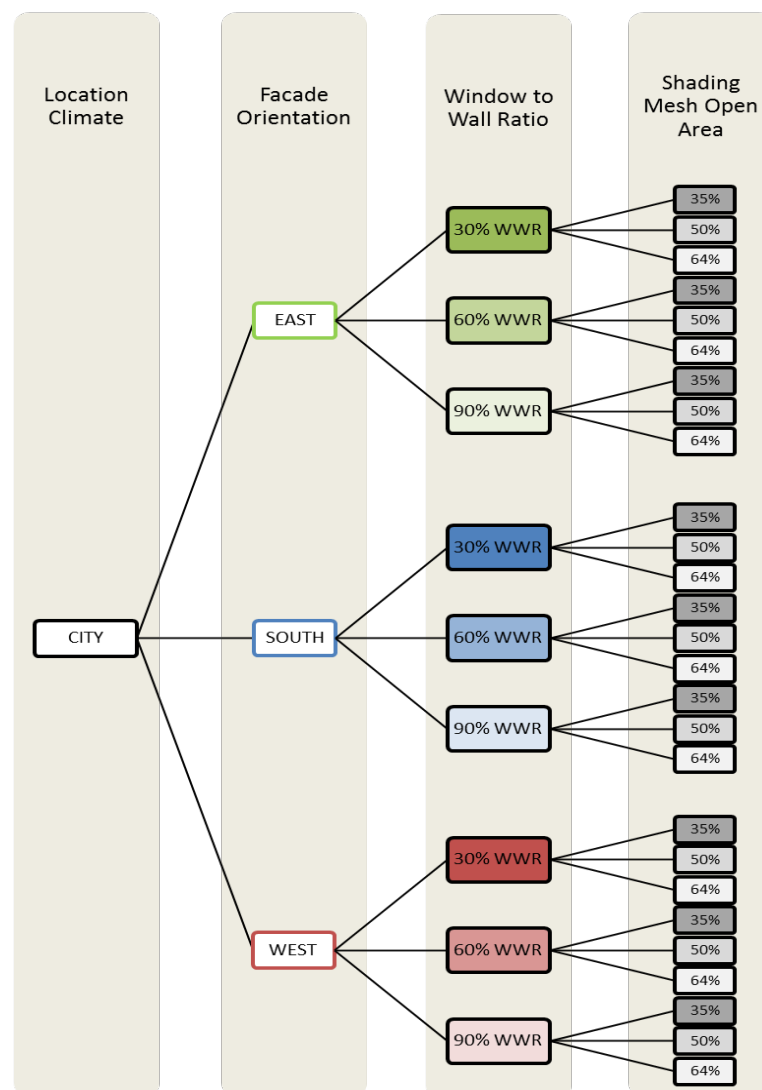


Figure 7. Overview of investigated key-design parameters

2.2 Hypothesis

This research is based on the suggestion that building shading strategies with static metal mesh screen shading devices may have a positive or negative impact on building performance according to location climate conditions.

2.2.1 Research questions

1. *Which is the most appropriate modelling method to address thermal simulation of metal mesh screen shading devices?*
 - As no prior case studies are published on the subject, this study will research the capabilities of available tools and propose an approach.
2. *Does the application of static mesh screens increase annual heating demand to such extent that cannot be covered by the savings achieved in cooling demand?*
 - Energy demand for heating and cooling will be juxtaposed and judged in reference to the total energy demand.
3. *Is there a type of mesh screen open area that is more appropriate for building shading?*
 - The likelihood of a best performing mesh screen will be assessed by reviewing the annual energy demand of all case models.
4. *Can office buildings without cooling systems achieve thermal comfort during summer with the application of metal mesh screen shading devices and natural ventilation strategies?*
 - The best performing screen will be analyzed in terms of summer overheating and thermal comfort for the case of an unconditioned unit with night natural ventilation cooling according to the adaptive comfort model of EN 15251.

2.3 Software tools

Metal mesh screens are virtually modelled and simulated in the manufacturing industry with specialized tools as GeoDict (GeoDict Software 2015). Such tools perform CFD simulations to define flow characteristics, filtration behavior, material porosity and other required properties for the development and production of meshes. Yet no literature is available on combining these material simulation tools with building performance simulation software.

The EnergyPlus v8.1 software, utilized in this work, has a detailed thermal model for shading devices with the important feature of calculating the natural convection airflow between the shading device and the glazing surface, based on the ISO 15099:2001 standard. Furthermore it considers absorbance and transmittance of the shading device for long-wave

radiation (IR) as well as direct and diffuse solar radiation. Inter-reflections between the shading layer and the glass are also calculated (DOE 2013b). However EnergyPlus as well as other building simulation tools are not capable of modelling the complex geometry of facade mesh screen shading devices that are usually constructed of woven wire and rods. For this reason three approximative modelling methods are investigated based on available tools and input options for complex shading systems. A thorough analysis is presented in section 2.5.

For modelling the fenestration systems of the case study models, WINDOW 7.3 software is used, a tool developed and annually upgraded by the Lawrence Berkeley National Laboratory (LBNL 2014). This software calculates U-value, solar heat gain coefficient, shading coefficient, and visible transmittance for the complete window system, as well as for the glazing and frame separately and has a direct link with EnergyPlus. It embodies the International Glazing Database which contains detailed optical data for several thousand international glass products (Lyons et al. 2010). A full layer-by-layer description of the optical and thermo-physical properties of glazing layers and gas fills of the modelled window can be imported into EnergyPlus either by using the full or average spectral calculation method or the bi-directional scattering distribution function method (BSDF). It also has the ability to model complex fenestration systems with multiple shading types.

2.4 Statistical Analysis

Information required for the parametric analysis concerns meteorological data for the different locations, technical characteristics of mesh screen shadings as well as building envelope properties and operating schedules for the thermal simulation models. Data are collected from online databases, manufactures technical documentations and by reviewing building regulations and standards as well as reference projects.

2.4.1 Climate data

Weather files for different European climate zone locations are acquired from the weather data database of the U.S. Department of Energy (2015). These are Typical Meteorological Year 2 (TMY2) data sets providing hourly values of solar radiation based on improved solar models as well as meteorological elements for a one year period. They consist of months selected from individual years and concatenated to form a complete year. Therefore they closely match the long-term average climatic conditions rather than being good indicators of conditions over the next year or five year period. On the contrary, they represent conditions judged to be typical over a long period of time, such as 30 years, and are more appropriate

for building energy simulation as they will result in predicted energy consumption that is closer to the long-term average (Crawley 1998).

2.4.2 Shade material properties

Technical data of the stainless steel mesh screen shading devices are collected from the manufactures product catalogues (GKD Creativeweave 2015). The material used is austenitic stainless steel AISI Type 316 and its properties are shown in Table 1. It has to be mentioned that these values refer to the screen material itself and not to the overall shading assembly.

Table 1. Properties of mesh screen shading material

	conductivity λ [W·m ⁻¹ ·K ⁻¹]	solar reflectance	visible reflectance	emissivity ϵ
SS AISI Type 316	16.3	0.55	0.25	0.28

2.4.3 Characteristics of the thermal simulation model

A hypothetical typical office space in the perimeter zone of a multistory building is used as the base model for the simulations. The unit is 6 m wide, 4 m deep and 3 m tall. It consists of three opaque inner walls and an exterior wall with glazing along the 6m dimension. Adiabatic heat transfer (no heat loss) is assumed for the three inner walls, floor and ceiling. This set-up facilitates a fair comparison of predicted energy demand and thermal performance due to different window and shading configurations.

Different key-design parameter constellations are prepared in OpenStudio SketchUp plug-in v1.5.3 and then imported in EnergyPlus v8.1 to obtain hourly values of energy demand, solar and daylight performance of the shading systems and space operative temperatures. The hourly data are then used to calculate daily, monthly and annual results, as required by each analysis stage.

Building envelope thermal properties

Building regulations for each geographical location are studied in order to determine the thermal properties of the exterior wall and window of the models. For Athens KENAK 2010 – Zone B is used, for Vienna OIB-Richtlinie 6 2011 and for London Building Regulation 2013 Part L2a. The exterior wall for all cases is a brick masonry wall with exterior thermal insulation and a rear ventilated exterior clinker facade. Thickness of the insulation and type of bricks are selected according to the common practices for new commercial building constructions in the three countries. Main difference is that in Athens 5 cm XPS insulation is used as in Vienna and London 20 cm glasswool, resulting in different U-values (Table 2). Wall constructions and material semantic properties are available in the appendix.

Table 2. U-values of external building envelope

	Exterior wall		Exterior window	
	regulation U-value [W·m ⁻² ·K ⁻¹]	model U-value [W·m ⁻² ·K ⁻¹]	regulation Uw [W·m ⁻² ·K ⁻¹]	model Uw [W·m ⁻² ·K ⁻¹]
ATH - GR	0.5	0.42	exterior window: 3.0	2.744
VIE - AT	0.35	0.144	non-residential: 1.7	1.193
LON - UK	0.26	0.144	non-residential: 1.6	1.193

The same principle of common practice also applies for the selection of windows. In Athens a window with clear double glazing and simple aluminum frame is used. In Vienna and London a double low-e thermal insulating glazing with composite wood-aluminum frame is selected. Window, glazing and frame U-values are calculated based on EN 673 standard and ISO 10077-1:2006 and shown in Tables 2 and 3.

Table 3. Window construction properties

Window construction*	Material layers**	Thickness [mm]	Window g value	Window T vis	Ug [W·m ⁻² ·K ⁻¹]	Uf [W·m ⁻² ·K ⁻¹]
ATH - GR	-clear glass	4.8	0.65	0.67	2.630	2.8
	-10% air / 90% argon	14				
	-clear glass	4.8				
VIE - AT	-clear glass	3.8	0.46	0.62	1.212	1.3
	-10% air / 90% argon	16				
LON - UK	-low-e glass	3.8				

*Calculation according to ISO 10077 / EN 673 for a 1230x1480 mm window, Class 2 edge correlation for air permeability

**Listed from exterior to interior surface

Operating schedules and internal loads

The following parameters are defined and kept constant for all simulation models:

- People
- Electrical equipment
- Electrical lights and daylighting control

It is supposed that two employees are working in the 24 m² office space. Internal loads from people are set at 115 W per person, for office light work according to Table 6.3 of ASHRAE Handbook Fundamentals 2001. Internal gains from electric equipment are calculated proportionally at 12.5 W·m⁻² from Table 11 of ASHRAE Handbook Fundamentals 2009. Typical occupancy schedule and equipment usage level for weekdays is shown in Figure 8. During weekends no occupants are present and no electric equipment is in use.

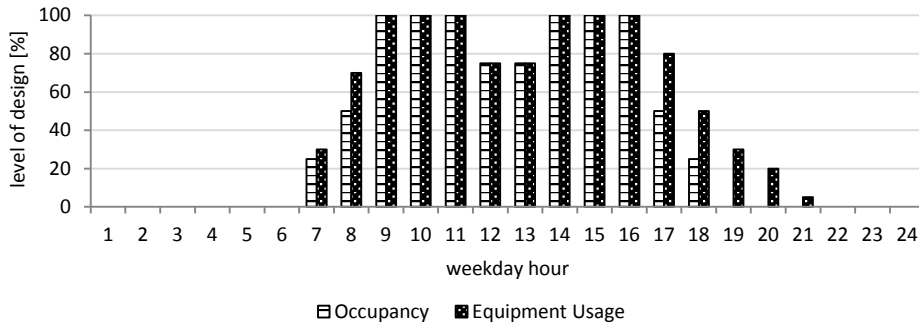


Figure 8. Office occupancy and equipment usage level

Internal gains from electrical lighting are set to $12 \text{ W}\cdot\text{m}^{-2}$ according to ASHRAE 90.1.2010 Standard. Lighting availability schedule is shown in Figure 9. There is also a daylighting control strategy with a continuous dimming system. When illuminance at the center of the office at the reference plane of 0.8 m above the floor exceeds 500 lux, lights are turned off. During weekends lighting availability is set at 5%.

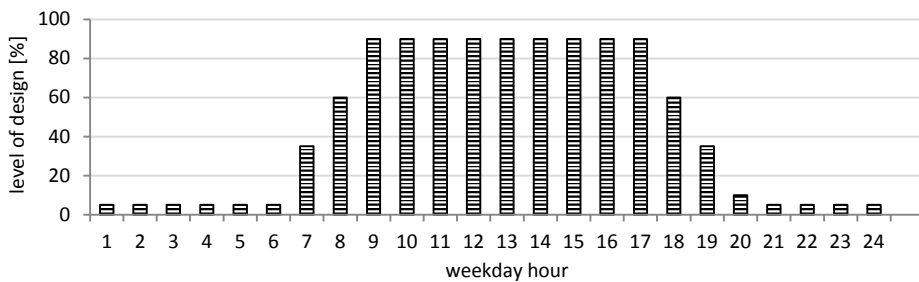


Figure 9. Lighting availability schedule

HVAC system

The office is served by mechanical ventilation with a design flow rate of $0.0085 \text{ m}^3\cdot\text{s}^{-1}$ per person (ASHRAE Standard 62-2001) on working days when occupants are present. Infiltration is set at a constant level of 0.2 ACH.

Heating and cooling are provided by an ideal loads air system with unlimited power capacity in order to calculate energy demand that ensures comfortable thermal conditions. The thermostat settings are 20°C for heating and 26°C for cooling during office working hours from 07:00 to 19:00, with a night and weekend setback temperature of 18°C for heating and 32°C for cooling.

2.5 Analysis of mesh screen modelling - calculation method

As there is no literature available at the moment about modelling and simulating mesh screens in building performance simulation tools, a study has been contacted for selecting the most appropriate input modelling and calculation approach.

2.5.1 Methods overview

EnergyPlus WindowMaterial:Screen – EPscr

The first modelling method focuses on the internal capabilities of EnergyPlus and utilizes the WindowMaterial:Screen modelling object. This object is commonly used to model insect screens but can also be used as a shading device for large glazing areas. It creates an exterior screen and assumes that the screen is made up of intersecting orthogonally-crossed cylinders with the same diameter (D) (Figure 10). The surface of the cylinders is assumed to be diffusely reflecting, having the optical properties of a Lambertian surface (DOE 2013a). The solar and visible transmission and reflection properties of the screen vary with the angle of incidence of solar radiation. The spacing (S) of the cylinders is supposed to be equal in both directions, vertical and horizontal, which is though not the case in most stainless steel mesh screens. Nonetheless, the appropriate spacing (S) and cylinder diameter (D) for the EPscr method can be calculated so that the open area of the screen matches that of the original geometry. Also material properties of the shade can be defined and its distance from the glazing can be set up to 1 meter.

This modeling method can be only combined with spectral optical data type calculation in EnergyPlus. In this work the Spectral Average approach is used, as it the default approach for glazing materials in EnergyPlus. It requires inputs of transmittance, front and back reflectance of solar spectrum and visible light, infrared transmittance, front and back emissivity and conductivity of each layer of the glazing. The determination for solar transmittance and reflectance are averaged over the solar spectrum, and the values for visible transmittance and reflectance are weighted average over the solar spectrum according to the response of the human eye (Lam et al. 2014).

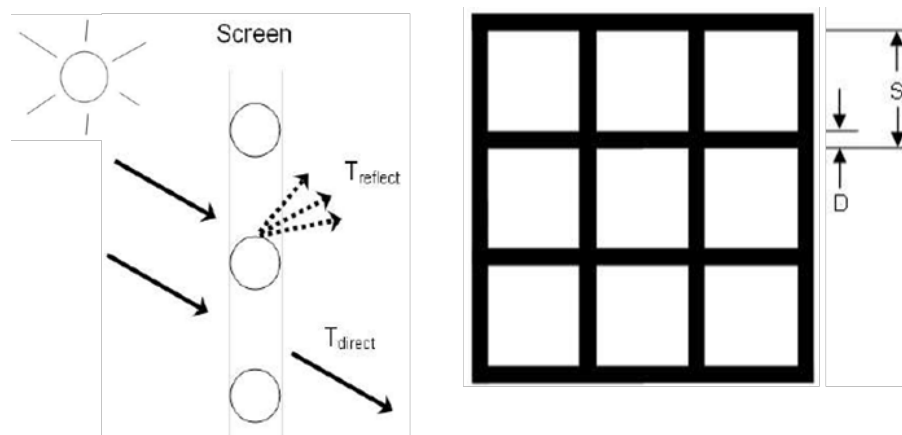


Figure 10. Geometry of WindowMaterial:Screen object
©EnergyPlus Input-Output Reference

WINDOW 7.3 Screen – WINscr

The second modelling method utilizes a recent capability of WINDOW software for defining perforated screen shading systems, first embedded in the 7.0 version in 2012. To better approximate the geometry of a mesh screen, a rectangular perforation is defined with the exact horizontal and vertical spacing characteristics of the original screen (Figure 11). In contrary to the EPscr method, width of vertical and horizontal opaque surfaces can vary and overall thickness of the shade can be defined independently. As in the EPscr, material properties of stainless steel can be applied to the screen and it is addressed as a Lambertian diffusely reflecting surface. The screen is then added to the exterior layer position of the modeled glazing system at the desired distance, thus creating a complex fenestration system (CFS).

WINDOW 7.3 can only export BSDF dataset for CFS, which are subsequently read and calculated by the BSDF optical data type in EnergyPlus. WINDOW incorporates the Klems radiosity-based method to generate BSDF data of multi-layered fenestration systems from the angularly resolved data of single layers (Klems 1994, Bueno et al. 2015). BSDF, which consists of Bi-directional Reflectance Distribution Function (BRDF) and Bi-directional Transmittance Distribution Function (BTDF), describes how light coming from a certain direction is transmitted and reflected in other directions. These directions are obtained by discretizing a hemisphere into 145 patches in the Klems basis (Mitchell et al. 2013). The process results in a matrix of 145 incoming by 145 outgoing directions, which fully optically characterizes the CFS.

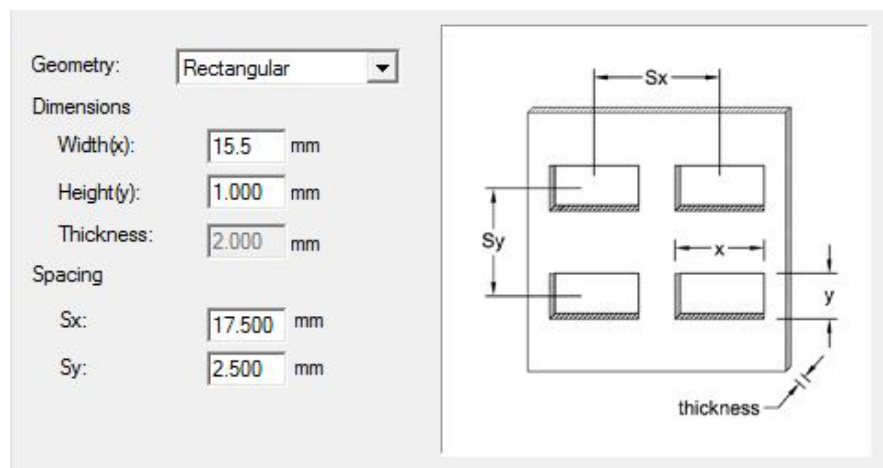


Figure 11. WINDOW 7.3 perforated screen input characteristics

Hand-drawn Screen – HANDscr

The third is a low-tech approach of drawing the screen geometry by hand. Here simplifications are also made, due to restrictions on geometry types and surfaces that thermal simulation tools like EnergyPlus accept. Curved surfaces, as cylinders, are not valid input. Due to the scale of the wires and rods, whose diameter ranges from 1.5 mm to 6 mm, scattering a cylinder in multiple flat surfaces is not possible so the hand-drawn mesh screen finally consists of only flat horizontal and vertical surfaces (Figure 12). Expect of diffuse solar and visible reflectance properties of the shading surfaces, no other material property can be given to the modelled screen.

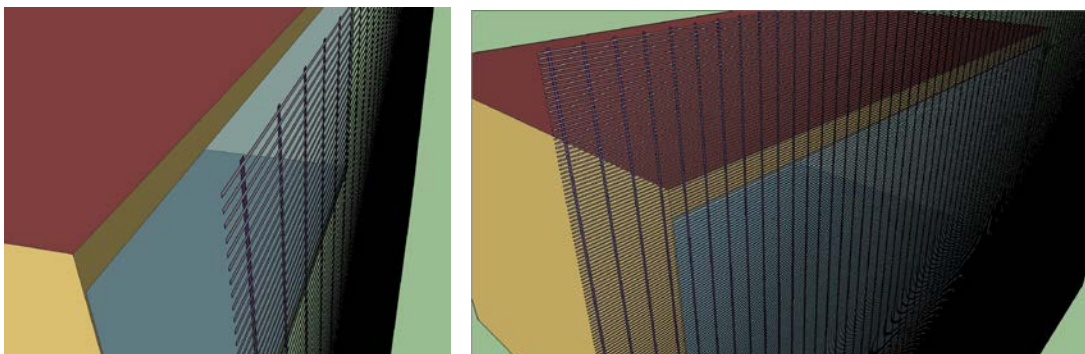


Figure 12. Hand-drawn screen geometry

2.5.2 Uncertainty analysis

An uncertainty analysis is performed to examine the credibility and identify possible limitations of the proposed modelling and calculation methods. The case of a south oriented, 90% WWR, located in Vienna office space is selected as the testbed. The tests involve the most translucent screen of 64% open area, where the actual geometry of the screen “holes” and the relation of vertical and horizontal elements has a significant difference between the square and rectangular opening approach.

Factor of scale

As the screen modelling in all three methods involves elements of about 3 mm thickness the accuracy of the simulation results is tested by analyzing and comparing the real dimension screen model with an 10 times enlarged test model. Results concerning total transmitted solar radiation of the window-shade system are presented in Figure 13. EPscr WINscr methods show tight correlation between the real scale and the 10 times bigger models, which proves their reliability. However, EPscr has constantly a larger solar radiation transmission rate by an average of $2.5 \text{ W}\cdot\text{m}^{-2}$, especially from March till September. The hand-drawn method also shows slightly worse correlation but mainly it documents a very

different performance than the other two. It is also the most time intensive, regarding modeling and calculation time and results in several warnings and errors when simulated. Therefore it rejected as an arbitrary and error prone modeling alternative.

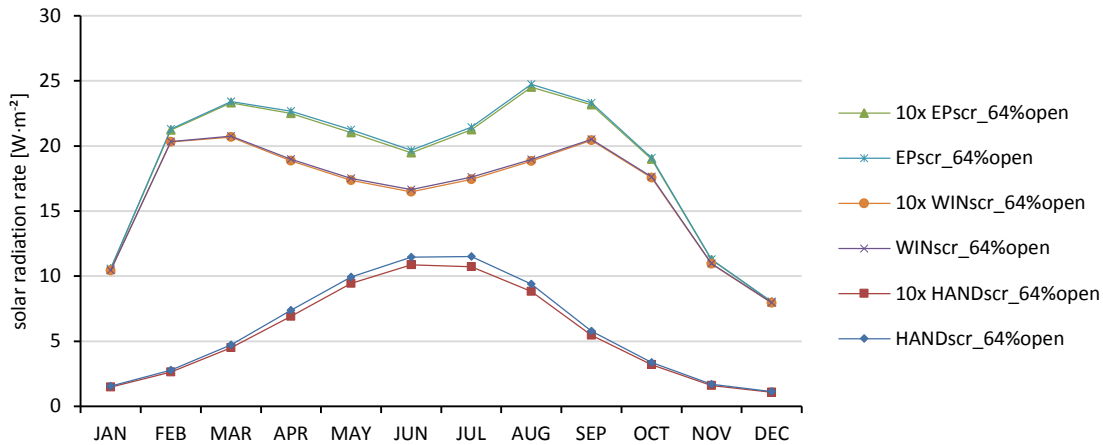


Figure 13. Analysis factor of scale: Window total transmitted solar radiation

Transmitted solar radiation and visible transmittance

EPscr and WINscr methods are tested regarding their visible transmittance and solar radiation transmittance. Results of the two methods for average monthly solar transmittance have an excellent correlation when no shading is applied (Figure 14), but with a shading screen the outcome varies especially for beam solar radiation (Figure 15). Incidental to this fact, although both results follow a similar trend, EPscr curve is constantly greater than WINscr during the March-September period.

On the other hand the two methods perform differently considering visible transmittance either with or without shading. Average space daylight illuminance, which has a direct relation with visible transmittance, is shown in Figure 16. Without shading EPscr method depicts higher space illuminance than WINscr, while with shading, this relation changes, as EPscr results in lower monthly averages and values have a greater divergence from April till August. A detailed comparison on hourly basis is performed for a summer month and can be found in the appendix.

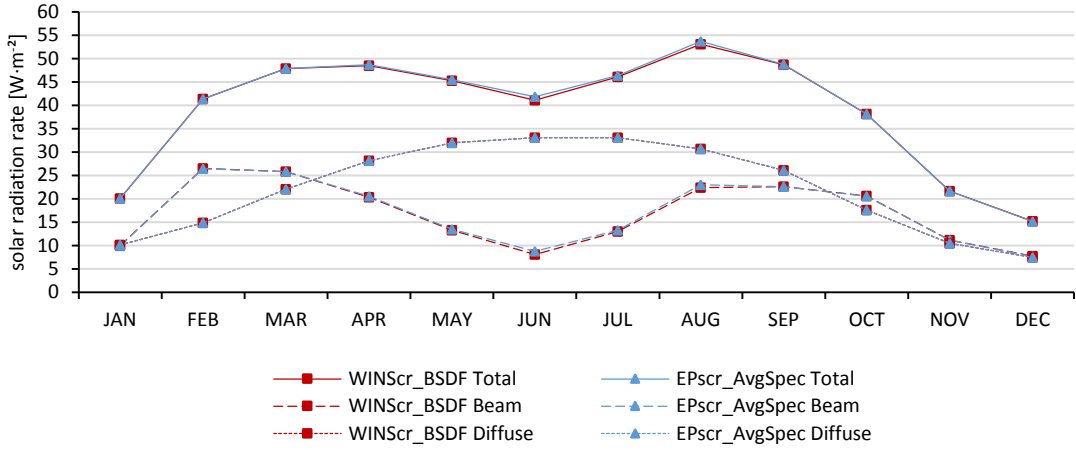


Figure 14. Window without shading screen: Transmitted solar radiation

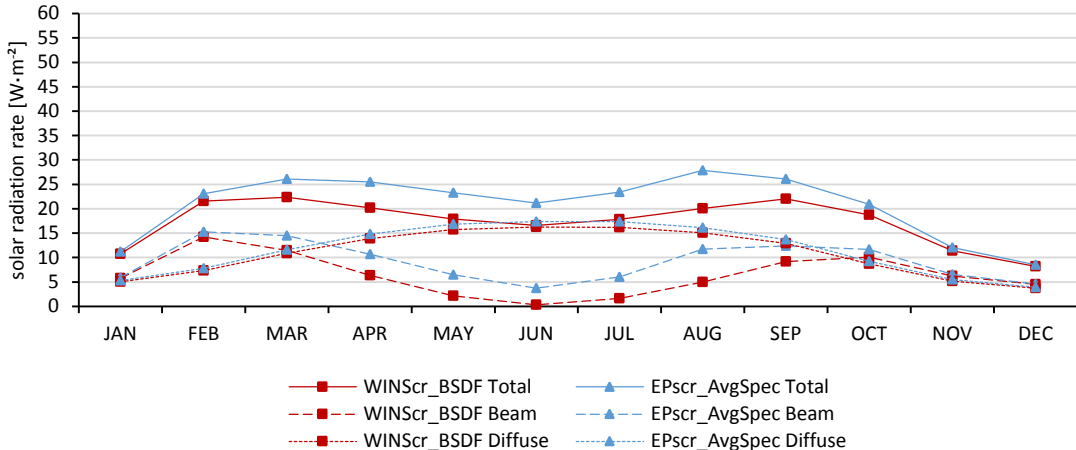


Figure 15. Window with shading screen: Transmitted solar radiation

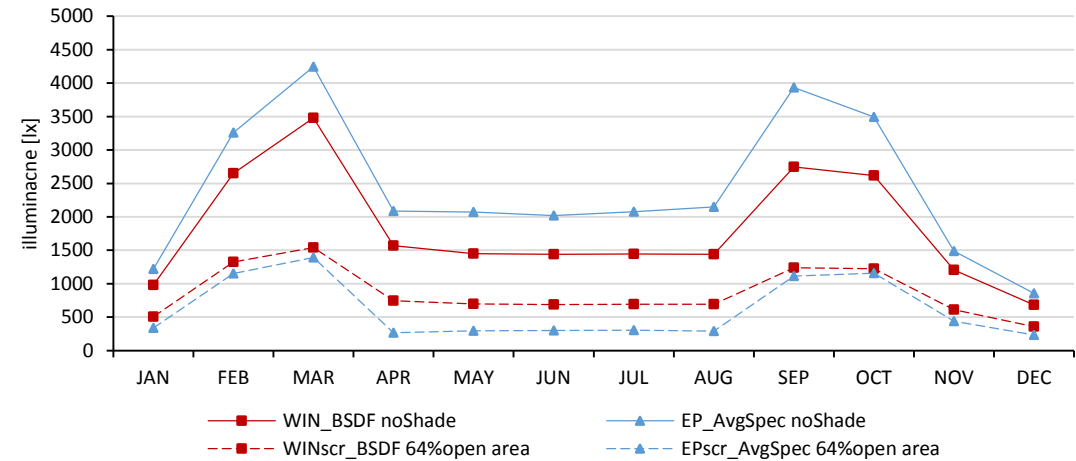


Figure 16. Average monthly daylight illuminance: with and without shading

Position of the shading screen

Compared to other window shading options such as exterior blinds, metal mesh screens are usually placed at a greater distance from the window. Testing the actual distance of the shading screen from the glazing showed that it does not influence the calculation results for solar radiation transmittance and space illuminance in both methods, when there is no other shading surface present. Average monthly values proved to be exactly the same (as shown in Figures 14, 15 and 16) for all tested setups, ranging from 20 cm to 100 cm.

However the size of the gap between the shade and the glazing does have an effect on thermal modelling of the window system and heat balance calculations. Double clear glass window and double low-e thermal insulating glass window were tested for various screen to glazing distances and weather files. Especially for the EPscr method, the analysis showed the glass construction in combination with the local weather conditions could result in severe errors that would terminate the simulation if the screen was placed far from the window. For the three locations that are in the focus of this study, the distance of 45 cm from the glazing was identified as error-free for all cases and within the usual installation range of metal mesh screens on building facades (see Appendix D Table 13).

Besides the distance of the screen, its size and position on the exterior wall are also important. Upon that issue, a limitation emerges for both modelling approaches is that a detailed shading screen can be modeled only in front of an actual window, as graphically shown in model a. of Figure 17. This screen would then affect only the window behind it but would not have any impact as shading surface for other adjacent windows on the same wall. Metal mesh screens on the other hand usually provide shading as second skin on a facade and their surface is not limited to that of a window (Figure 17, b.). The extra shading surface outside the window surface would provide protection from solar penetration from the sides and above, depending on the angle of the sun. To overcome this barrier, the study makes the assumption that there is a surrounding shade outside of the window area (Figure 17, c.), where a detailed screen is created by either the EPscr or WINscr methods (Figure 17, d.). The surrounding shading surface is modelled as a translucent shading layer, given the reflectance properties of stainless steel and degree of translucency according to the open area of the mesh. Facades with high WWR require much smaller surfaces of such surrounding shade than those with lower WWR. The translucent surface would also then shade the opaque exterior walls of the facade, as it is the case in real applications.

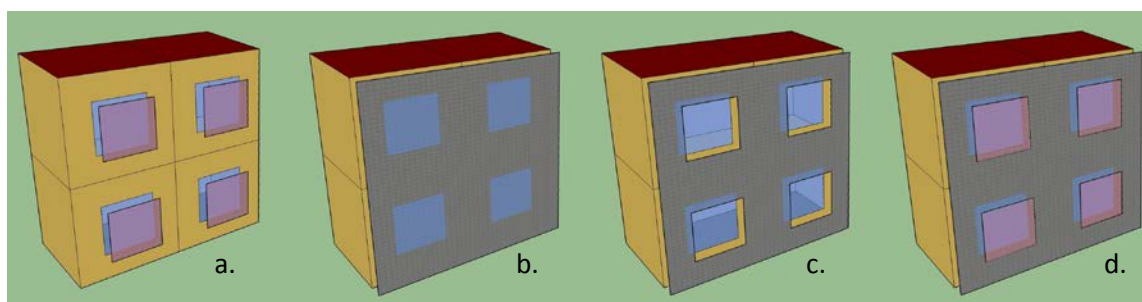


Figure 17. Example for modelling position of metal mesh screen shading
 a. screen created by EPscr or WINscr method, b. normal application of a metal mesh screen,
 c. surrounding shading surface, d. final mesh screen shading model

2.5.3 Comprehensive test and statistical comparison

Due to the notable differences in the performance of the two modelling approaches, a comprehensive test for the location of Vienna is performed, evaluating and comparing the effect of the energy performance for every set-up of key-design parameters. Therefore heating, cooling, lighting as well as total annual energy demand was calculated by both methods for all orientations, WWR and types of mesh screens. For all cases scenarios, all parameters are kept identical except of the modelling of the window-shade system. The percent error of the two modelling method are presented in the graphs below. WINscr results are compared in reference to those of EPscr for different shading conditions.

Figure 18 shows that the WINscr method predicts always lower energy demand for heating, whether with or without shading. The two methods are deviating less for cases with 35% and 50% open area shadings, with an error up to 10% and more when the most translucent shading of 64% open area or when no shade are applied.

WINscr predicts always slightly higher cooling energy demand when no shade is applied as seen in Figure 19. However with a shading screen it predicts constantly lower energy demand for 50% open area screen. The WINscr and EPscr results are similar for the 64% open area screen, at east or west orientation and higher WWR. On a south facade or with low WWR ratio, WINscr method calculates lower cooling demand. For the 35% open area screen, WWR also plays an important role, as for higher ratios, WINscr predicts higher consumption than the EPscr method.

Although the error for heating and cooling demand EPscr and WINscr range mostly between $\pm 20\%$, Figure 21 depicts that lighting does not follow this tendency. When no shading is applied, WINscr with BSDF optical data calculation predicts higher energy consumption for electrical lighting. On the other hand, for any type of shading its results are significantly lower than EPscr with average spectral data calculation. This derives from the different

daylight space illuminance that the two methods calculate, as presented in the previous section.

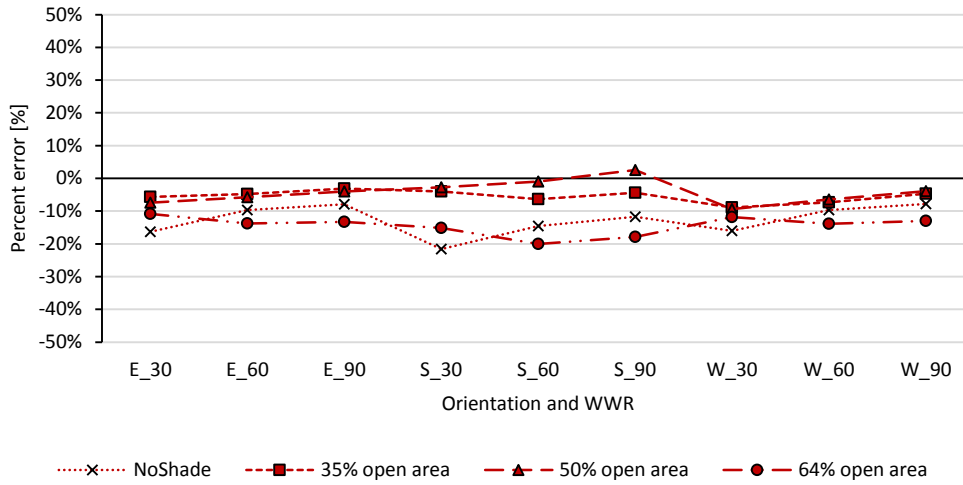


Figure 18. Percent error of WINscr annual heating energy demand in reference to EPscr method

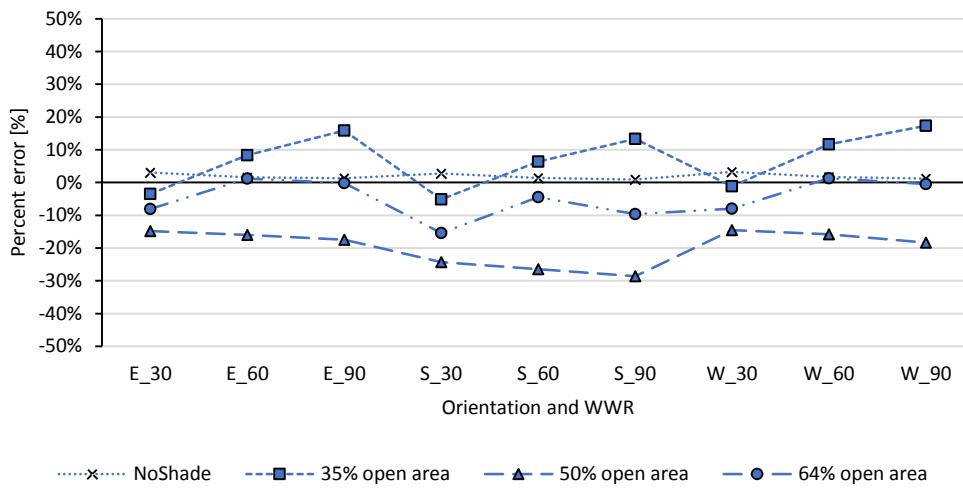


Figure 19. Percent error of WINscr annual cooling energy demand in reference to EPscr method

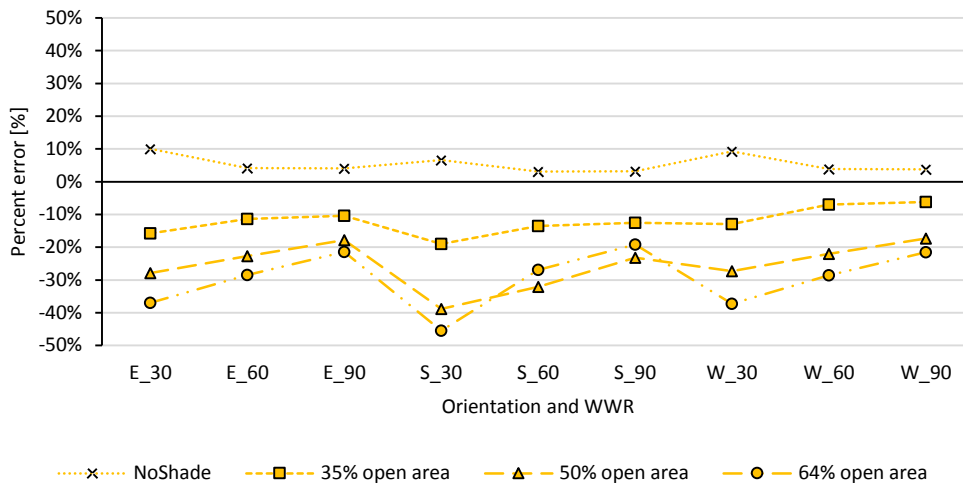


Figure 20. Percent error of WINscr annual lighting energy demand in reference to EPscr method

Overall WINscr method predicts lower annual energy demand when a screen is applied, while without any shade results are relatively similar with EPscr (Figure 21). The difference between the two methods becomes more obvious when screens with larger open area ratio are applied on the building facades. Figure 22 shows a boxplot of the error range per shading condition for the total energy demand.

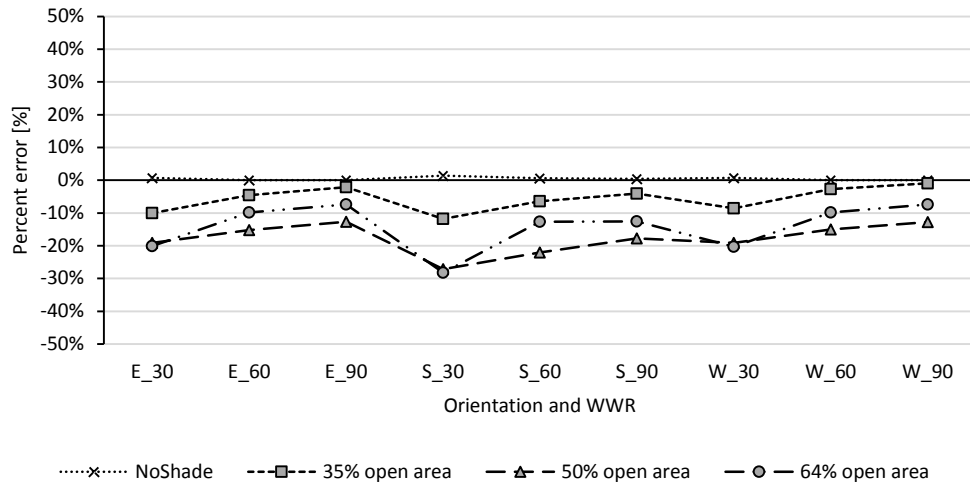


Figure 21. Percent error of WINscr total annual energy demand in reference to EPscr method

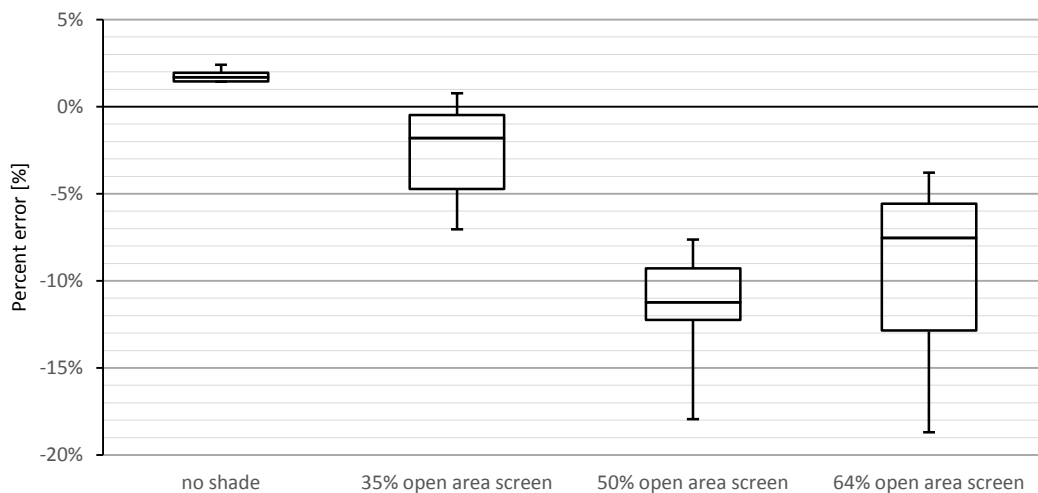


Figure 22. Boxplot of percent error of WINscr total annual energy demand results in reference to EPscr method for four different shading conditions

2.5.4 Remarks, barriers and selection of method

Table 4 shows the computational time of the three initial modelling approaches, measured on a PC with Intel Core i7 @ 3.33GHz. As already discussed HANDscr is rejected as a highly error prone alternative and also extremely time consuming. The WINscr method takes 6 times more to complete than the EPscr, as it handles much more detailed input data.

Table 4. Average simulation time of modelling - calculation methods

Modelling approach	Average time [s]
EPscr	50
WINscr	310
HANDscr	4320

The two methods have significant differences in calculating visible transmittance, thus resulting in great variations in the daylight controlled electrical lighting energy demand. It has to be mentioned that for EPscr results of transmitted solar radiation through the window and space illuminance do not have the expected relationship (Figure 23). Higher transmitted solar radiation would result in higher space illuminance levels. To the contrary, although EPscr has always higher transmitted solar radiation than WINscr, WINscr method always calculates higher space illuminance levels. An interpretation of this results would be that WINscr illuminance levels describe the highest possible performance and in reality values could range between the outcomes of the two modelling methods.

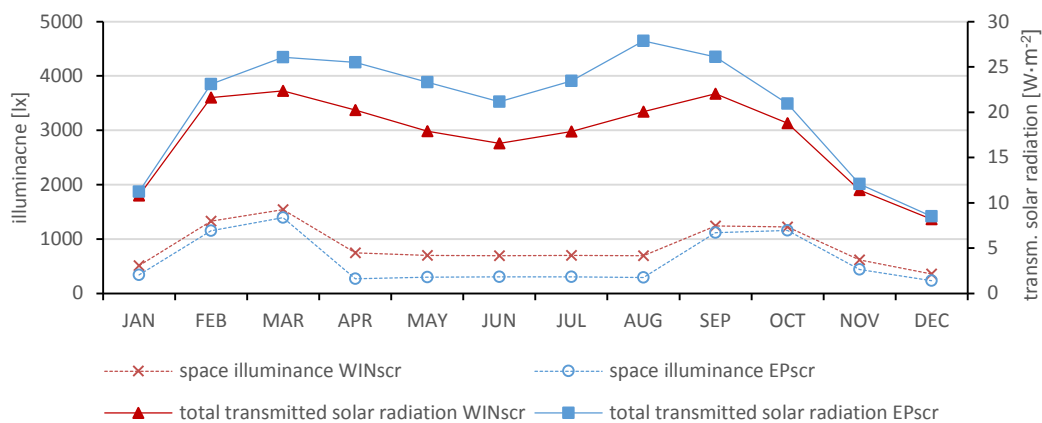


Figure 23. Relationship of EPscr and WINscr for space illuminance and transmitted solar radiation from a window with 64% open area mesh screen shading

As already stated EPscr and WINscr use different optical data types for their calculations, average spectral and BDSF respectively. The BDSF calculation method is much more sensible to variation of the input values as it uses bi-directional reflectance distribution function and bi-directional transmittance distribution function and has discretization for each incident angle, analyzed in detailed matrices (Lam et al. 2014). This is the only glazing modeling and calculation method to do so and therefore is highly sensitive to the incident angle, crucial factor when calculating performance of complex shading systems.

In general the two methods provide similar but different results. An actual measurement of a mesh screen shading device would provide valuable information but unfortunately no resources were available for such an experiment during this study.

Reviewing published literature showed that several studies have used BSDF for simulation of complex fenestration systems (CFS). The radiosity-based algorithm used by the WINDOW software and in this occasion by the WINscr method has been validated in providing accurate BSDF data in the case of CFS with venetian blinds (Molina et al. 2015). Fernandes et al. (2015) use BSDF data and EnergyPlus in their research of static angular selective shading systems which block or filter direct sunlight and admit daylight within specific range of incident solar angles. Bueno et al. (2015) state that the use of BSDF datasets to represent the scattering properties of CFS permits evaluation of a broad variety of systems.

As it has not been possible to experimentally measure a steel mesh screen shading device and compare its performance with simulation results, for this thesis the WINscr method with BSDF calculation is selected to proceed for assessing the impact of all key-design parameters and discussing the energy and thermal performance of the studied office space.

2.6 Results evaluation criteria

Simulation results of the parametric analysis are evaluated in terms of the predicted energy demand, when the office unit implements daylighting control and is mechanically conditioned by an active HVAC system and as described in 2.4.3. Annual heating, cooling, electrical lighting and total energy demand are examined separately. Consequent to that the impact of the four key-design factors - location and climate, orientation, WWR and mesh screen type – is going to be assessed and highlight the best performing combinations.

Based on the results of energy performance, the best performing metal mesh screen shading type is analyzed for its thermal performance according to the adaptive comfort model of Standard EN 15251 (CEN 2007). Overheating and thermal comfort are studied for the summer month's period, when the office unit is operating without active mechanical cooling under various night ventilation scenarios. The goal is to identify the potential of using metal mesh screen shading devices on office buildings with passive summer night cooling strategies. That would concern buildings with no summer air conditioning or cases where the installed ventilation systems are not providing cooling.

2.6.1 Adaptive comfort model of EN 15251

Halawa and Van Hoof (2012) state that the adaptive approach to thermal comfort has gained a significant status in the building science community for evaluating naturally ventilated buildings, describing comfort temperatures as a function of the outdoor air temperature. As people adapt to weather and temperature changes through the year, the main responsibility for attaining thermal comfort is given to the individual. Adaptation takes

the form of changing the clothing insulation degree or regulating the indoor thermal environment for example by opening windows, operating local fans, etc.. Also the type of the building plays an important role on the expectations that people have for thermal comfort. EN 15251 proposes therefore four categories as seen in Table 5.

Table 5. Suggested applicability of the categories of EN 15251

Category	Explanation
I	High level of expectation only used for spaces occupied by very sensitive and fragile persons
II	Normal expectation for new buildings and renovations
III	A moderate expectation (used for existing buildings)
IV	Values outside the criteria for the above categories (only acceptable for a limited periods)

Furthermore EN 15251 relies on actual weather data for defining the outdoor temperature and not on historic monthly means, providing higher variability [Nicol and Humphreys 2010]. Thereby the model is based on an exponentially weighted running mean of the outdoor air temperature (Formula 1). The weighting given to the outside temperatures is higher for recent days, reducing with distance back in time as people adapt to the conditions.

$$T_{rm} = (1 - a) \cdot \{T_{ed-1} + a \cdot T_{ed-2} + a \cdot T_{ed-3} \dots\} \quad (1)$$

where:

T_{rm} running mean outdoor temperate of the actual day [°C]

T_{ed-1} daily mean outdoor temperature of the previous day [°C]

T_{ed-2} daily mean outdoor temperature of the day before the previous day [°C]

a constant between 0 and 1, it is suggested that 0.8 is used

Comfort temperature for non-mechanically cooled buildings in free-running mode is calculated according to the running mean of the outdoor temperature using formula 2.

$$T_{comf} = 0.33 \cdot T_{rm} + 18.8 \quad (2)$$

where:

T_{comf} comfort temperature [°C]

T_{rm} running mean outdoor temperature [°C]

The allowable maximum difference between this comfort temperature and the actual indoor operative temperature (T_{op}) is given in terms of the mentioned categories (± 2 Kelvin for category I, ± 3 Kelvin for II and ± 4 Kelvin for III) resulting in maximum (T_{max}) and minimum (T_{min}) acceptable indoor temperatures. This means that the limiting temperatures vary with the running mean of the outdoor temperature (Figure 24). Comfort temperature

limits for non-mechanically cooled buildings according to EN 15251). These limits are valid when for the upper limit $T_{\max} 10^{\circ}\text{C} < T_{\text{rm}} < 30^{\circ}\text{C}$ and for the lower limit $T_{\min} 15^{\circ}\text{C} < T_{\text{rm}} < 30^{\circ}\text{C}$. For running mean outdoor temperatures below 15°C , there is a set minimum acceptable comfort temperature based on the categories as stated in Table A.3 of standard EN15251.

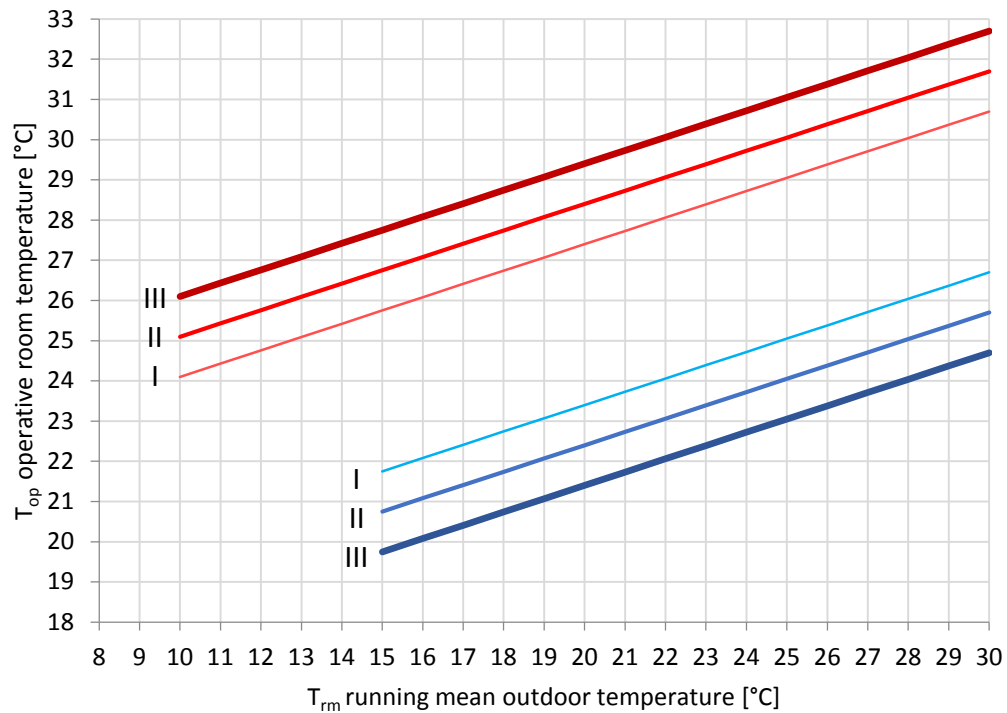


Figure 24. Comfort temperature limits for non-mechanically cooled buildings according to EN 15251

2.6.2 Summer overheating

Summer overheating is evaluated in this study by the number of hours that exceed the upper limit of comfort temperature (T_{\max}) by one degree or more [CIBSE 2013]. Hourly temperature difference is calculated using formula 3.

$$\Delta T = T_{op} - T_{max} \quad (3)$$

where:

ΔT difference between actual and maximum operative temperature, always rounded to the nearest whole degree [°C]

T_{op} actual operative temperature [°C]

T_{max} maximum acceptable operative temperature [°C]

These hours are accumulated for the summer period and presented as an overheating rate as means of comparison.

3 RESULTS

3.1 Overview

Simulation results are presented in two sections in this chapter. First section contains results for annual energy demand of an office unit with an active HVAC system, grouped in the three studied European climate zones. Second part presents results of the feasibility analysis on building thermal performance in the summer period, when metal mesh screen shading is applied on an office unit without active cooling, under various night ventilation scenarios.

3.2 Predicted annual energy demand

For each location graphs of predicted annual energy demand are presented for the three metal mesh screen types of 35%, 50% and 64% mesh open area. Heating, cooling, electrical lighting and their sum are shown separately. The amount of beam and diffuse solar radiation entering the room through window is also depicted as window transmitted solar radiation energy, providing information for the solar performance of the shading device in relation to orientation and WWR. A comparison of the annual total energy demand provides a quick overview of the energy performance of every setup of the key-design parameters.

3.2.1 Location: Athens, Greece

In all cases, dominant energy consumer is cooling and as expected, annual heating energy demand is kept to minimum levels. The increase of WWR in the office unit brings an increase at the total energy demand for all types of mesh screens. For the screen with 35% open area total energy demand ranges from 66 to 80 Kwh·m⁻² (Figure 25), for 50% from 55 to 84 Kwh·m⁻² (Figure 26) and for 64% 60 to 131 Kwh·m⁻² (Figure 27).

Figure 28 displays an overview of the annual total energy demand for four different shading conditions, including the case with no shading on the window. The 50% open area mesh screen is identified as the best performing shading strategy for almost all orientations and WWR. A denser screen of 35% open area would perform slightly better on an eastern facade with 60% or 90% WWR, or on a western facade with 90% WWR.

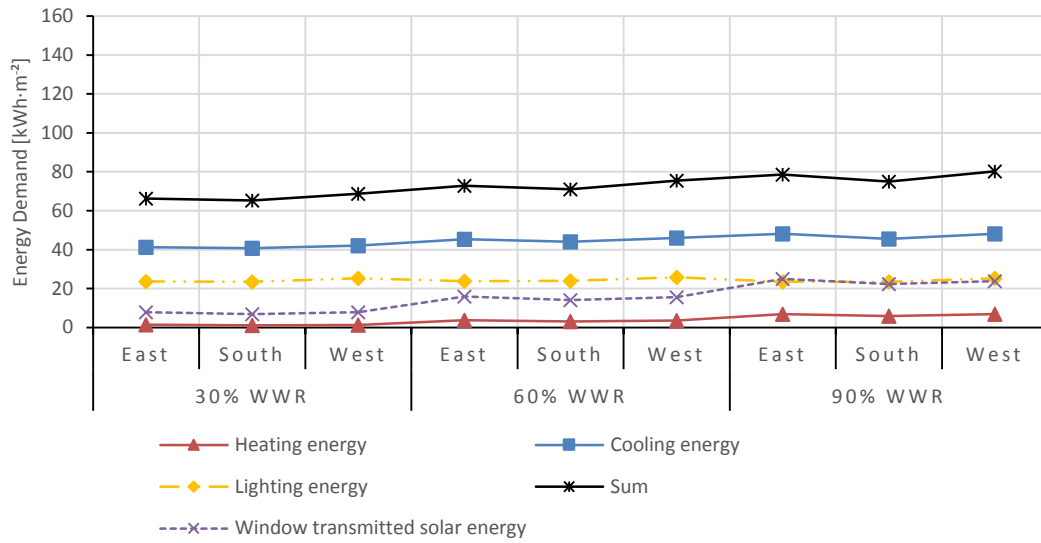


Figure 25. Athens - annual energy demand of 35% open area shading screen

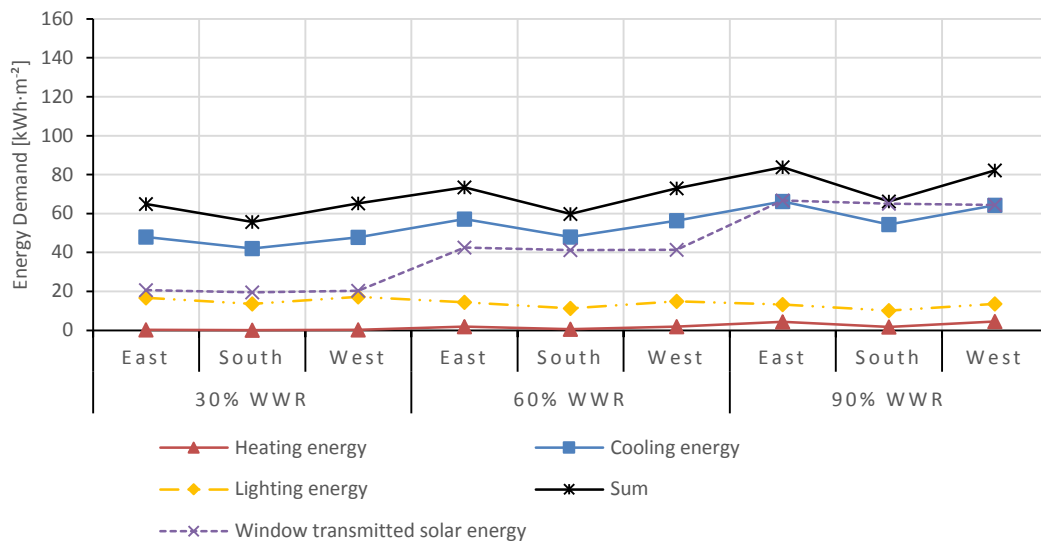


Figure 26. Athens - annual energy demand of 50% open area shading screen

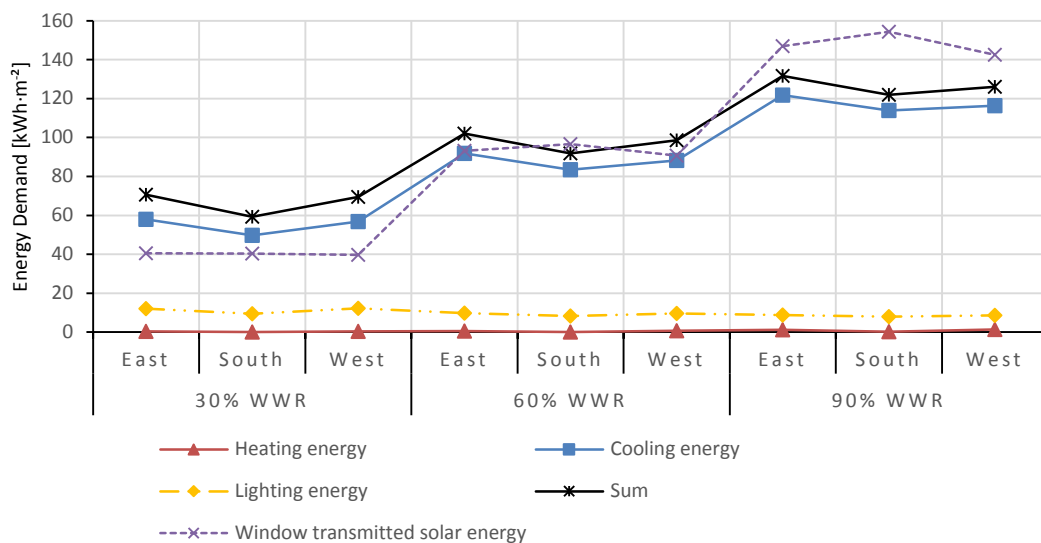


Figure 27. Athens - annual energy demand of 64% open area shading screen

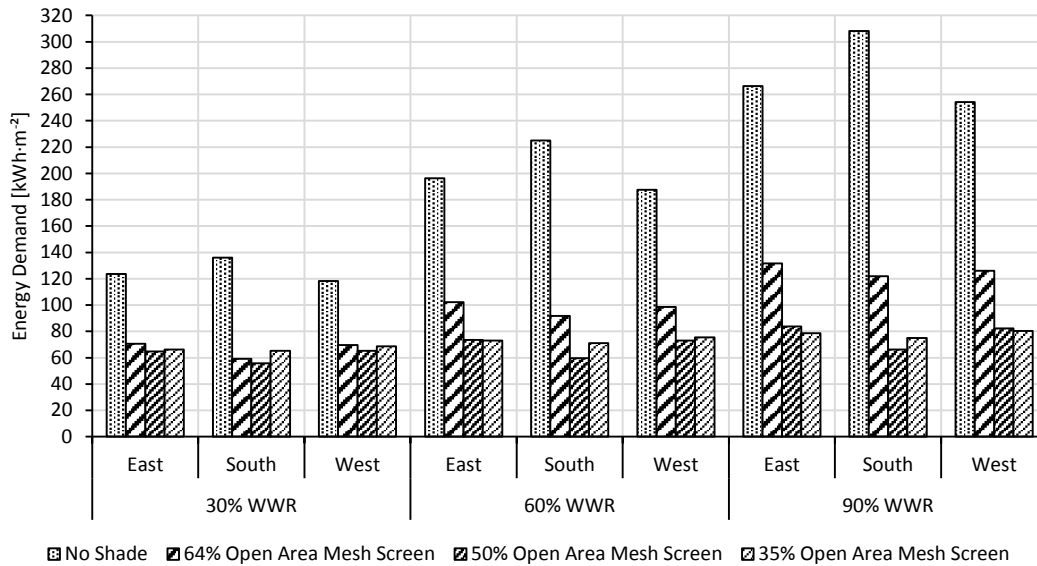


Figure 28. Athens - annual total energy demand

3.2.2 Location: Vienna, Austria

For the 35% open area screen, lighting has the higher energy demand, expect the cases with 90% WWR, where heating is higher. Shading with a 50% open area screen has balanced energy consumption between heating, cooling and lighting. With a 64% open area screen, cooling becomes dominant energy consumer. As expected, the increase of WWR in the office unit brings an increase at the total energy demand for all types of mesh screens. For the screen with 35% open area total energy demand ranges from 54 to 74.5 $\text{kWh}\cdot\text{m}^{-2}$ (Figure 29), for 50% from 42 to 71.5 $\text{kWh}\cdot\text{m}^{-2}$ (Figure 30) and for 64% 40 to 88 $\text{kWh}\cdot\text{m}^{-2}$ (Figure 31).

Figure 28 displays an overview of the annual total energy demand for four different shading conditions, including the case with no shading on the window. The 50% open area mesh screen is identified as the best performing shading strategy for almost all orientations and WWR. A more translucent screen of 64% open area would perform slightly better on a southern facade with 30% WWR.

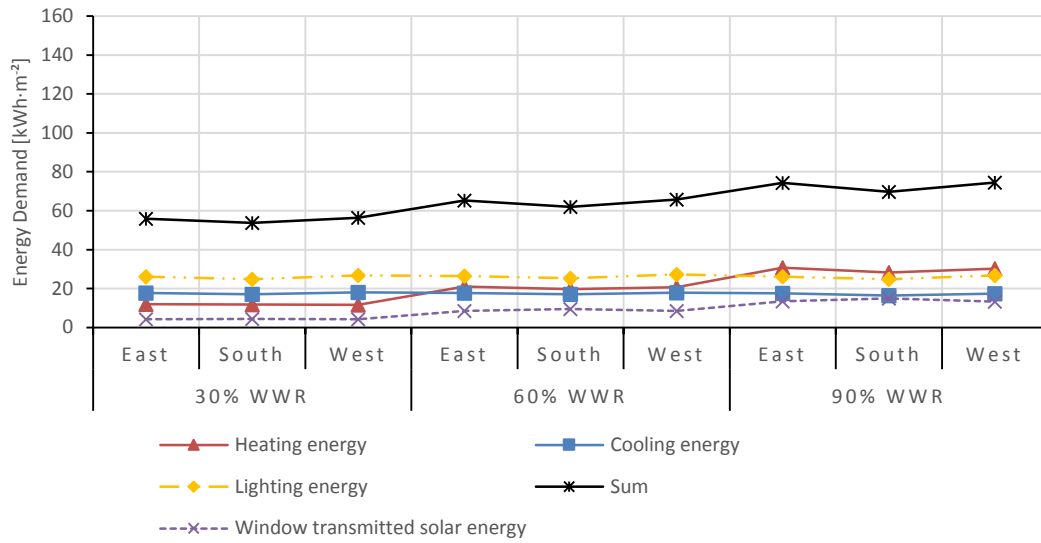


Figure 29. Vienna - annual energy demand of 35% open area shading screen

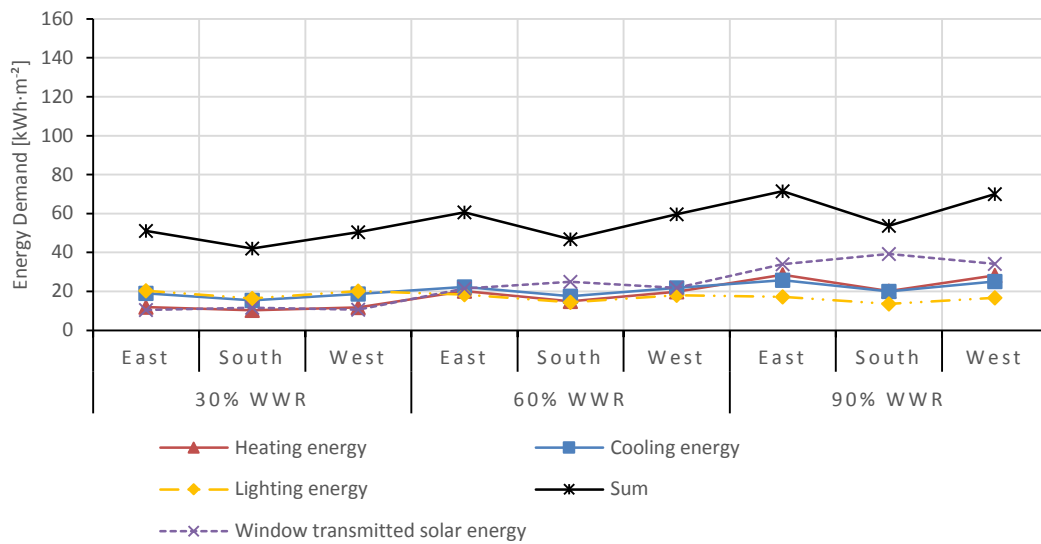


Figure 30. Vienna - annual energy demand of 50% open area shading screen

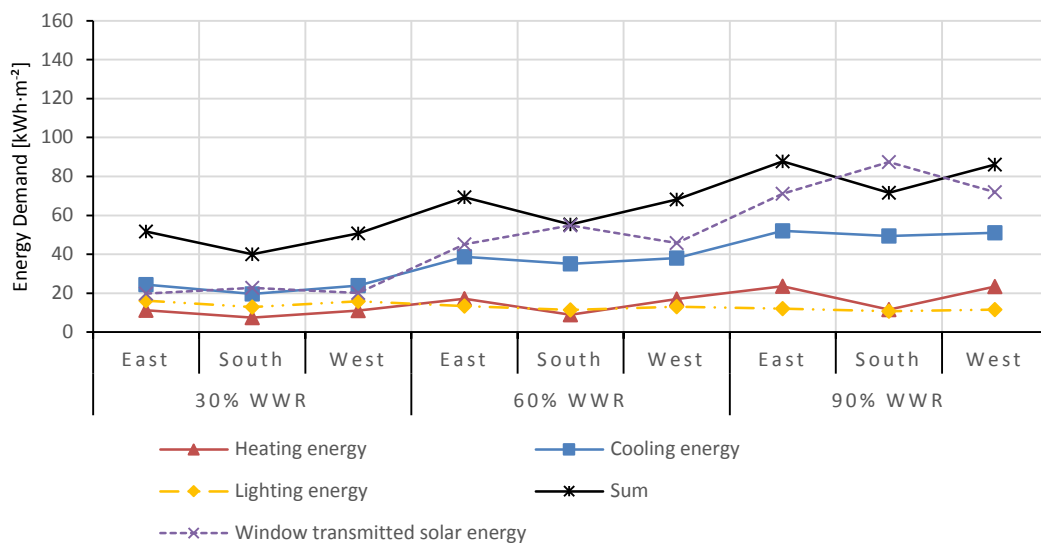


Figure 31. Vienna - annual energy demand of 64% open area shading screen

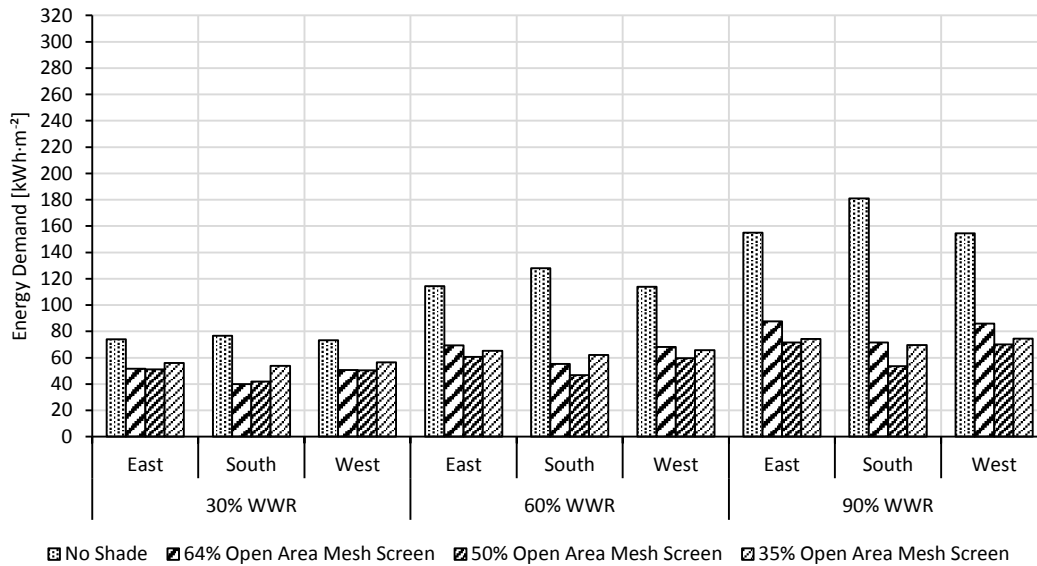


Figure 32. Vienna - annual total energy demand

3.2.3 Location: London, United Kingdom

For the 35% and 50% open area screens, lighting has the higher energy demand for all orientations and WWR. With a 64% open area screen, lighting and cooling have equally the highest energy demand, but as WWR increases cooling becomes also here the highest energy consumer. As in the previous locations, the increase of WWR in the office unit brings an increase at the total energy demand for all types of mesh screens. For the screen with 35% open area total energy demand ranges from 37 to 52 $\text{Kwh}\cdot\text{m}^{-2}$ (Figure 33), for 50% from 27 to 46 $\text{Kwh}\cdot\text{m}^{-2}$ (Figure 34) and for 64% 26 to 61 $\text{Kwh}\cdot\text{m}^{-2}$ (Figure 35).

Figure 36 displays an overview of the annual total energy demand for four different shading conditions, including the case with no shading on the window. The 50% open area mesh screen is identified as the best performing shading strategy for almost all orientations and WWR. A more translucent screen of 64% open area would perform slightly better on an eastern or southern facade with 30% WWR.

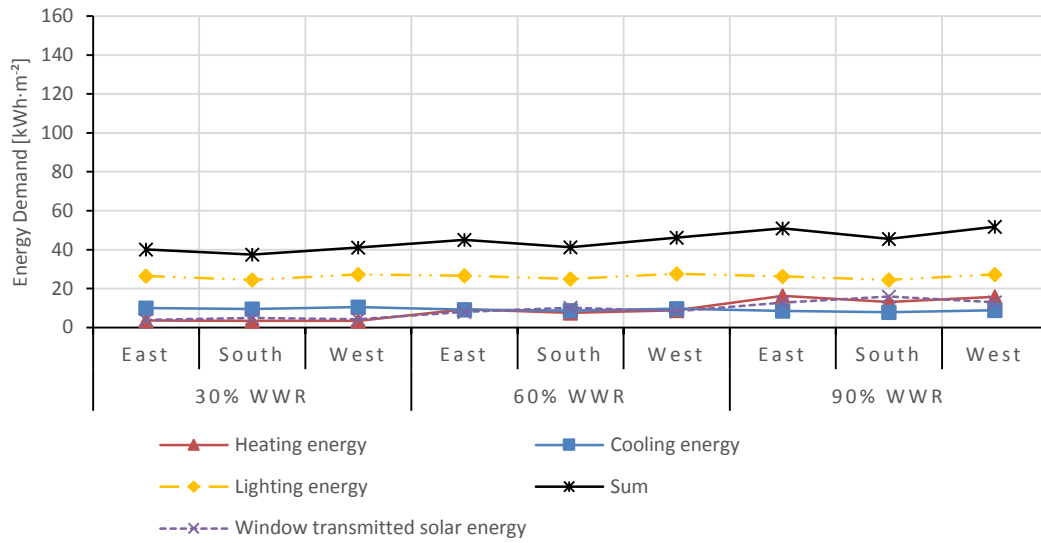


Figure 33. London - annual energy demand of 35% open area shading screen

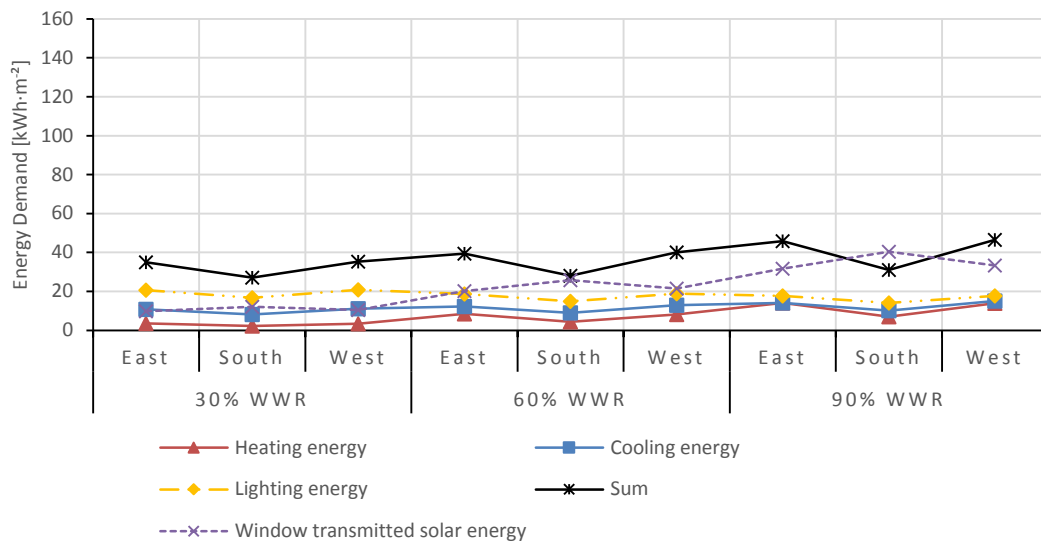


Figure 34. London - annual energy demand of 50% open area shading screen

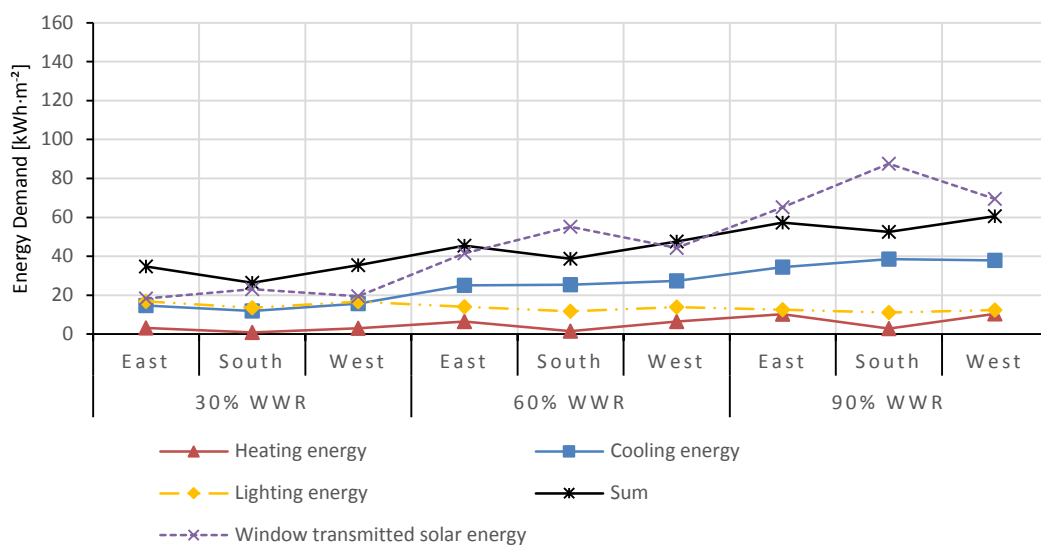


Figure 35. London - annual energy demand of 64% open area shading screen

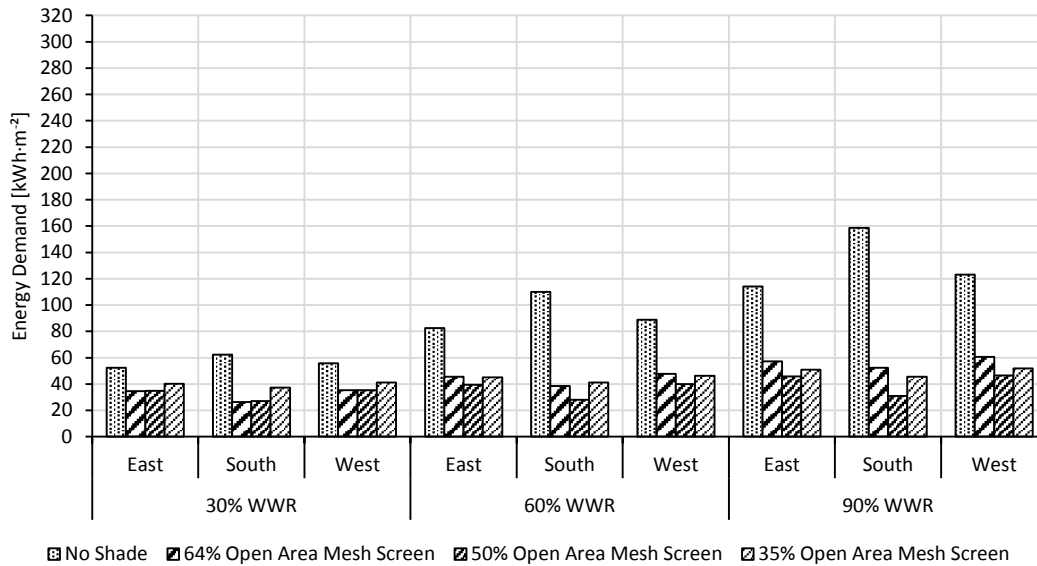


Figure 36. London - annual total energy demand

3.3 Feasibility study on summer thermal performance

An overview of the results presented in section 3.2 and especially in Figures 28, 32 and 36 leads to the observation that models with 50% open area mesh screen shading devices perform in general better in terms of predicted energy consumption at all locations and most facade orientations and window to wall ratios. For this reason, this type of mesh screen is selected for a further analysis on its thermal performance by means of a feasibility study on metal mesh screen shading on buildings without active cooling during the summer period. Criteria of the analysis, as discussed in section 2.6., are based on adaptive comfort model of EN 15251. The standard can be applied on buildings with mechanical ventilation and no active cooling function through the system. It describes that “mechanical ventilation without cooled air (in summer) may be used, but the opening and closing of windows must be given first priority in regulating the indoor climate” (CEN 2007). Parameters of the analysis are summarized below.

Based on parameters defined in section 2.4.3 with the following remarks:

- Study of the summer period: June - August
- Shading type: 50% open area metal mesh screen
- No active mechanical cooling:
 - mechanical ventilation operates in the morning but does not provide cooling
 - morning ventilation:

weekdays: $0.0085 \text{ m}^3 \cdot \text{s}^{-1}$ per person resulting in about 1 ACH

weekends: off

- Natural free cooling through night ventilation:
 - five different night ventilation scenarios (0 ACH, 1 ACH, 2 ACH, 4 ACH and 8 ACH)
 - occurring every night and always from 22:00 till 07:00
- Constant infiltration of 0.2 ACH
- Clothing insulation in summer: 0.5 clo
- Building category according to EN 1521: Category II
 - minimum comfort temperature for this category is 20.75°C

3.3.1 Summer overheating and thermal comfort

Table 6 summarizes the rate of comfortable hours for all night ventilation scenarios. Results are graphically presented in Figures 37, 38 and 39 for the three climate zone locations respectively. The highest rate of hours within thermal comfort are recorded for the scenario with the highest air changes (8 ACH) in the case of Athens and for those with low rate of air changes (1 ACH or 2 ACH) in the cases of Vienna and London. Rate of overheating hours is presented in Figures 40, 41 and 42. No cooling via night ventilation results in extreme overheating for models in all locations. Night cooling strategies prove effective for Vienna and London but in the case of Athens, even with high rate of night ventilation summer overheating hours reach an average of 50%.

Table 6. Summer thermal comfort for an office space with 50% open area mesh screen shading device: percent of comfort hours according to adaptive comfort model of EN15251 for the June-August period

	night ventilation scenario	30% WWR			60% WWR			90% WWR		
		East	South	West	East	South	West	East	South	West
Athens	0 ACH	0%	0%	0%	0%	1%	0%	0%	3%	0%
	1 ACH	5%	12%	5%	3%	12%	3%	3%	12%	2%
	2 ACH	16%	32%	15%	9%	29%	8%	7%	27%	7%
	4 ACH	43%	56%	43%	28%	48%	28%	23%	42%	22%
	8 ACH	58%	67%	58%	42%	57%	43%	34%	50%	36%
Vienna	0 ACH	0%	6%	0%	0%	10%	0%	2%	12%	1%
	1 ACH	63%	80%	64%	45%	70%	47%	34%	61%	37%
	2 ACH	82%	86%	83%	69%	80%	70%	56%	71%	59%
	4 ACH	77%	72%	76%	74%	74%	74%	63%	71%	65%
	8 ACH	64%	58%	63%	67%	65%	67%	62%	64%	62%
London	0 ACH	11%	25%	9%	12%	27%	9%	14%	35%	12%
	1 ACH	85%	90%	84%	75%	85%	72%	66%	79%	62%
	2 ACH	78%	69%	80%	80%	75%	79%	74%	74%	71%
	4 ACH	55%	49%	55%	63%	57%	63%	63%	60%	62%
	8 ACH	48%	44%	49%	57%	52%	56%	58%	56%	56%

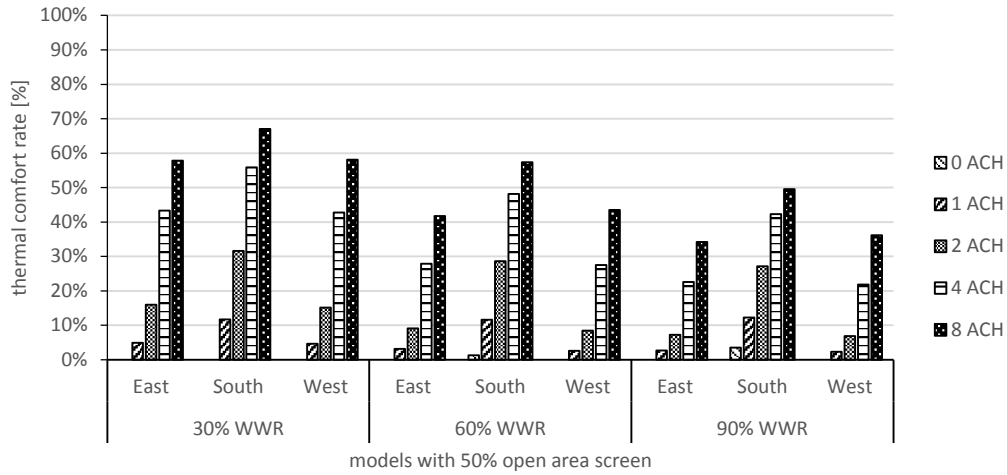


Figure 37. Athens - summer thermal comfort for different night ventilation scenarios (June-August), shading mesh screen with 50% open area

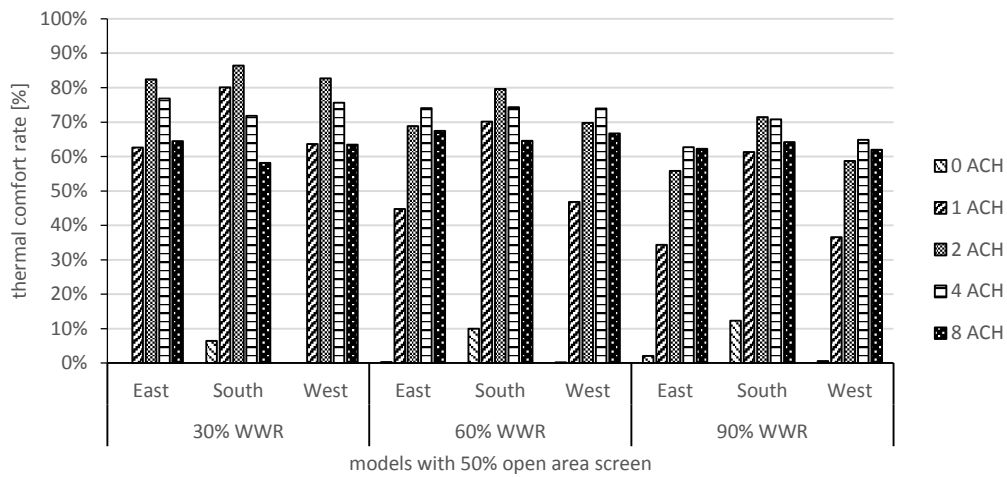


Figure 38. Vienna - summer thermal comfort for different night ventilation scenarios (June-August), shading mesh screen with 50% open area

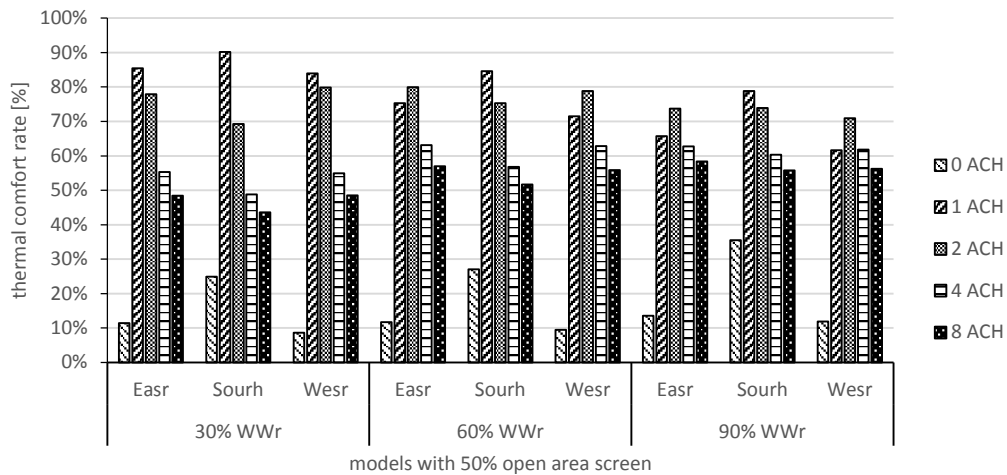


Figure 39. London - summer thermal comfort for different night ventilation scenarios (June-August), shading mesh screen with 50% open area

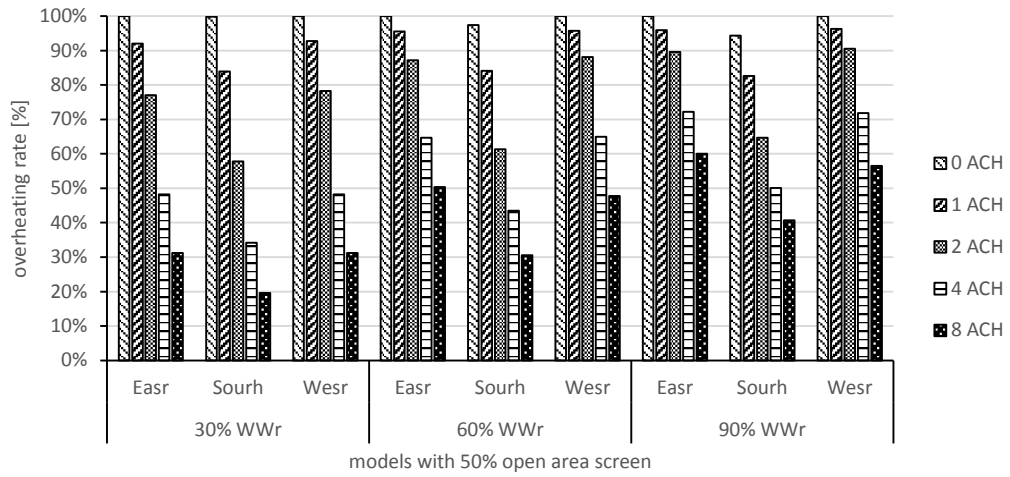


Figure 40. Athens - summer overheating (June-August), hours exceeding Tmax ($\Delta T \geq 1$)

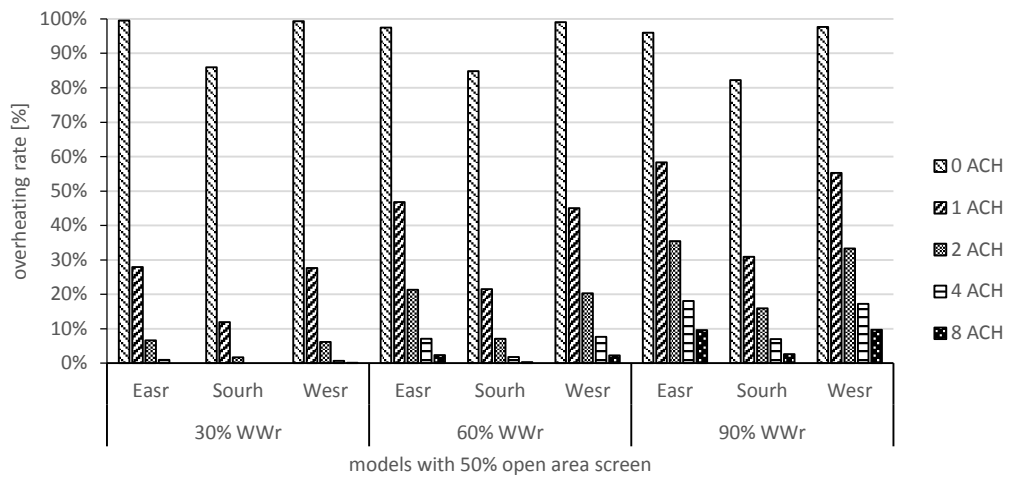


Figure 41. Vienna - summer overheating (June-August), hours exceeding Tmax ($\Delta T \geq 1$)

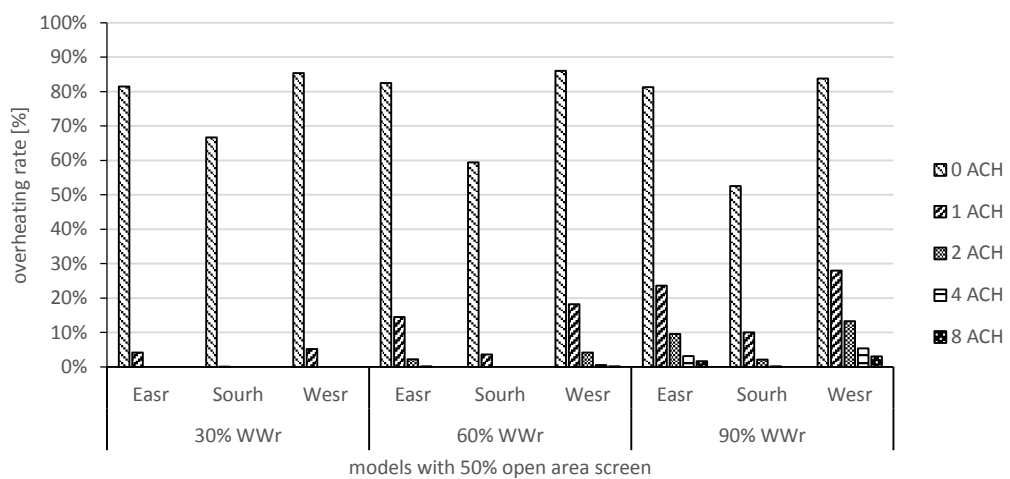


Figure 42. London- summer overheating (June-August), hours exceeding Tmax ($\Delta T \geq 1$)

3.3.2 Thermal comfort for selected night ventilation scenarios

The distribution of summer indoor operative temperatures is presented in the following charts for selected night ventilation scenarios for each location. Results presented in the previous section 3.3.1 indicate that for south oriented facades, no matter the WWR, there is a night ventilation scenario that achieves higher thermal comfort rates. For Athens this is the night ventilation scenario with 8 ACH. For Vienna the 2 ACH scenario and for London the 1 ACH scenario. Figure 43, 44 and 45 depict the temperature distribution during the three months of the summer period based on adaptive comfort model of EN 15251, for the three locations respectively.

Comfortable temperatures in a category II building according to EN 15251 are defined for 80% of acceptability rate. Values that lay between the $T_{\min} - T_{\max}$ range are considered as comfortable. In the case of Athens the running mean outdoor temperature exceeded the specified domain limit of 30°C four times during the summer period. In this case the adaptive comfort model is not applicable and room operative temperatures of these occasions are regarded as non-comfortable.

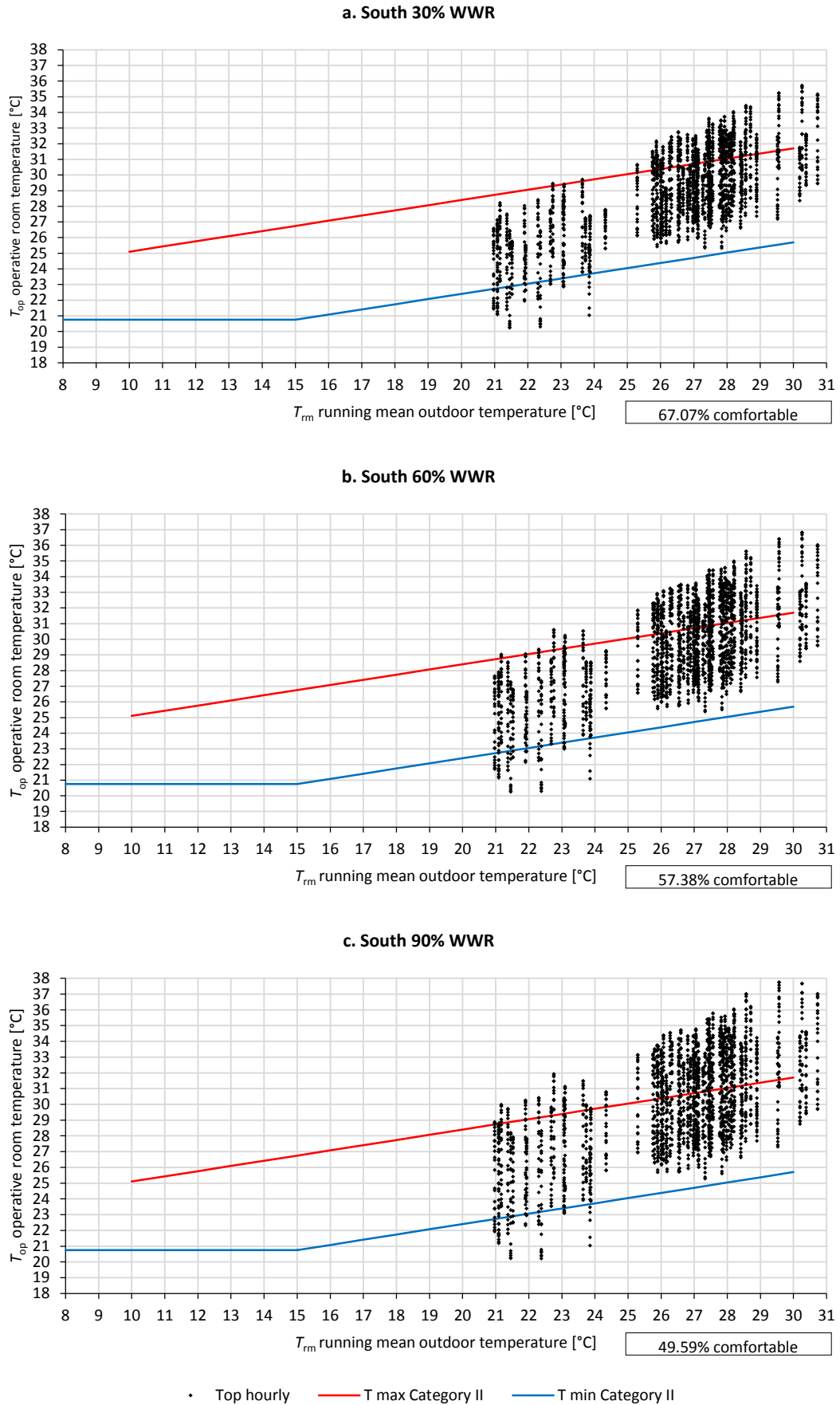


Figure 43. Athens - summer period (June-August) temperature distribution according to EN 15251, shading mesh screen with 50% open area on a south facade and 8 ACH night ventilation scenario

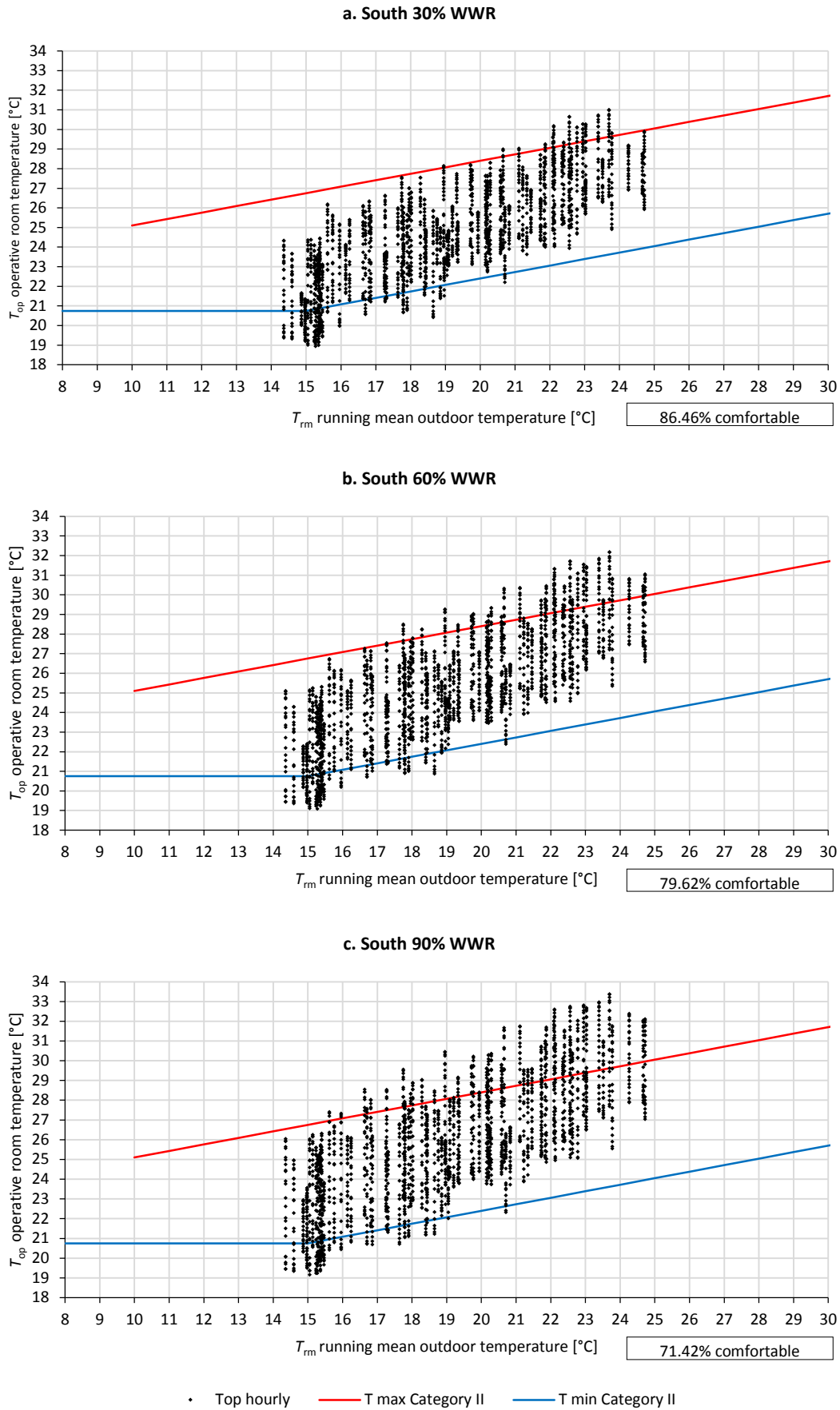


Figure 44. Vienna - summer period (June-August) temperature distribution according to EN 15251, shading mesh screen with 50% open area on a south facade and 2 ACH night ventilation scenario

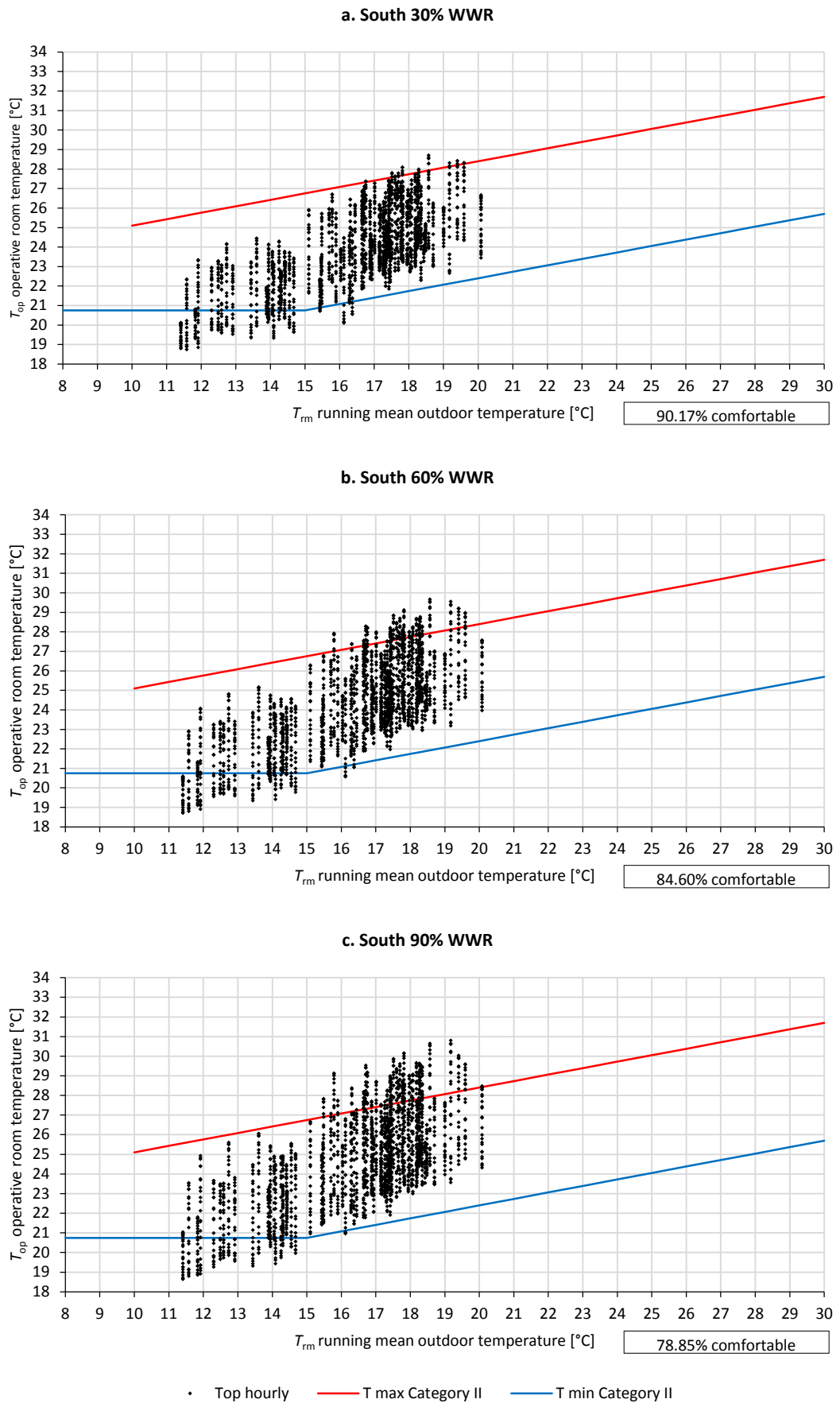


Figure 45. London - summer period (June-August) temperature distribution according to EN 15251, shading mesh screen with 50% open area on a south facade and 1 ACH night ventilation scenario

4 DISCUSSION

4.1 Overview

As stated in section 2.5.4, this work evaluates the outcome of the WINscr modelling and calculation method. Although the actual calculations for predicted energy demand of the simulation models may differ, the trends and remarks which are discussed in this chapter are the same for both methods on all simulated cases. This provides a further validation of the impact the studied key-design parameters have on an office space with metal mesh screen shading.

4.2 Energy performance

Results presented in section 3.2 are analyzed according to the four key-design parameters addressed in this study. Through a critical scope, this section derives to suggestions on the application of metal mesh screen shading devices on office buildings.

4.2.1 Location - Climate

Figure 46 shows the range of results for total annual energy demand in the three cities, located in different climate zones. Results of the base cases of each orientation-WWR scenario when no shade is applied are also depicted. As expected, applying a shade on a facade reduces significantly the energy demand by decreasing the need for cooling. However, as seen in Table 7, the average energy demand including heating, cooling and lighting for an office space with metal mesh screen shading in Athens is 29% higher compared to Vienna and 91% higher compared to London. The reason for this is that cooling load predictions in Athens are dramatically higher for every parameter constellation in order to maintain the room temperature at the set-point of 26°C (Figure 47). This supports the argument that for a mechanically cooled building in Athens, providing shade only be means of metal mesh screen shading will prove inefficient in terms of energy performance. Best energy performance results for all climate zones come from cases of south oriented facade with only 30% WWR. For Vienna and London shading would require to be more translucent though than in Athens, thus letting more solar radiation pass through and having higher solar gains.

Table 7. Average energy demand and best performing case for the three climate zones

total annual energy demand [Kwh·m ⁻²]	Athens	Vienna	London
average	79.6	61.6	41.7
best performing constellation	55.7 South_30WWR_50%mesh	40.0 South_30WWR_64%mesh	26.3 South_30WWR_64%mesh

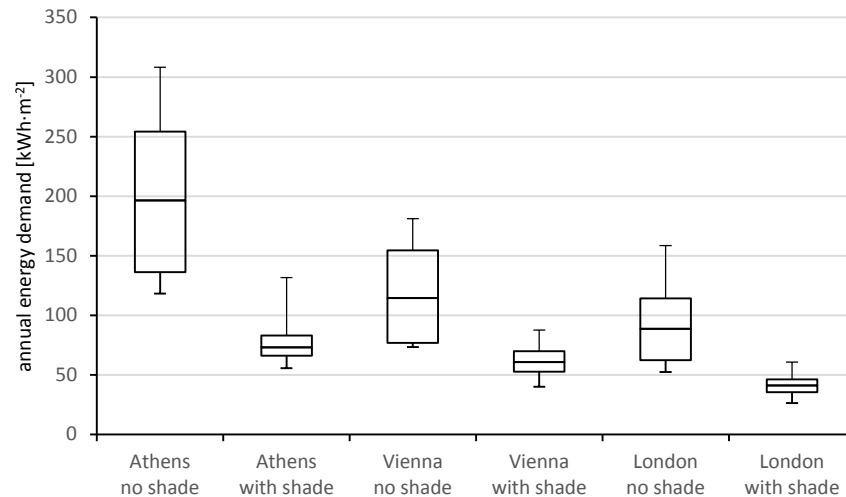


Figure 46. Boxplots of total annual energy demand for the three climate zones, with or without window shading

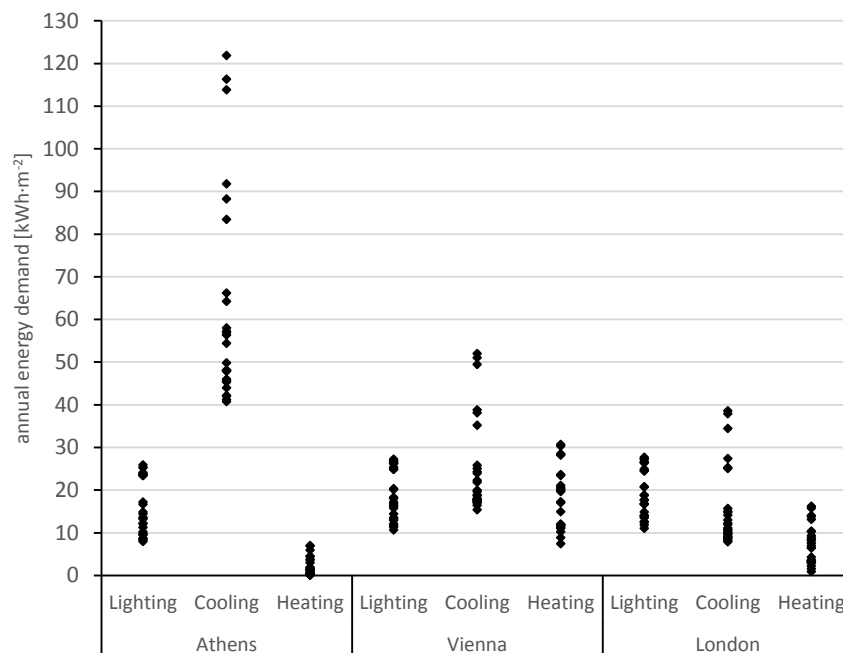


Figure 47. Distribution of annual energy demand results in the three climate zones

4.2.2 Facade orientation

By reviewing the results of total annual energy demand presented in Figures 28, 32 and 34, metal mesh screen shadings prove to be more effective when applied on a south oriented facade. In all locations and for all WWRs and types of mesh screen, the energy demand is lower compared to east and west facing spaces, therefore total annual energy savings presented in Table 8 are always higher in the south orientation. The explanation for this condition lays in the solar elevation angle. When the sun is the East or West its altitude is lower and therefore solar radiation can penetrate easier the open area of the mesh screen shading. During the summer, when the sun's path is higher, eastern and western facades

with mesh screen shading will generally result in higher cooling loads than those which are south oriented. For the last, the static geometry of the screen would provide better shading conditions. During winter on the other hand, when the sun is orbiting at a lower altitude, the penetration of solar radiation through the screen will occur on all three orientations. However, the hours when the sun is located in the east or the west are fewer and those facades cannot benefit as much as the south facade from solar gains. This results in higher heating loads for eastern and western room orientations as it can be seen in graphs of section 3.2.

Table 8. Annual energy savings in comparison to base cases without shading (marked red is the highest reduction achieved)

		30% WWR			60% WWR			90% WWR			
		East	South	West	East	South	West	East	South	West	
Mesh screen open area [%]	Athens	35	37%	42%	33%	54%	60%	51%	63%	68%	61%
		50	38%	48%	35%	54%	64%	52%	61%	71%	60%
		64	34%	45%	32%	41%	52%	40%	45%	55%	45%
	Vienna	35	17%	21%	16%	33%	41%	33%	43%	52%	43%
		50	21%	32%	21%	36%	50%	37%	44%	60%	45%
		64	21%	33%	21%	31%	45%	31%	36%	51%	37%
	London	35	14%	26%	16%	32%	48%	35%	43%	59%	46%
		50	20%	37%	23%	37%	57%	40%	46%	67%	49%
		64	21%	38%	23%	32%	50%	34%	39%	55%	40%

4.2.3 Window to wall ratio (WWR)

As regards WWR, calculated results confirm a logical expectation. The larger the WWR of an exterior facade, the larger the energy consumption as well as the window transmitted solar radiation energy. Nonetheless, when comparing models with shading to those without, facades with 90% WWR display the highest energy savings potential (Table 8). This trend is also presented in Figures 48, 49 and 50 for Athens, Vienna and London respectively. Since metal mesh screens are often applied on glass curtain wall facades on office buildings, analysis of the results leads to some suggestions on their application. In climate zones in southern Europe, like the one of Athens, eastern and western oriented facades would require a denser mesh in order to keep cooling loads lower while in the south a mesh with medium open area ratio, like the 50%, would provide higher energy savings. In central and northern European climate zones, for all orientations a mesh screen with open area close to 50% would perform better. A more translucent mesh would fit facades with low WWR in Vienna and London but is not recommended for the case of Athens.

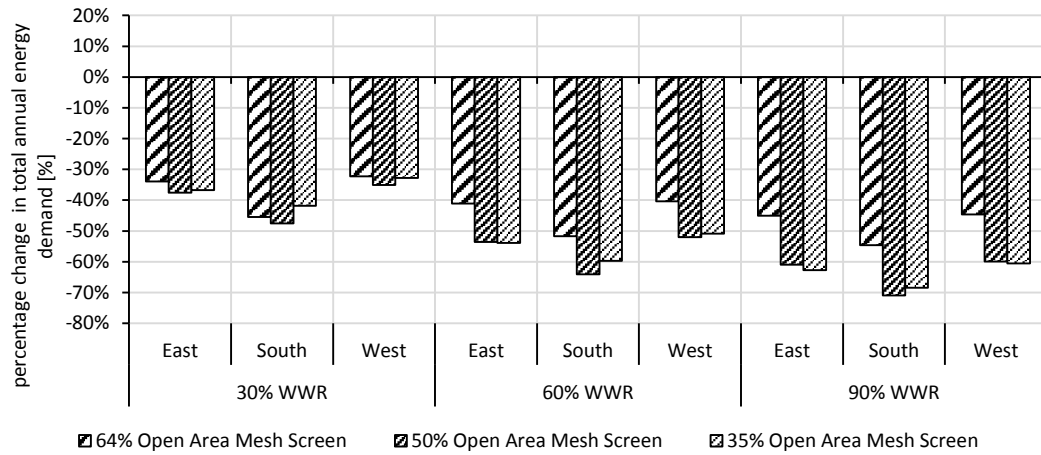


Figure 48. Athens - energy savings compared to base cases without shading

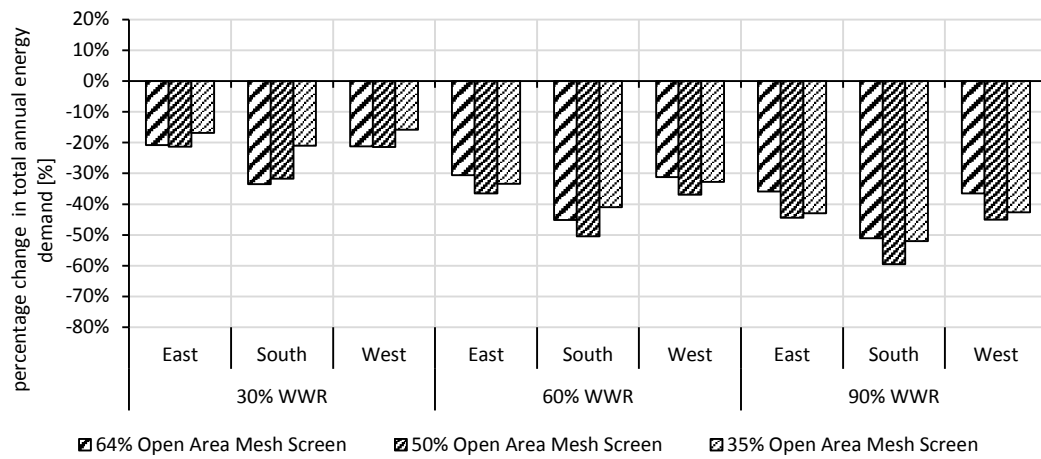


Figure 49. Vienna - energy savings compared to base case without shading

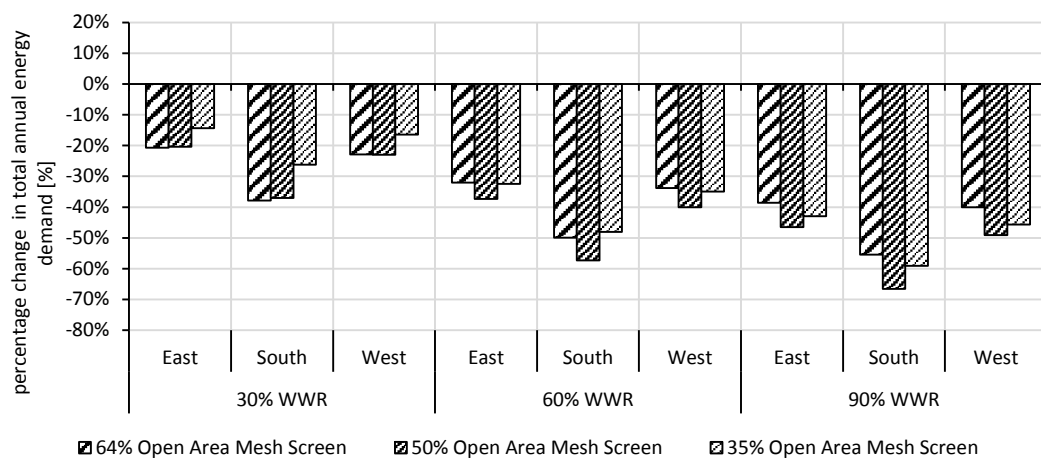


Figure 50. London - energy savings compared to base case without shading

4.2.4 Type of metal mesh screen

The type of mesh screen used for shading is an essential factor affecting the final energy performance. It is already discussed that a denser or looser mesh has different effect on each orientation-WWR combination. As seen in Figures 48, 49 and 50 there is a mesh screen type that generally provides higher energy savings in the vast majority of simulated scenarios and that is the 50% open area mesh (OAM). Climate conditions also influence the potential for energy savings. Greater energy demand reduction when applying metal mesh screens on an unshaded facade is recorded in the case of Athens, where the worst performing model achieves 32% (west_30WWR_64OAM) and the best one 71%. In Vienna, worst case performance results in 16% (west_30WWR_35OAM) savings and best 60%. For London these values are defined at 14% (east_30WWR_35OAM) and 67%. Best performance is always reported in south oriented 90% WWR facade with 50% OAM (Table 7). This implies that for Athens such kind of shading is beneficial for reducing energy consumption at least by 30%, mainly by decreasing cooling loads. However, as discussed in section 4.2.1 it should not be the only type of shading provided and should be coupled with other means of shading strategies in order to achieve lower cooling energy demand. In Vienna and London reduction greater than 30% occurs in cases with 60% and 90% WWR. For facades with lower amount of transparent surfaces, a more translucent mesh such as the 64% OAM can also surpass this limit when placed on a south oriented wall. Table 9 lists the best performing mesh screen types according to the energy demand reduction they achieve and therefore would be best suited for a shading device. For results where the amount of reduction differs less than 1%, two types of meshes are listed. In the majority of the studied cases a 50% OAM screen would be the most energy efficient choice.

Table 9. Best performing type of screen in terms of energy demand reduction: suggested mesh open area

		30% WWR	60% WWR	90% WWR
Athens	East	35/50	35/50	35
	South	50	50	50
	West	50	35/50	35/50
Vienna	East	50/64	50	50
	South	50/64	50	50
	West	50/64	50	50
London	East	50/64	50	50
	South	50/64	50	50
	West	50/64	50	50

Figure 51 presents the ranges of total annual energy demand pro type of mesh screen and location. The fact that the 50% OAM performs better can be also confirmed by the minimum

and median values of this type of screen which are always lower than those of 35% and 64% OAM for the same location. Another point is that the dense of 35% OAM shows less fluctuations in energy demand regarding orientation and WWR of the facade, with an average of $16.5 \text{ Kwh}\cdot\text{m}^{-2}$ min-max difference. 50% OAM has an average min-max range of $25.8 \text{ Kwh}\cdot\text{m}^{-2}$ and 64% OAM $50 \text{ Kwh}\cdot\text{m}^{-2}$.

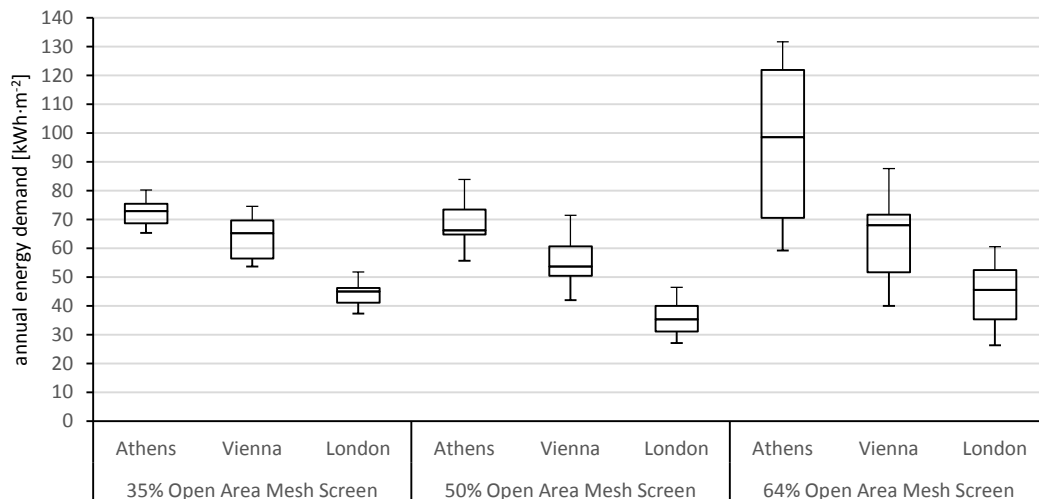


Figure 51. Boxplots of total annual energy demand for type of mesh screen and climate zone

Another observation from results in section 3.2 which was also expected is that the denser the screen the higher the electrical lighting consumption, as daylight availability decreases. Also heating loads are generally increasing due to the reduction of window solar gains. In order to assess the impact on heating loads and electrical lighting by the application of a permanent shading mesh screen surface on the exterior facade results are compared in reference to a base case where no shading is applied. For that cases where the highest increase in heating loads occurs (in reference to the model with no shade, where there is maximum solar gains), comparison of heating loads and electrical lighting increase in comparison to cooling loads savings is presented in Figure 52. The case where the highest increase in heating demand for all types of mesh screens is recorded in Athens at east_90WWR and in Vienna at south_90WWR. In London highest heating loads increases are found at south_90WWR for 35% OAM, east_90WWR for 50% OAM and west_90WWR for 64% OAM. In every occasion the decrease of cooling loads can easily cover the occurred increases in every climatic condition. It is thereby demonstrated that the application of static mesh screens is a rational shading strategy for European climates and it does not increase annual heating demand to such extent that cannot be covered by the savings achieved in cooling demand.

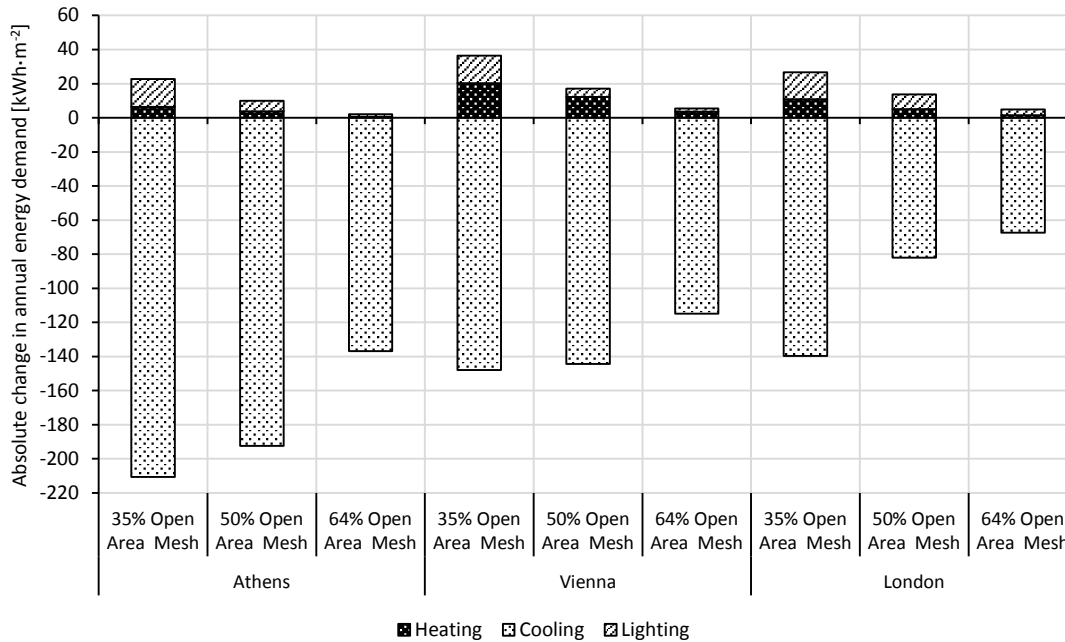


Figure 52. Absolute change in annual energy demand for heating, cooling and electrical lighting

4.3 Summer thermal comfort

For evaluating the potential of the metal mesh screen shading devices to provide a comfortable indoor climate a feasibility study was performed for an office space without active cooling during the summer period and results were presented in section 3.3. The analysis focused on the 50% OAM screen as it is that one that proves more suitable for building shading. Results of section 3.3.1 showed that depending on the climate conditions nighttime natural ventilation for the June-August period can be effective for locations such as Vienna and London, but comfort hours remain at low levels for Athens, even with high night air change rates. Figure 53 presents the range of results of overheating and comfort hours for the selected night ventilation scenarios per location. In Athens, with 8 ACH, comfortable hours have a mean valued of 50% of the time and maximum of 67%, which is calculated for the 30% WWR south facade. Such orientation and WWR has the highest amount of comfortable hours also in Vienna with 2 ACH scenario and London with 1 ACH scenario, nevertheless in these cases maximum values reach 86% and 90% respectively for the selected scenarios and mean values of 73% and 77%. This statistic supports the argument that an office building could function without active cooling, given the fact that the window surface of the facade is not extensive.

Another point that should be stressed is that high night ventilation air change rates (e.g. 8 ACH) can prove counterproductive in summer for Vienna and London by dropping indoor temperature to such extent so that in the morning the space would require heating to reach comfortable levels. However results imply that west and east oriented office spaces with

large exterior glazing surfaces in these climate zones would require higher air change rates than south spaces to achieve a high rate of comfortable hours. For Vienna a night ventilation with 4 ACH and for London with 2 ACH would result in higher rate of comfortable temperatures.

As already stated, south oriented facades in all locations recorded the highest rate of comfortable hours. Charts in Figures 54, 55 and 56 show the cumulative frequency of operative room temperatures for the summer period in the three climate zones for the selected, best performing ventilation scenario per location. If the temperature of 28°C is set as a reference, then it can be observed that in Athens only 36% of the hours are below this limit for the low WWR model and 26% for the high WWR glass curtain wall model. Therefore achieving thermal comfort only by means of metal mesh screen shading in Athens and no active cooling is not possible.

On the other hand, in Vienna 88% of the summer period hours are calculated below 28°C for a 30% WWR facade and 73% for a curtain wall glass system. In London results range from 99% to 89% respectively. These leads to the suggestion that 50% OAM screen can prove beneficial on south facades in central and northern European climates by providing overheating protection and maintaining a comfortable temperature in summer when combined with a suitable night ventilation cooling strategy. This may not eliminate the need of active cooling systems in all cases, but it can decrease it to a large extent.

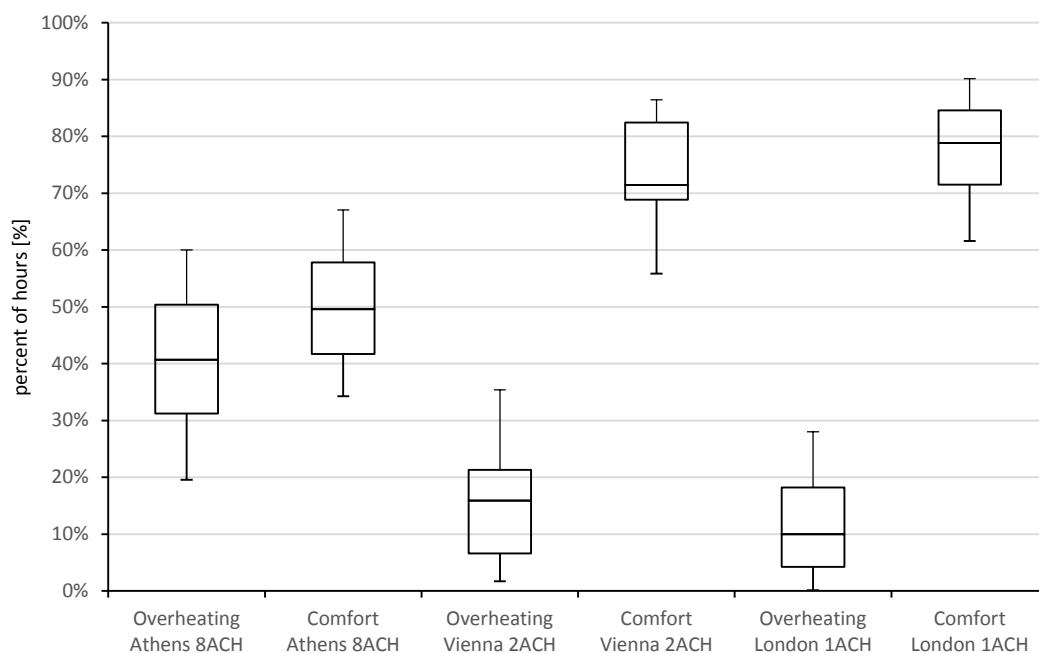


Figure 53. Boxplot of overheating and comfort rates for the selected night ventilation scenarios

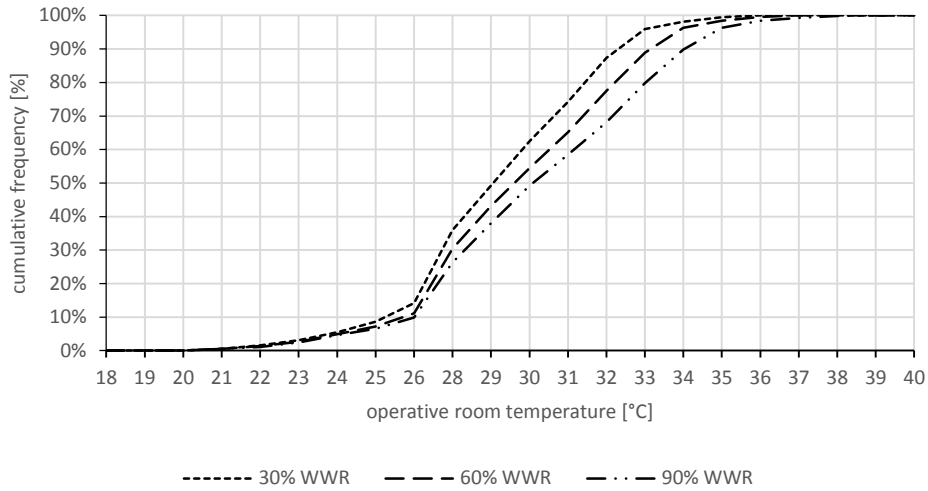


Figure 54. Athens – cumulative frequency of operative room temp. for the summer period (Jun.-Aug.), shading mesh screen with 50% open area on a south facade and 8 ACH night ventilation scenario

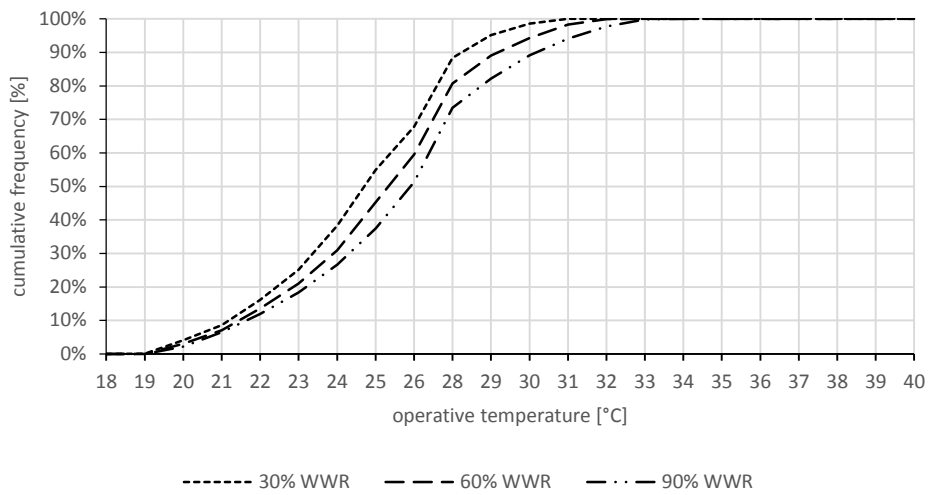


Figure 55. Vienna – cumulative frequency of operative room temp. for the summer period (Jun.-Aug.), shading mesh screen with 50% open area on a south facade and 2 ACH night ventilation scenario

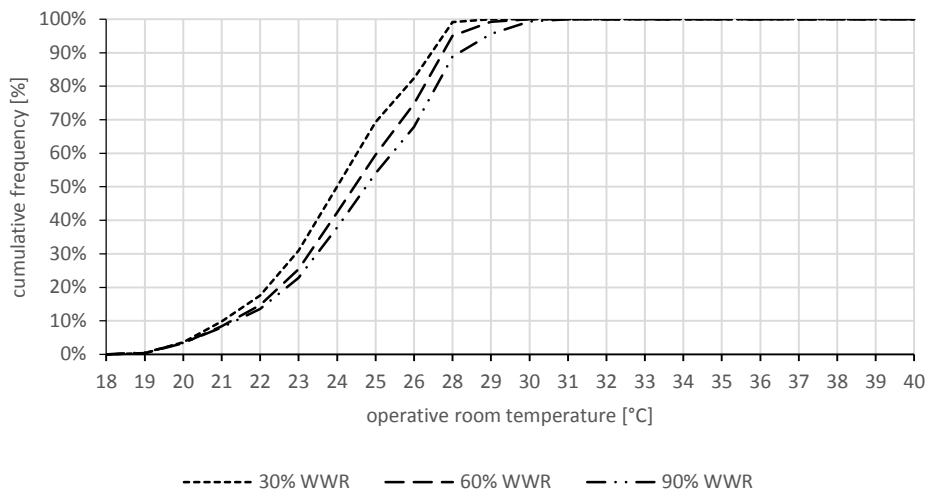


Figure 56. London – cumulative frequency of operative room temp. for the summer period (Jun.-Aug.), shading mesh screen with 50% open area on a south facade and 1 ACH night ventilation scenario

5 CONCLUSION

In the course of this work, the performance of a rather new alternative of solar shading options for non-residential buildings was assessed. Using building performance simulation the study addressed the impact of applying external metal mesh screen shading devices on the energy demand and thermal behavior of a typical office space. The influence of parameters as mesh screen translucency, window to wall ratio and facade orientation was investigated under different European climatic conditions in regards to the annual energy demand for heating, cooling and electrical lighting with daylight control.

Series of simulations were performed using EnergyPlus, taking into account local building construction standards and typical office occupancy and operation schedules. In order to do so an uncertainty analysis was carried out to define the most suitable modelling approach of the shading screens. Since the complicated micro-scale geometry of the meshes cannot be accurately represented in building energy modeling tools, simplifications were made and alternative methods were tested. However this denotes the incapability of actual simulation tools to assess shading systems with complex geometry, which may extend outside of the window frame and simultaneously have an influence on more than one glazing surfaces as well as on opaque facade elements. The analysis led to results that showed similar trends but different actual values. Significant differences were documented in calculating visible transmittance, thus resulting in great variations in the daylight controlled electrical lighting energy demand. On the other hand the distance of the screens from the window had an unnoticeable effect on the results. Lacking experimental physical measurements, a modelling approach was selected based on literature review.

Results indicate that highest energy savings are calculated for South orientations with 50% translucent screens. Facades with large amount of glazing area as curtain wall systems showed the largest potential for energy savings. For East and West orientations of facades with small WWR, a denser screen would be more suitable in southern European climates and contrariwise a more open screen would be advised in central and northern regions. Furthermore the predicted reduction of cooling loads when applying such a shading device can easily cover the increase of annual heating demand and electrical lighting consumption.

Regarding summer indoor climate requirements, comfortable conditions can be passively achieved in central and northern European climates with mesh screen shading and an appropriate night ventilation strategy. On the other hand, results depicted that there is a need of active cooling systems in southern regions, decreasing though cooling demand to a large extent.

Minimal maintenance costs e.g. for cleaning, durability and resistance to weather conditions as well as desire for unobstructed outside views can lead planners to the choice of metal mesh screens in order to realize a solar shading concept with the static character of a second skin facade. The study concludes that the application of such devices can be considered as a sensible alternative and that the permanent character of the construction, affecting solar radiation transmittance all over the year, will not be detrimental to the building performance.

Further research on comparing external mesh screen shades and other common types of commercial building solar control strategies, as exterior blinds, permanent louvers or building overhangs and fins, would provide further information concerning advantages and disadvantages of each approach. However the present study can help planners, who intend to utilize metal mesh screen devices on office building facades, to choose the appropriate application and characteristics of the shade according to climatic criteria and architectural intentions.

6 INDEX

6.1 List of Abbreviations

ACH - Air Changes per Hour

AEC - Architecture, Engineering and Construction

AISI - American Iron and Steel Institute

ASHRAE - American Society of Heating, Refrigerating, and Air-Conditioning Engineers

BRDF - Bi-directional Reflectance Distribution Function

BSDF - Bi-directional Scattering Distribution Function

BTDF - Bi-directional Transmittance Distribution Function

CFD - Computational Fluid Dynamics

CFS - Complex Fenestration System(s)

HVAC - Heating, Ventilation and Air Conditioning

OAM - Open Area Mesh

OIB - Österreichisches Institut für Bautechnik

WWR – Window to Wall Ratio

6.2 List of Figures

Figure 1. National Library of France, Dominique Perrault (1989-1995).....	5
Figure 2. Stainless steel shading mesh screen made of woven wire and rods, Scale 1:2	6
Figure 3. Alpenland office building, St. Pölten – Austria	6
Figure 4. Hospital, Seville – Spain	7
Figure 5. Aedas Holland Park School, London – U.K.	7
Figure 6. Office building, Brest – Northwest France	7
Figure 7. Overview of investigated key-design parameters.....	9
Figure 8. Office occupancy and equipment usage level.....	14
Figure 9. Lighting availability schedule.....	14
Figure 10. Geometry of WindowMaterial:Screen object	15
Figure 11. WINDOW 7.3 perforated screen input characteristics.....	16
Figure 12. Hand-drawn screen geometry.....	17
Figure 13. Analysis factor of scale: Window total transmitted solar radiation.....	18
Figure 14. Window without shading screen: Transmitted solar radiation.....	19
Figure 15. Window with shading screen: Transmitted solar radiation	19
Figure 16. Average monthly daylight illuminance: with and without shading.....	19
Figure 17. Example for modelling position of metal mesh screen shading a. screen created by EPscr or WINscr method, b. normal application of a metal mesh screen, c. surrounding shading surface, d. final mesh screen shading model.....	21
Figure 18. Percent error of WINscr annual heating energy demand in reference to EPscr method	22
Figure 19. Percent error of WINscr annual cooling energy demand in reference to EPscr method	22
Figure 20. Percent error of WINscr annual lighting energy demand in reference to EPscr method	22
Figure 21. Percent error of WINscr total annual energy demand in reference to EPscr method	23
Figure 22. Boxplot of percent error of WINscr total annual energy demand results in reference to EPscr method for four different shading conditions.....	23
Figure 23. Relationship of EPscr and WINscr for space illuminance and transmitted solar radiation from a window with 64% open area mesh screen shading.....	24
Figure 24. Comfort temperature limits for non-mechanically cooled buildings according to EN 15251	27
Figure 25. Athens - annual energy demand of 35% open area shading screen.....	29

Figure 26. Athens - annual energy demand of 50% open area shading screen.....	29
Figure 27. Athens - annual energy demand of 64% open area shading screen.....	29
Figure 28. Athens - annual total energy demand	30
Figure 29. Vienna - annual energy demand of 35% open area shading screen.....	31
Figure 30. Vienna - annual energy demand of 50% open area shading screen.....	31
Figure 31. Vienna - annual energy demand of 64% open area shading screen.....	31
Figure 32. Vienna - annual total energy demand	32
Figure 33. London - annual energy demand of 35% open area shading screen.....	33
Figure 34. London - annual energy demand of 50% open area shading screen.....	33
Figure 35. London - annual energy demand of 64% open area shading screen.....	33
Figure 36. London - annual total energy demand.....	34
Figure 37. Athens - summer thermal comfort for different night ventilation scenarios (June-August), shading mesh screen with 50% open area	36
Figure 38. Vienna - summer thermal comfort for different night ventilation scenarios (June-August), shading mesh screen with 50% open area	36
Figure 39. London - summer thermal comfort for different night ventilation scenarios (June-August), shading mesh screen with 50% open area	36
Figure 40. Athens - summer overheating (June-August), hours exceeding T_{max} ($\Delta T \geq 1$).....	37
Figure 41. Vienna - summer overheating (June-August), hours exceeding T_{max} ($\Delta T \geq 1$).....	37
Figure 42. London- summer overheating (June-August), hours exceeding T_{max} ($\Delta T \geq 1$).....	37
Figure 43. Athens - summer period (June-August) temperature distribution according to EN 15251, shading mesh screen with 50% open area on a south facade and 8 ACH night ventilation scenario.....	39
Figure 44. Vienna - summer period (June-August) temperature distribution according to EN 15251, shading mesh screen with 50% open area on a south facade and 2 ACH night ventilation scenario.....	40
Figure 45. London - summer period (June-August) temperature distribution according to EN 15251, shading mesh screen with 50% open area on a south facade and 1 ACH night ventilation scenario.....	41
Figure 46. Boxplots of total annual energy demand for the three climate zones, with or without window shading.....	43
Figure 47. Distribution of annual energy demand results in the three climate zones	43
Figure 48. Athens - energy savings compared to base cases without shading.....	45
Figure 49. Vienna - energy savings compared to base case without shading	45
Figure 50. London - energy savings compared to base case without shading	45

Figure 51. Boxplots of total annual energy demand for type of mesh screen and climate zone	47
Figure 52. Absolute change in annual energy demand for heating, cooling and electrical lighting.....	48
Figure 53. Boxplot of overheating and comfort rates for the selected night ventilation scenarios.....	49
Figure 54. Athens – cumulative frequency of operative room temp. for the summer period (Jun.-Aug.), shading mesh screen with 50% open area on a south facade and 8 ACH night ventilation scenario	50
Figure 55. Vienna – cumulative frequency of operative room temp. for the summer period (Jun.-Aug.), shading mesh screen with 50% open area on a south facade and 2 ACH night ventilation scenario	50
Figure 56. London – cumulative frequency of operative room temp. for the summer period (Jun.-Aug.), shading mesh screen with 50% open area on a south facade and 1 ACH night ventilation scenario	50
Figure 57. Types of metal mesh screens	63
Figure 58. Reflectance and emittance of building materials	68
Figure 59. Analysis factor of scale: Window Beam Transmitted Solar Radiation Energy	70
Figure 60. Analysis factor of scale: Window Diffuse Transmitted Solar Radiation Energy	70
Figure 61. Percentage difference for annual window total transmitted solar radiation energy between "Shadow Calculation: 1" and "Shadow Calculation: 20" (day interval for shadow calculations in EnergyPlus).....	71
Figure 62. Total Transmitted Solar Radiation Rate per window surface area without additional surrounding shading surfaces	71
Figure 63. Space daylight illuminance	
Figure 64. Total transmitted beam solar radiation rate per window area	
Figure 65. Total transmitted diffuse solar radiation rate per window area	73
Figure 66. Effective Window System Solar Transmittance	74
Figure 67. Effective Window System Solar Reflectance.....	74
Figure 68. Effective Window System Solar Absorbance.....	74
Figure 69. Athens annual heating energy demand of WINscr and EPscr methods.....	75
Figure 70. Athens annual cooling energy demand of WINscr and EPscr methods	75
Figure 71. Athens annual lighting energy demand of WINscr and EPscr methods.....	76
Figure 72. Athens total annual energy demand of WINscr and EPscr methods	76
Figure 73. Vienna annual heating energy demand of WINscr and EPscr methods.....	77
Figure 74. Vienna annual cooling energy demand of WINscr and EPscr methods	77

Figure 75. Vienna annual lighting energy demand of WINscr and EPscr methods	78
Figure 76. Vienna total annual energy demand of WINscr and EPscr methods	78
Figure 77. London annual heating energy demand of WINscr and EPscr methods	79
Figure 78. London annual cooling energy demand of WINscr and EPscr methods	79
Figure 79. London annual lighting energy demand of WINscr and EPscr methods.....	80
Figure 80. London total annual energy demand of WINscr and EPscr methods.....	80

6.3 List of Tables

Table 1. Properties of mesh screen shading material.....	12
Table 2. U-values of external building envelope.....	13
Table 3. Window construction properties	13
Table 4. Average simulation time of modelling - calculation methods	24
Table 5. Suggested applicability of the categories of EN 15251	26
Table 6. Summer thermal comfort for an office space with 50% open area mesh screen shading device: percent of comfort hours according to adaptive comfort model of EN15251 for the June-August period	35
Table 7. Average energy demand and best performing case for the three climate zones.....	42
Table 8. Annual energy savings in comparison to base cases without shading (marked red is the highest reduction achieved)	44
Table 9. Best performing type of screen in terms of energy demand reduction: suggested mesh open area	46
Table 10. Shading device technical data	63
Table 11. Building elements material semantic properties	69
Table 12. Constant properties of simulation models.....	69
Table 13. Analysis of EPscr method about the screen distance from the glazing - EnergyPlus terminates unexpectedly: convergence error in SolveForWindowTemperatures	72

6.4 List of Formulas

Formula 1, T_{rm}	26
Formula 2, T_{conf}	26
Formula 3, ΔT	27

7 LITERATURE

Aebischer, B., Catenazzi, G., and Jakob, M., 2007. Impact of climate change on thermal comfort, heating and cooling energy demand in Europe. In *Proceedings eceee 2007 Summer Study Saving energy – Just do it!*, 4-9 June 2007, La Colle sur Loup, France, pp. 859-870.

ASHRAE, 2001a. *Standard 62-2001. Ventilation for acceptable indoor air quality*. Atlanta, GA: American Society of Heating, Refrigeration and Air Conditioning Engineers.

ASHRAE, 2001b. *Handbook Fundamentals*. Atlanta, GA: American Society of Heating, Refrigerating and Air Conditioning Engineers.

ASHRAE, 2009. *Handbook Fundamentals*. Atlanta, GA: American Society of Heating, Refrigerating and Air Conditioning Engineers.

ASHRAE, 2010. *Standard 90.1-2010*. Atlanta, GA: American Society of Heating, Refrigerating and Air Conditioning Engineers.

Ballard Bell, V., and Rand, P. 2006. *Materials for Architectural Design*. London: Laurence King Publishing Ltd., pp. 185.

Bellia, L., De Falco, F. and Minichiello F., 2013. Effects of solar shading devices on energy requirements of standalone office buildings for Italian climates. *Applied Thermal Engineering* 54 (5), pp. 190-201.

Brownell, B. (ed.), 2006. *Transmaterial: a catalog of materials that redefine our physical environment*. New York: Princeton Architectural Press, pp. 63.

Bueno, B., Wienold, J., Katsifaraki, A., and Kuhn, T.E., 2015. Fener: A Radiance-based modelling approach to assess the thermal and daylighting performance of complex fenestration systems in office spaces. *Energy and Buildings* 94, pp. 10-20.

CEN, 2007. *Standard EN15251: Indoor environmental input parameters for design and assessment of energy performance of buildings addressing indoor air quality, thermal environment, lighting and acoustics*, Brussels: European Committee for Standardisation.

CIBSE, 2013. *CIBSE TM 52: The limits of thermal comfort, avoiding overheating in European buildings*, London: The Chartered Institution of Building Services Engineers.

Crawley, D.B., 1998. Which weather data should you use for energy simulations of commercial buildings?. *Am. Soc. Heat. Refrig. Air Cond. Eng. Trans.*, 104 (2), pp. 498-515.

Dubois, M.-C., 1997. *Solar Shading and Building Energy Use*. Report TABK-97/3049. Lund: Dept. of Building Science, Lund Univ. Quoted in Nikolaou, T., Stavrakakis, G., Skias, I., and Kolokotsa, D., 2007. Contribution of shading in improving the energy performance of

buildings In *2nd PALENC Conference and 28th AIVC Conference on Building Low Energy Cooling and Advanced Ventilation Technologies in the 21st Century*. Crete: Ilioptopos Synedreia, pp. 718-722.

Eskeland, G.S. and Mideksa, T.K., 2010. Electricity demand in a changing climate. *Mitigation and Adaptation Strategies for Global Change* 15 (8), pp. 877-897.

European Commission, 2015. Buildings. <<https://ec.europa.eu/energy/en/topics/energy-efficiency/buildings>> accessed 09.09.2015.

Fernandes, L.L., Lee, E.S., McNeil, A., Jonsson, J.C., Nouidui, T., Pang, X., and Hoffmann, S., 2015. Angular selective window systems: Assessment of technical potential for energy savings. *Energy and Buildings* 90, pp. 188-206.

GeoDict, 2015. <<http://www.geodict.com/Solutions/aboutGD.php>> accessed 02.06.2015.

Givoni, B., 1998. *Climate Considerations in Building and Urban Design*. USA: John Wiley & Sons.

GKD Creativeweave, 2015. Mesh types. <<http://www.gkd.de/en/architectural-mesh/mesh-types.html>> accessed 11.10.2015.

GKD Metalfabrics, 2015. Metalfabrics. <<http://www.gkdmalfabrics.com/metalfabrics.html>> accessed 11.10.2015.

Greek Government Gazette, 2010. FEK 407/2010 Regulation on the Energy Performance of Buildings – KENAK. Athens: National Printing Office.

Halawa, E., and Van Hoof, J., 2012. The adaptive approach to thermal comfort: A critical overview. *Energy and Buildings* 51, pp. 101-110.

Haver and Boecker Wire Weaving Division, 2014. Architectural wire mesh. <<http://www.diedrahtweber.com/en/applications-products/architectural-wire-mesh/facade/sun-protection.html>> accessed 30.01.2014.

HM Government, 2013. *Building Regulations Part L2A Conservation of Fuel and Power in new buildings other than dwellings*. UK: NBS-RIBA Enterprises Ltd.

Hunn, B.D., Grasso, M.M., Jones, J.W., and Hitzfelder J.D., 1993. Effectiveness of Shading Devices on Buildings in Heating Dominated Climates. *ASHRAE Trans.* 99 (1), pp. 207-222. Quoted in Nikolaou, T., Stavrakakis, G., Skias, I., and Kolokotsa, D. 2007. Contribution of shading in improving the energy performance of buildings In *2nd PALENC Conference and 28th AIVC Conference on Building Low Energy Cooling and Advanced Ventilation Technologies in the 21st Century*. Crete: Ilioptopos Synedreia, pp. 718-722.

- Klems, J., 1994. A new method for predicting the solar heat gain of complex fenestration systems. I Overview and derivation of the matrix layer calculation. *Am. Soc. Heat. Refrig. Air Cond. Eng. Trans.*, 100 (1), pp. 1065–1072.
- Lam, T.C., Ge, H., and Fazio, P., 2014. Study of different glazing modelling approaches in assessing energy performance of curtain wall systems using EnergyPlus. In: *IBPSA-Canada eSIM 2014 Conference Proceedings*, 7-10 May 2014, Ottawa, Canada.
- LBNL, 2014. Lawrence Berkeley National Laboratory WINDOW 7.3. <<https://windows.lbl.gov/software/window/window.html>> accessed 17.02.2015.
- Lee, E.S. and Tavit, A., 2007. Energy and visual comfort performance of electrochromic windows with overhangs. *Building and Environment* 42 (6), pp. 2439-2449.
- Lee, E.S., DiBartolomeo, D.L. and Selkowitz, S.E., 1998. Thermal and daylighting performance of an automated Venetian blind and lighting system in a full-scale private office. *Energy and Buildings* 29 (12), pp. 47-63.
- Littlefair, P., Ortiz, J. and Das-Bhaumik, C., 2010. A simulation of solar shading control on UK office energy use. *Building Research and Information* 38 (10), pp. 638-646.
- Lyons, P., Wong, J., and Bhandari, M., 2010. A comparison of window modelling methods in EnergyPlus 4.0. In: *IBPSA-USA 4th SimBuild Conference Proceedings*, 11-13 August 2010, New York City, pp. 177-184.
- Mitchell, R. et al., 2013. THERM 6.3 / WINDOW 6.3 NFRC Simulation Manual. <<https://windows.lbl.gov/software/NFRC/SimMan/NFRCsim6.3-2013-07-Manual.pdf>> accessed 28.08.2015.
- Molina, G., Bustamante, W., Rao, J., Fazio, P., & Vera, S., 2015. Evaluation of radiance's genBSDF capability to assess solar bidirectional properties of complex fenestration systems. *Journal of Building Performance Simulation* 8 (4), pp. 216-225.
- Nicol, F., and Humphreys, M., 2010. Derivation of the adaptive equations for thermal comfort in free-running buildings in European standard EN15251. *Building and Environment* 45 (1), pp. 11-17.
- Österreichisches Institut für Bautechnik (OIB), 2011. *OIB-Richtlinie 6: Energieeinsparung und Wärmeschutz*.
- Palmero-Marrero, A.I. and Oliveira, A.C., 2010. Effect of louver shading devices on building energy requirements. *Applied Energy* 87 (6), pp. 2040-2049.

Peel, M.C., Finlayson, B.L., and McMahon, T. A., 2007. Updated world map of the Köppen-Geiger climate classification. *Hydrology and Earth System Sciences Discussions* 4(2), pp. 439-473.

Sherif, A., El-Zafarany, A. and Arafa. R., 2012. External perforated window Solar Screens: The effect of screen depth and perforation ratio on energy performance in extreme desert environments. *Energy and Buildings* 52 (9), pp. 1-10.

Simmler H. and Binder B., 2008. Experimental and numerical determination of the total solar energy transmittance of glazing with venetian blind shading. *Building and Environment* 43 (2), pp. 197-204.

Treado, S., Barnett, J., and Remmert, W., 1984. Effectiveness of Solar Shading for an Office Building. NBS Building Science Series 161. Washington: National Bureau of Standards. Quoted in Nikolaou, T., Stavrakakis, G., Skias, I., and Kolokotsa, D., 2007. Contribution of shading in improving the energy performance of buildings In 2nd PALENC Conference and 28th AIVC Conference on Building Low Energy Cooling and Advanced Ventilation Technologies in the 21st Century. Crete: Ilioptopos Synedreia, pp. 718-722.

Tsangrassoulis, A., Santamouris, M. and Asimakopoulos, D., 1996. Theoretical and experimental analysis of daylight performance for various shading systems. *Energy and Buildings* 24 (10), pp. 223-230.

Tzempelikos, A. and Athienitis, A.K., 2007. The impact of shading design and control on building cooling and lighting demand. *Solar Energy* 81 (3), pp. 369-382.

Ürge-Vorsatz, D., Cabeza, L.F., Serrano, S., Barreneche, C., and Petrichenko, K., 2015. Heating and cooling energy trends and drivers in buildings. *Renewable and Sustainable Energy Reviews* 41 (1), pp. 85-98.

U.S. Department of Energy, 2013a. *EnergyPlus Input-Output Reference - The encyclopedic reference to EnergyPlus input and output*. Washington, DC: U.S. Department of Energy, pp. 125-130.

U.S. Department of Energy, 2013b. *EnergyPlus Engineering Reference - The reference to EnergyPlus calculations*. Washington, DC: U.S. Department of Energy, pp. 316.

U.S. Department of Energy, 2015. Weather Data. <http://apps1.eere.energy.gov/buildings/energyplus/weatherdata_about.cfm;jsessionid=5D2362036DDEC6E2C47E2C0172019B58.eere?CFID=4040361&CFTOKEN=f86c185c8a41b8b2-5E91E33D-AE06-D154-EF1EBE8AEAEED5D0> accessed 02.02.2015.

US Department of Energy, EnergyPlus. <<https://energyplus.net/>> accessed 02.02.2015.

U.S. Energy Information Administration, 2015. How much energy is consumed in residential and commercial buildings in the United States?. <<http://www.eia.gov/tools/faqs/faq.cfm?id=86&t=1>> accessed 28.09.2015.

Watts, A., 2011. *Modern Construction Envelopes*. Vienna: Springer WienNewYork, pp. 54-63.

Zumtobel, 2013. *The lighting handbook*. 4th ed. Dornbirn: Zumtobel Lighting GmbH.

APPENDIX

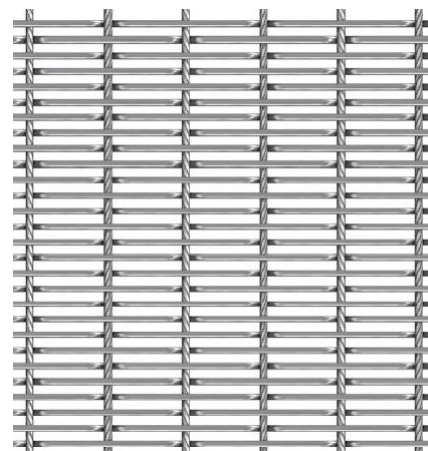
A. Metal mesh screen technical characteristics

Table 10. Shading device technical data

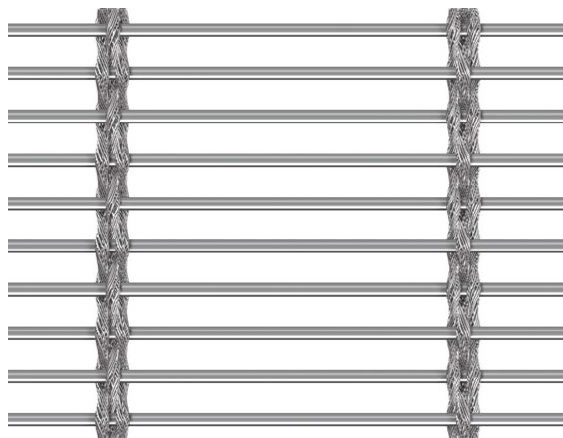
Type	Omega 1510	Omega 1520	Tigris
Manufacturer	GKD	GKD	GKD
Material	AISI Type 316 Stainless Steel	AISI Type 316 Stainless Steel	AISI Type 316 Stainless Steel
Open area	ca. 35.4%	ca. 50.6%	ca. 64.1%
Wire diameters			
cable	2 mm	2 mm	3 x 2 mm
rod	1.5 mm	1.5 mm	2 mm
Cable pitch	17.5 mm	17.5 mm	80 mm
Weft wire pitch	2.5 mm	3.5 mm	10 mm
Thickness	ca. 4.5 mm	ca. 4.5 mm	ca. 6.2 mm
Weight	ca. 6.65 kg·m ⁻²	ca. 5.2 kg·m ⁻²	ca. 6 kg·m ⁻²
Maximum mesh width	8 m	8 m	8 m
Standard mesh width		6 m	6 m
Standard fixing detail	inserted round bar with eye-bolts	inserted round bar with eye-bolts	inserted round bar with eye-bolts



OMEGA 1510



OMEGA 1520

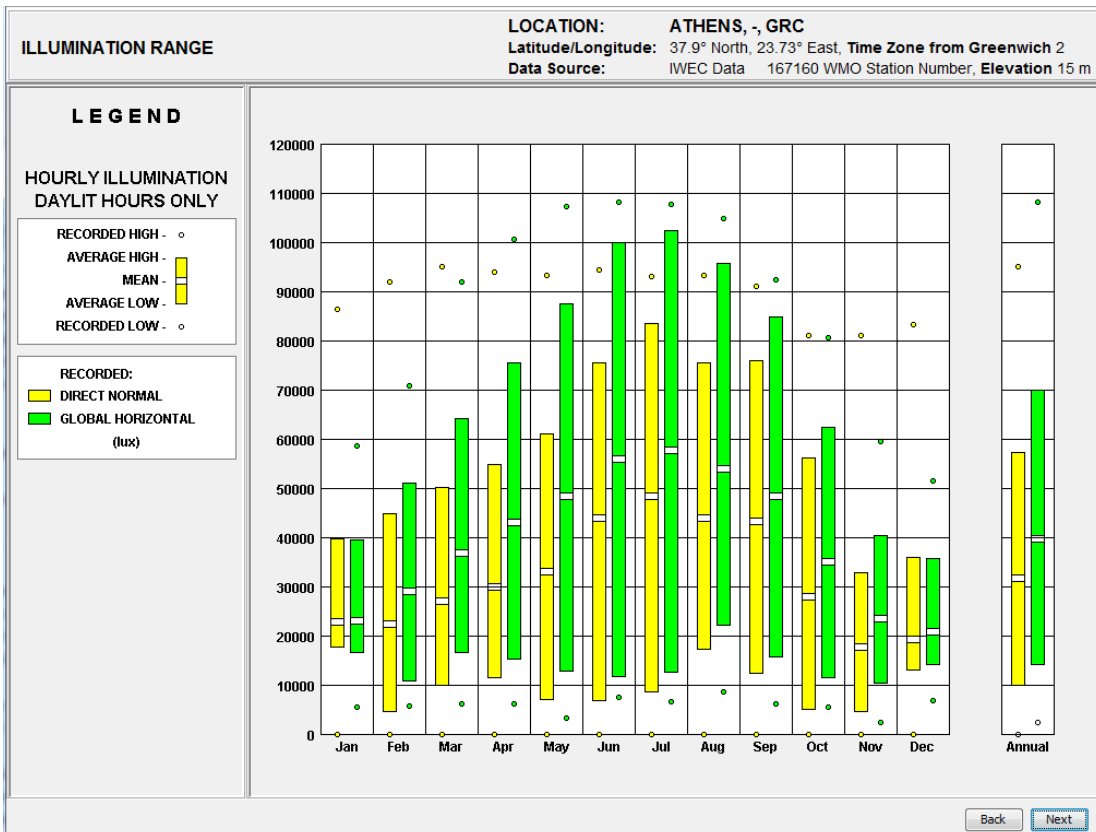
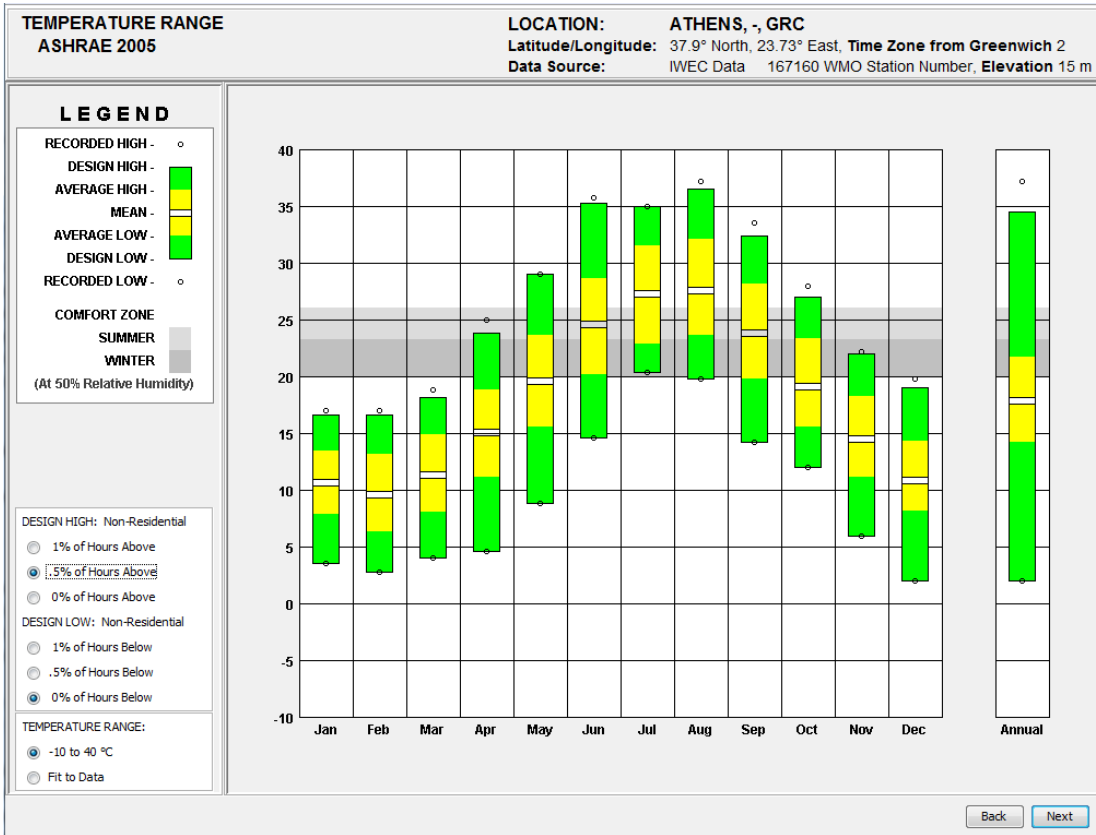


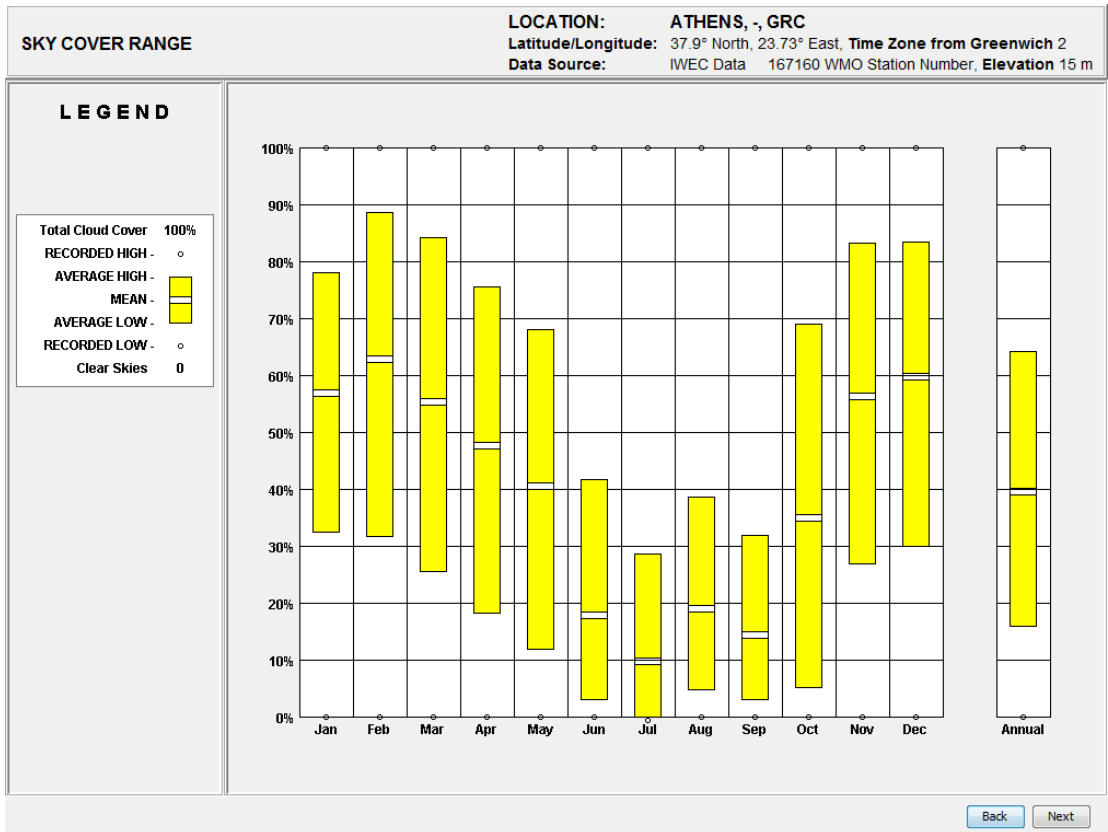
TIGRIS

Figure 57. Types of metal mesh screens

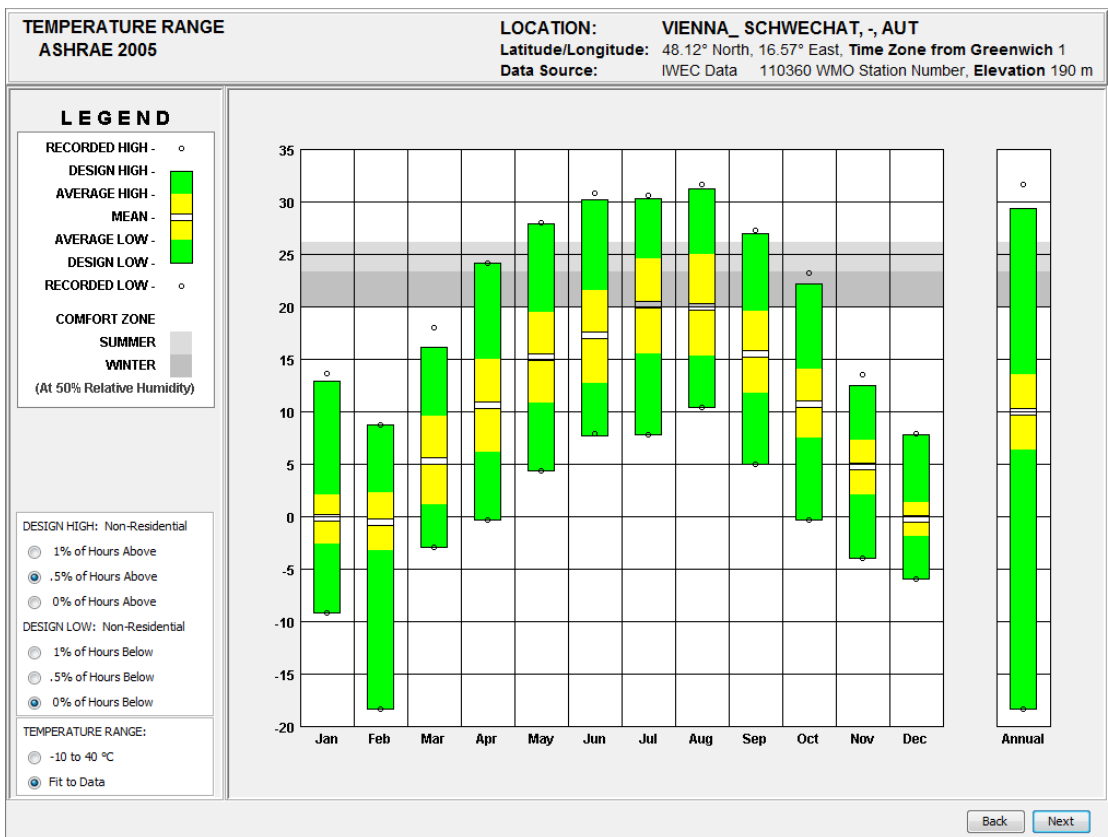
B. Climate data

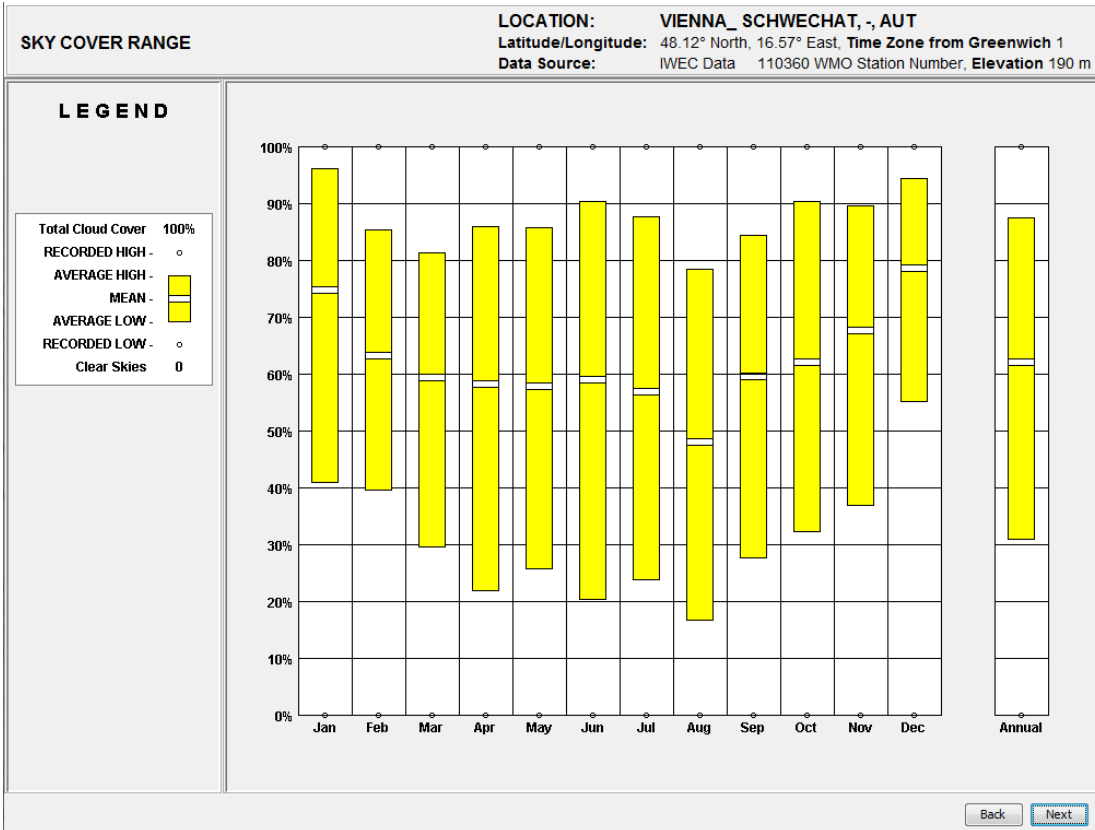
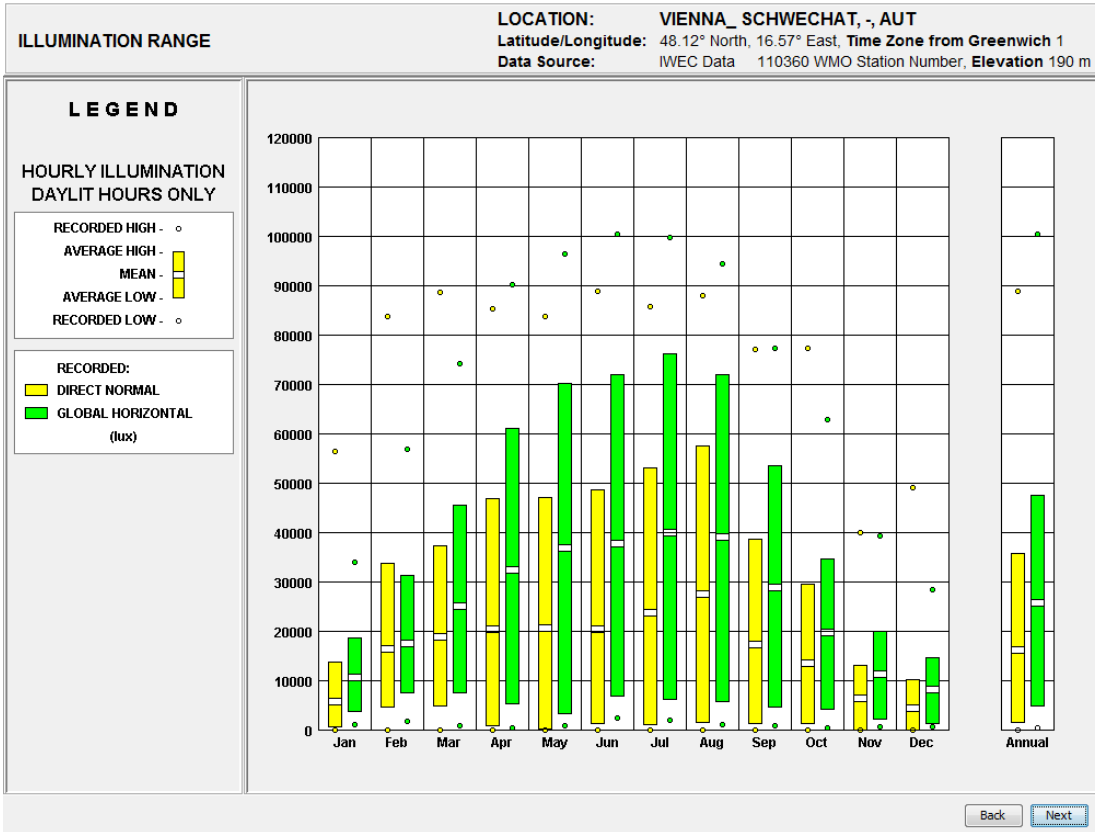
Location Athens



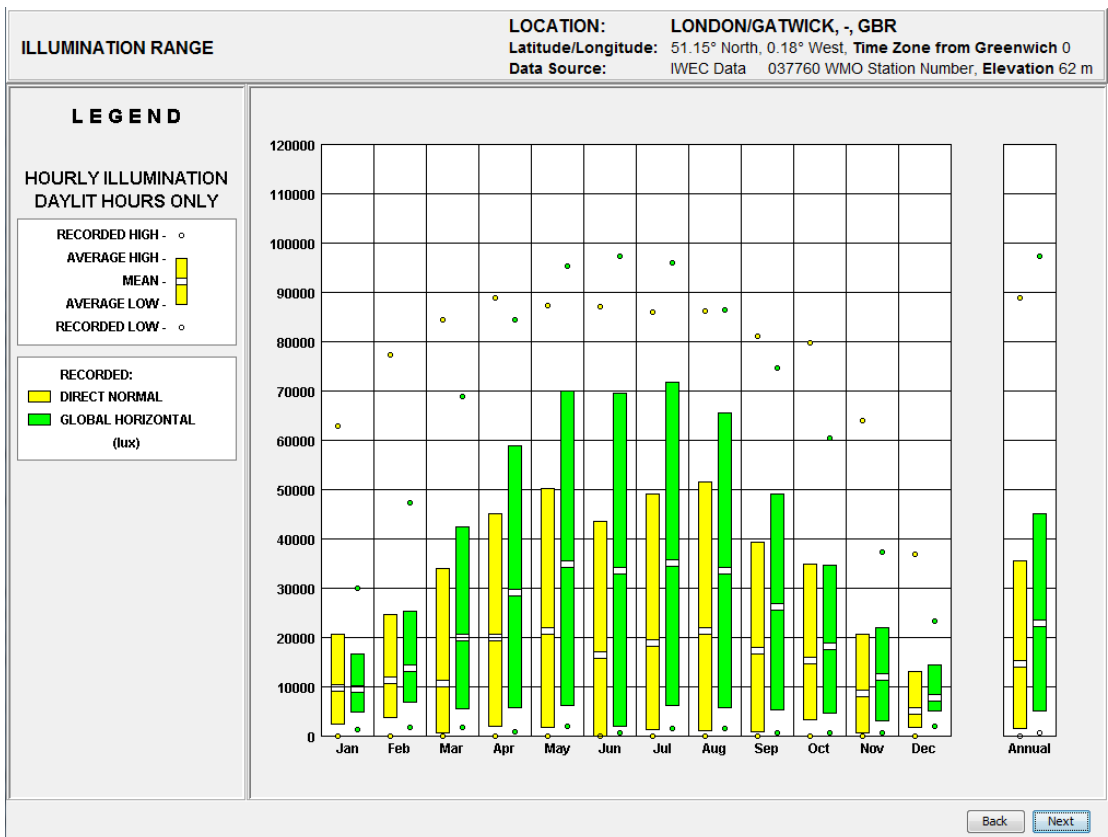
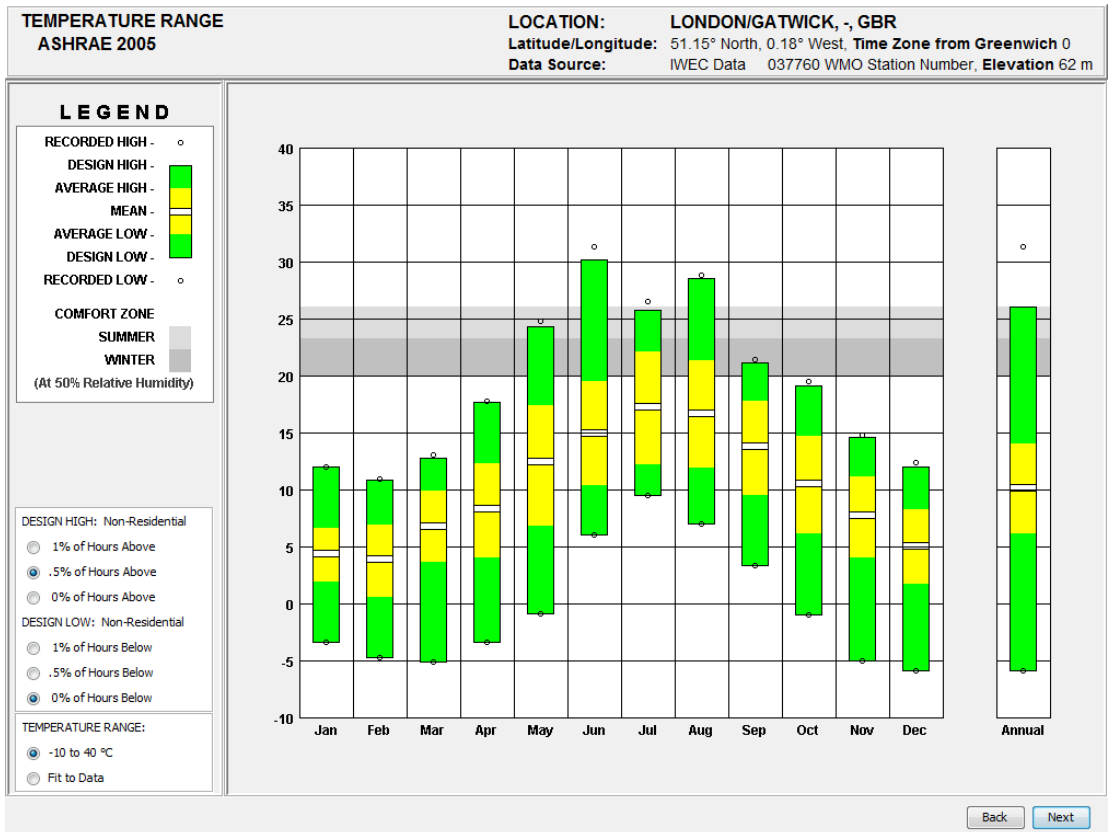


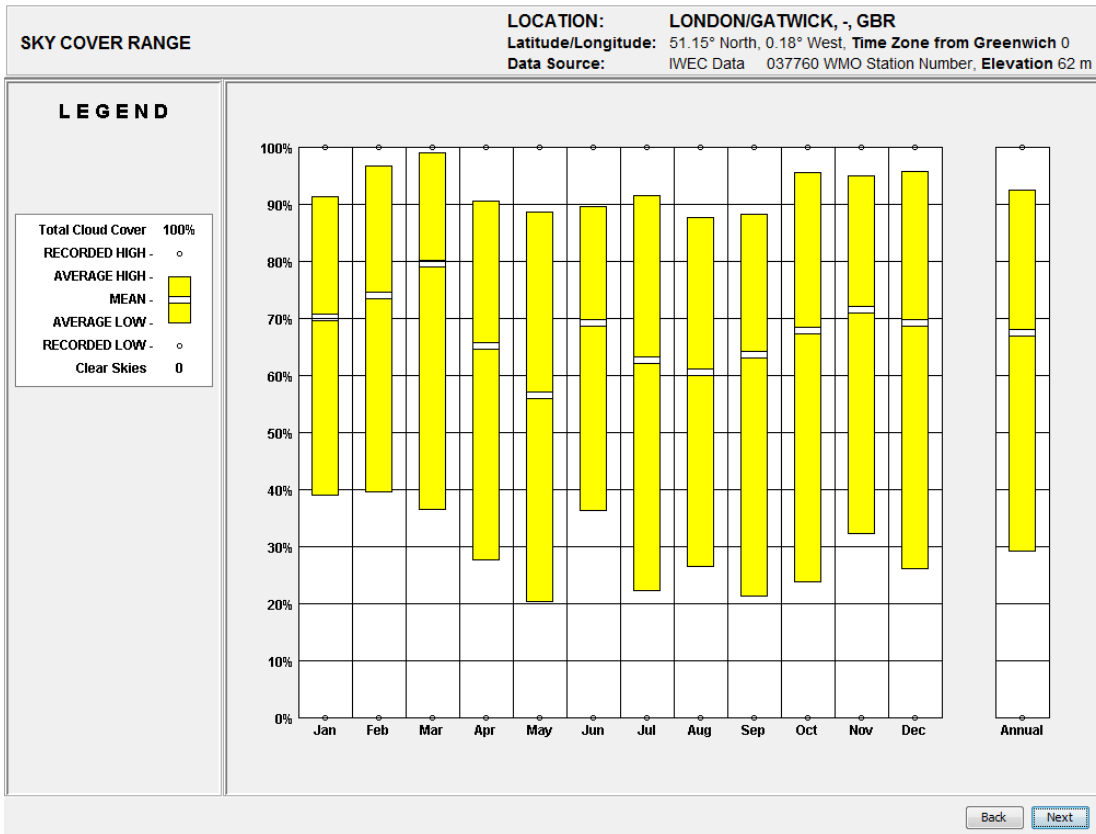
Location Vienna



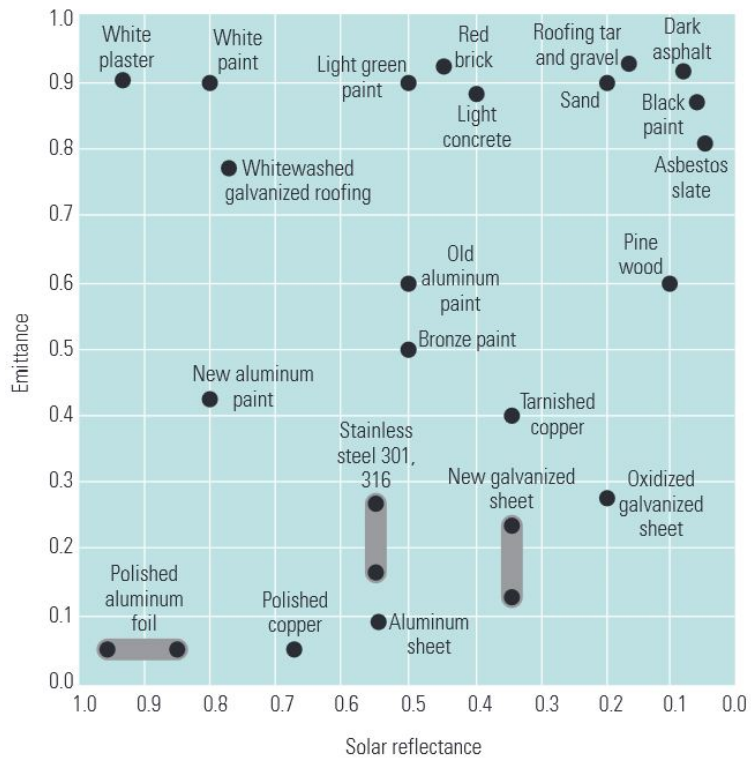


Location London





C. EnergyPlus simulation parameters



Courtesy: Florida Solar Energy Center

Figure 58. Reflectance and emittance of building materials

Table 11. Building elements material semantic properties

Building element	Material	Thickness "d" [m]	Conductivity "λ" [W·m ⁻¹ ·K ⁻¹]	Specific heat capacity "c" [J·kg ⁻¹ ·K ⁻¹]	Density „ρ“ [kg·m ⁻³]	Thermal resistance [m ² ·K·W ⁻¹]
Exterior Wall ATH - GR	Clinker	0.12	0.96	1000	2000	
	Air cavity	0.04				0.15
	XPS insulation	0.05	0.037	1400	30	
	Vertically perforated brick	0.20	0.39	1000	1000	
	Lime plaster	0.015	0.87	1000	1400	
Exterior Wall VIE -AT LON - UK	Clinker	0.12	0.96	1000	2000	
	Air cavity	0.04				0.15
	PE film	0.008	0.27	1000	800	
	Glasswool WLG035	0.25	0.035	800	20	
	Honeycomb porous brick	0.20	0.27	1000	800	
	Lime plaster	0.015	0.87	1000	1400	

Table 12. Constant properties of simulation models

EnergyPlus Simulation Parameters	
Version	8.1
Terrain	City
Loads convergence tolerance value	0.04
Temperature convergence tolerance value	0.4 Δ °C
Solar distribution	Full exterior with reflections
Shadow calculation method	Average over days in frequency
Shadow calculation frequency	20
Maximum figures in shadow overlap calculations	150000
Shadow polygon clipping algorithm	Sutherland Hodgman
Sky diffuse modeling algorithm	Simple sky diffuse modeling
Inside surface convection algorithm	TARP
Outside surface convection algorithm	DOE-2
Heat balance algorithm	Conduction transfer function
Surface temperature upper limit	2000 °C
Minimum surface convection heat transfer coefficient	0.1 W·m ⁻² ·K ⁻¹
Maximum surface convection heat transfer coefficient	0.1 W·m ⁻² ·K ⁻¹
Simulation timesteps per hour	6

D. Uncertainty analysis of modelling methods

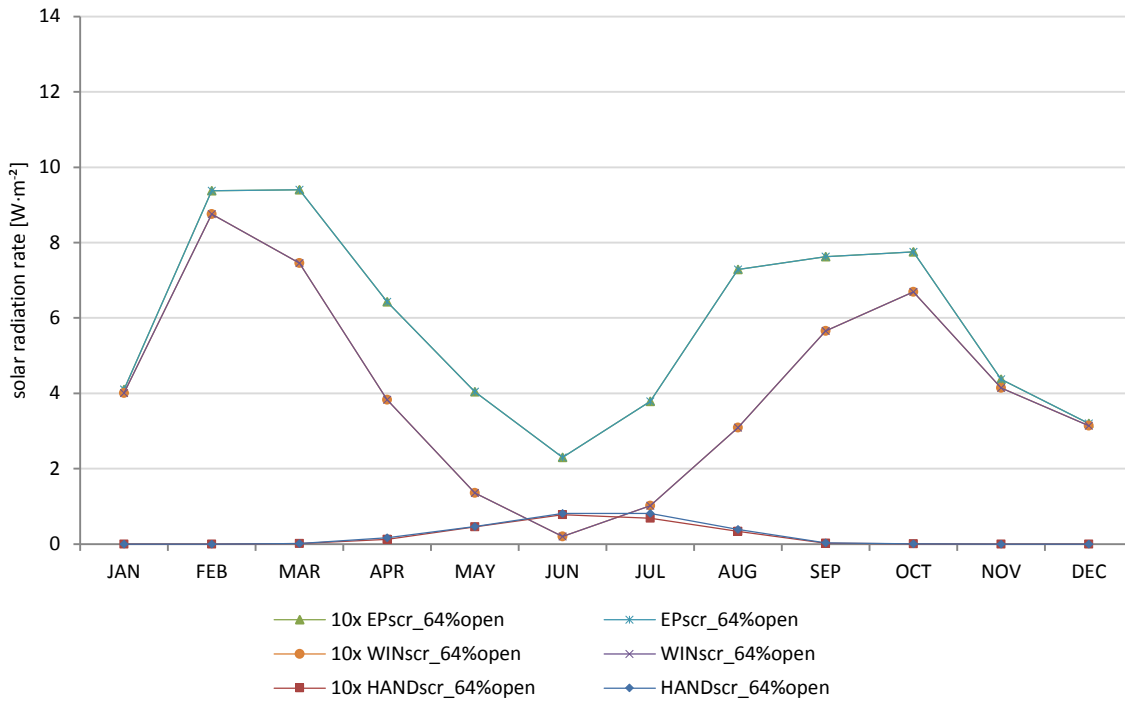


Figure 59. Analysis factor of scale: Window Beam Transmitted Solar Radiation Energy

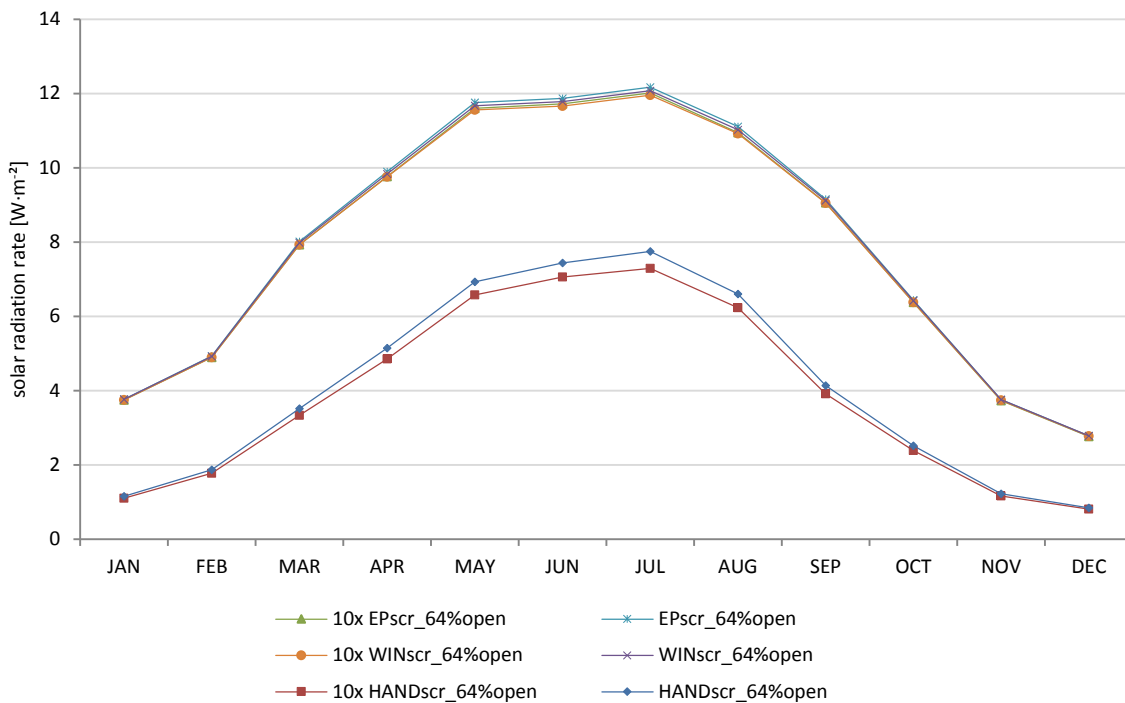


Figure 60. Analysis factor of scale: Window Diffuse Transmitted Solar Radiation Energy

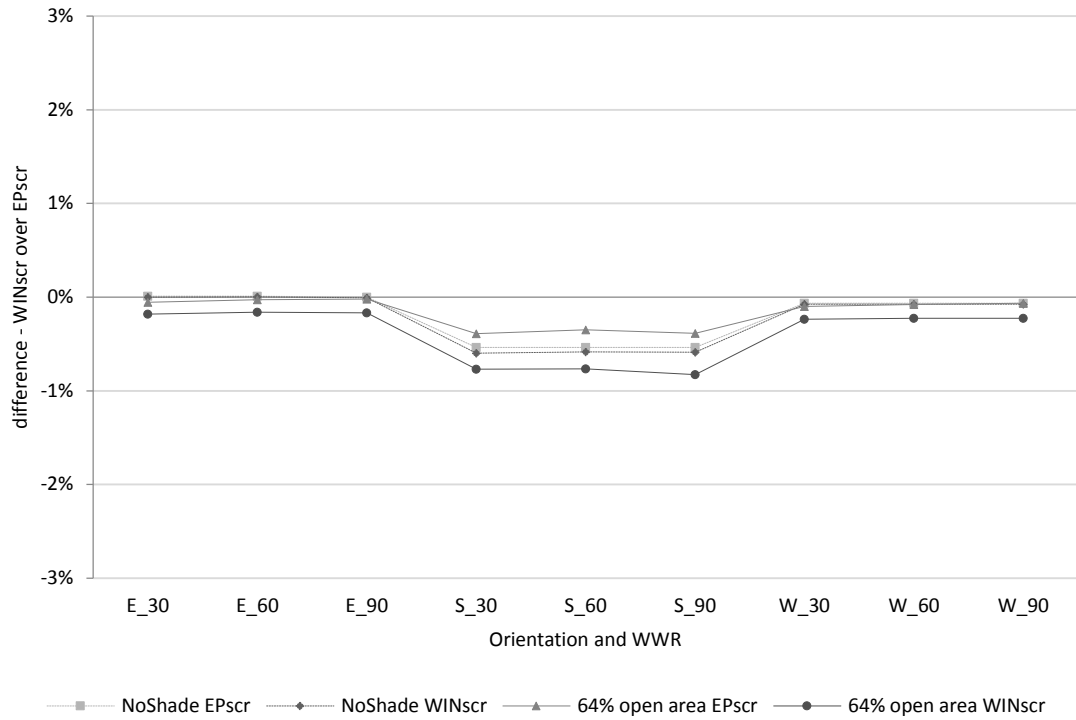


Figure 61. Percentage difference for annual window total transmitted solar radiation energy between "Shadow Calculation: 1" and "Shadow Calculation: 20" (day interval for shadow calculations in EnergyPlus)

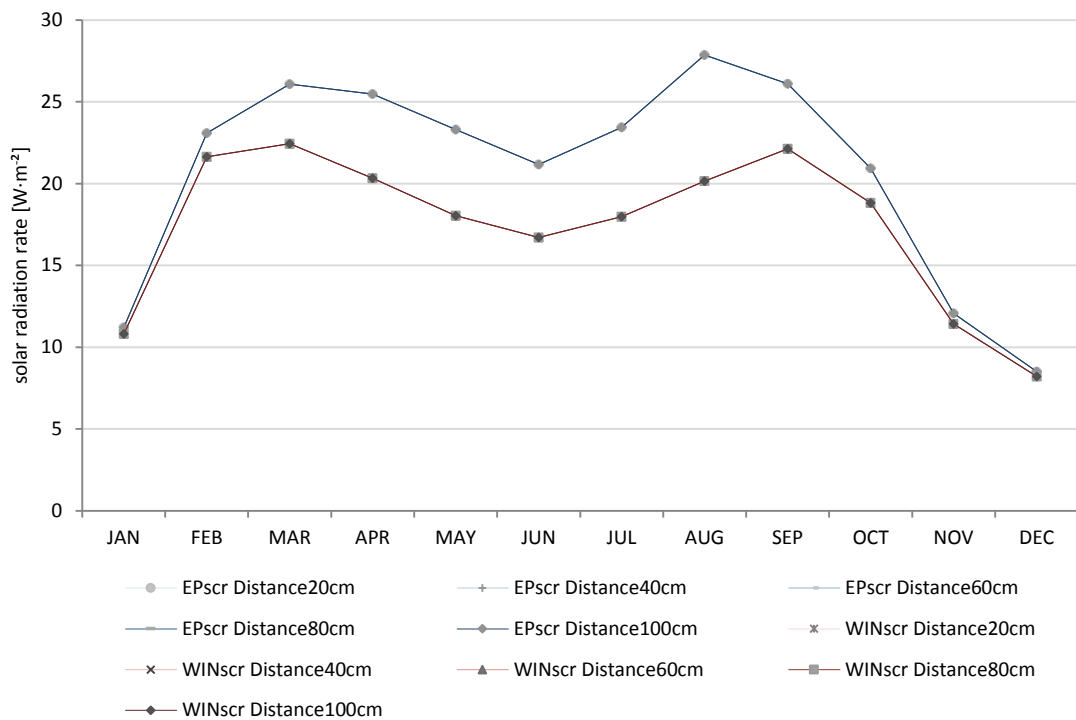


Figure 62. Total Transmitted Solar Radiation Rate per window surface area without additional surrounding shading surfaces

Detailed results for solar transmittance and optical performance of the window-shading system in one summer month

Screen at 45 cm, South, 90% WWR, Vienna, 64% Open Area Mesh, month: June

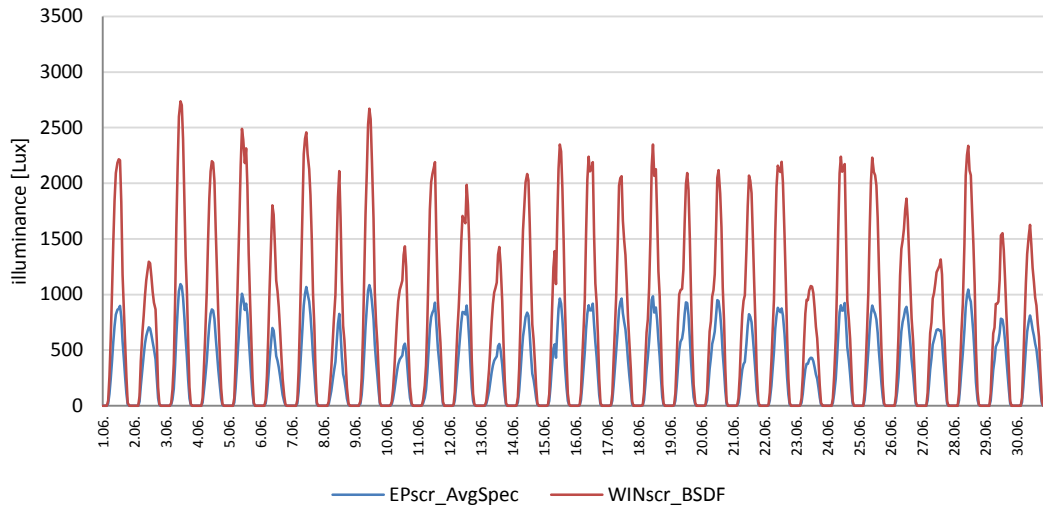


Figure 63. Space daylight illuminance

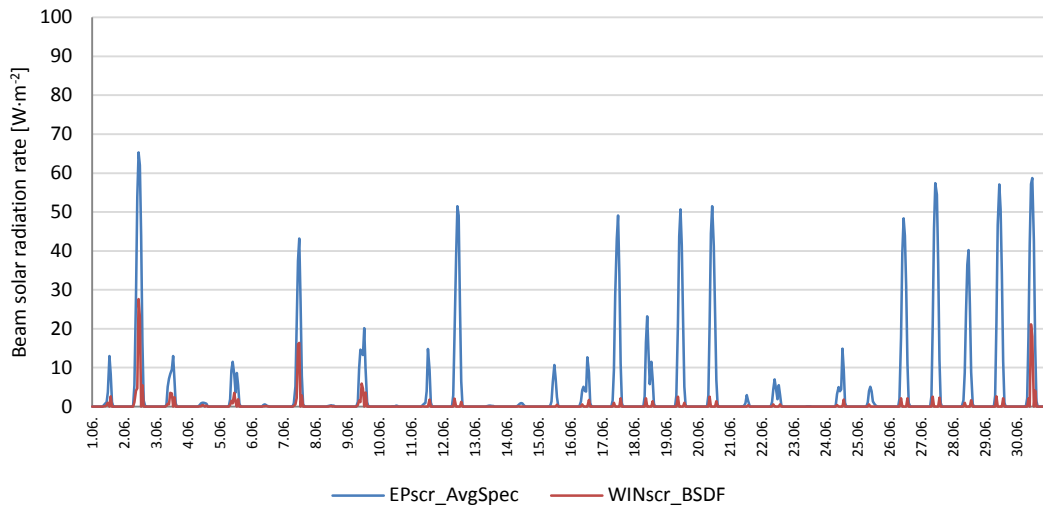


Figure 64. Total transmitted beam solar radiation rate per window area

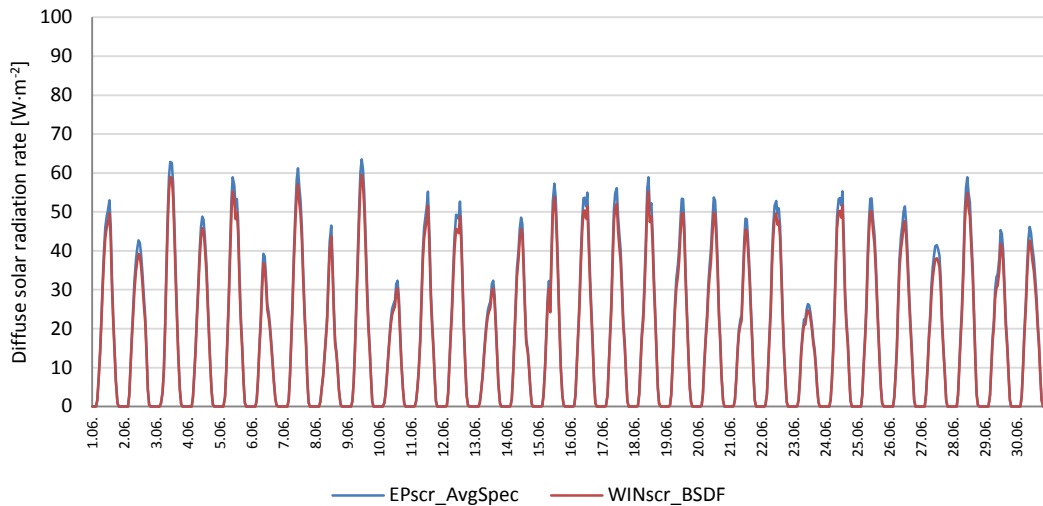


Figure 65. Total transmitted diffuse solar radiation rate per window area

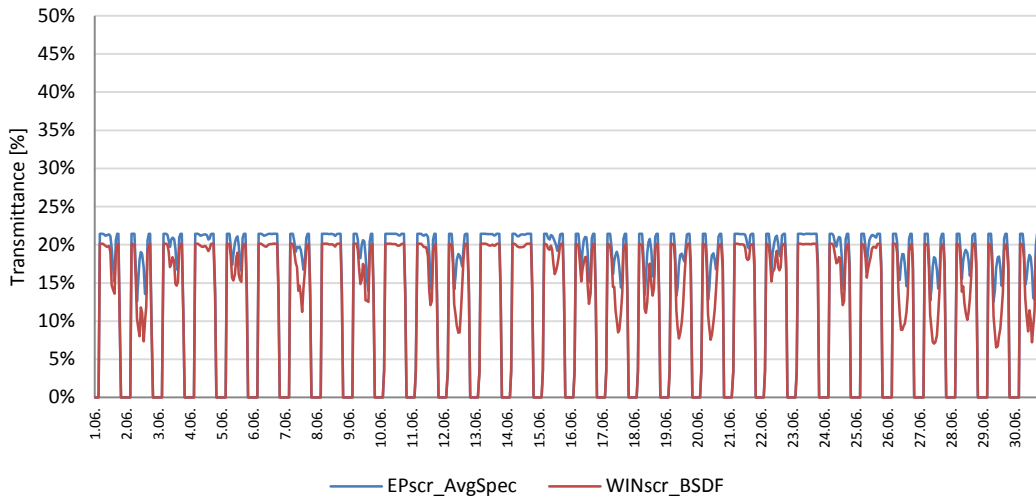


Figure 66. Effective Window System Solar Transmittance

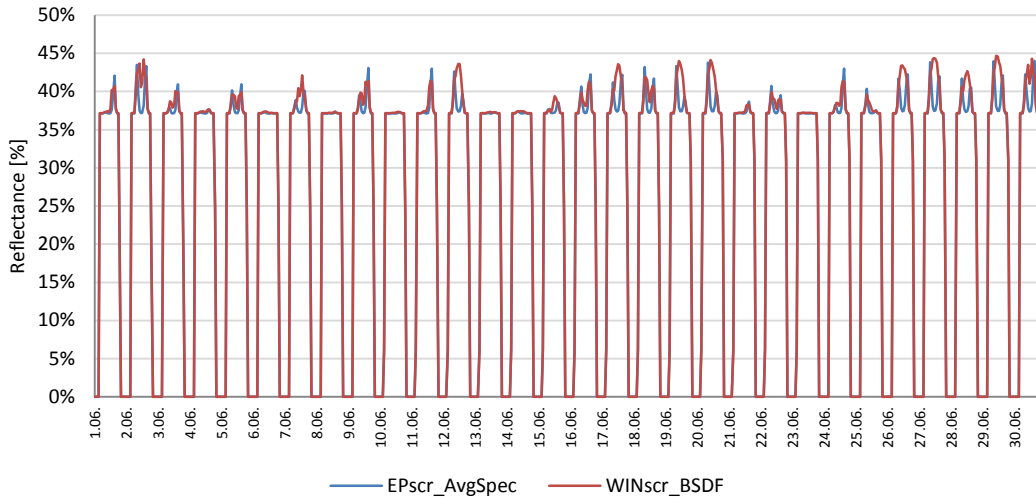


Figure 67. Effective Window System Solar Reflectance

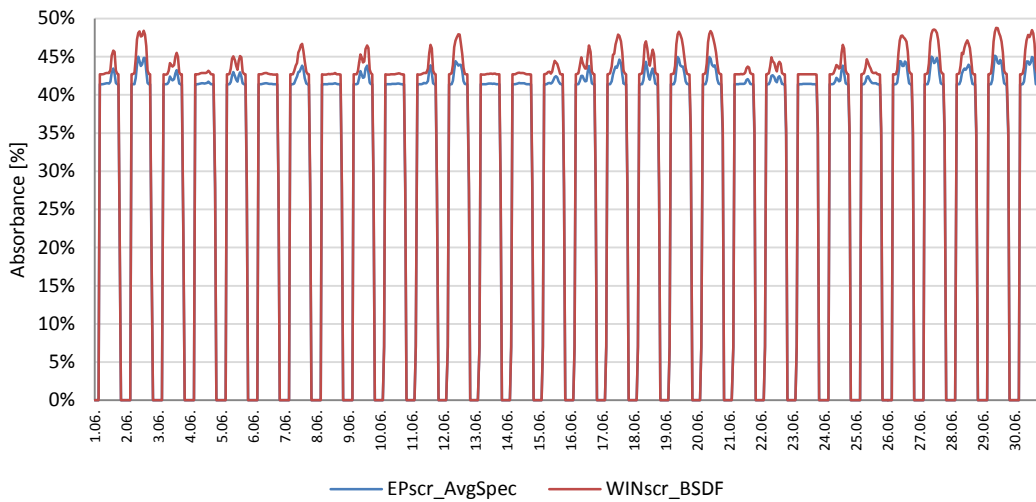


Figure 68. Effective Window System Solar Absorbance

E. Energy performance results for WINscr and EPscr methods

Location Athens



Figure 69. Athens annual heating energy demand of WINscr and EPscr methods

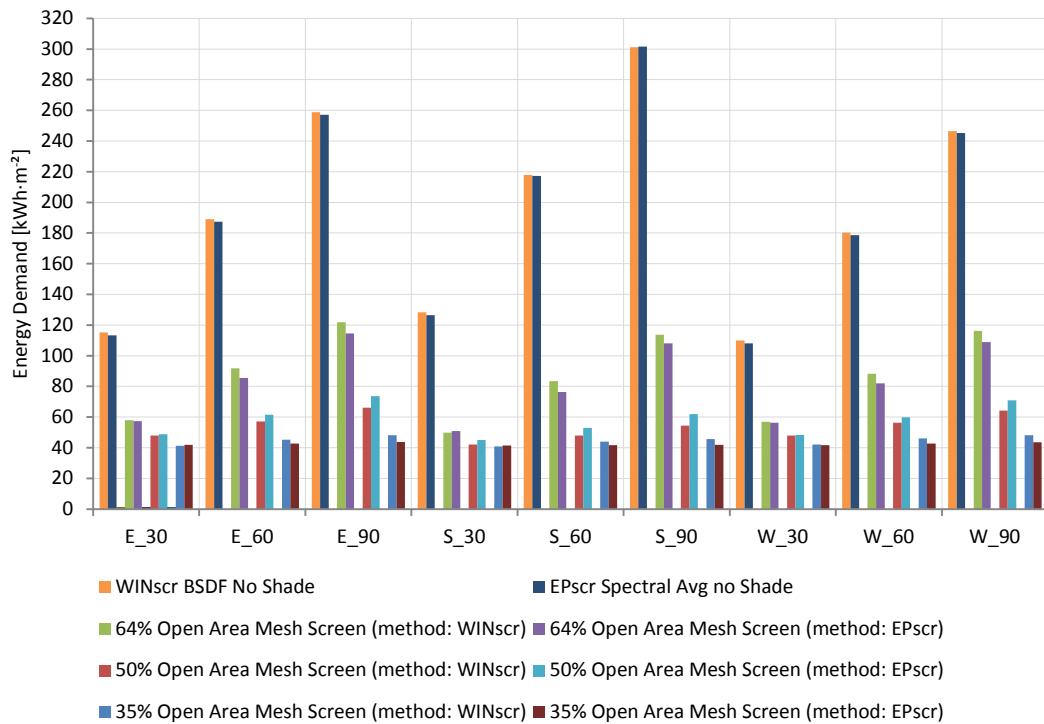


Figure 70. Athens annual cooling energy demand of WINscr and EPscr methods

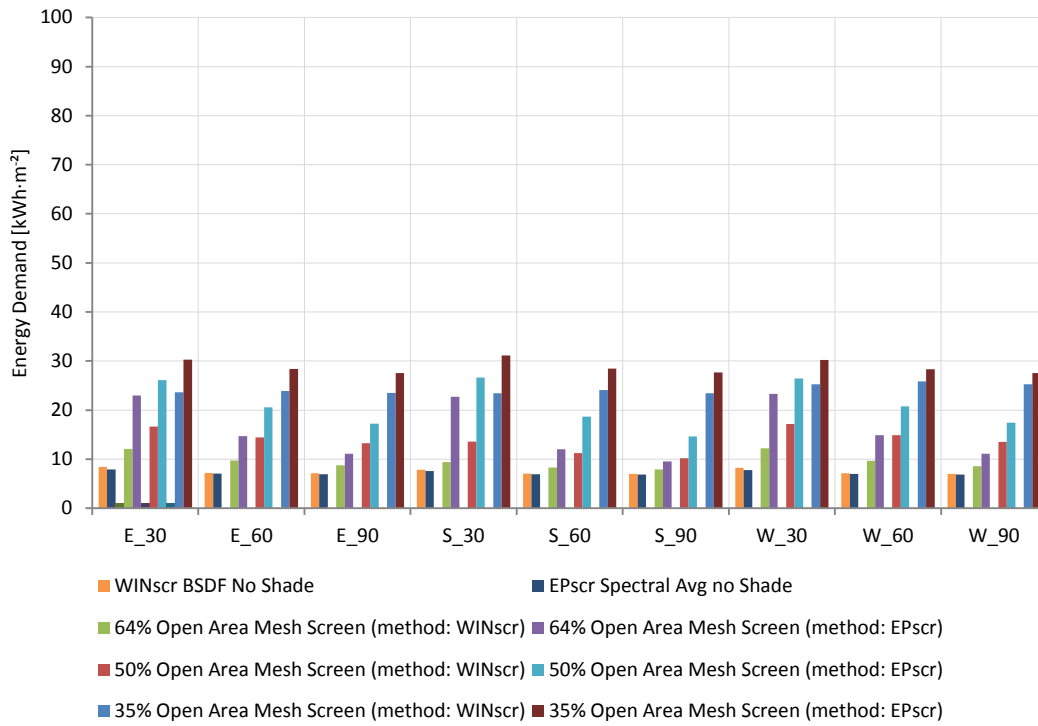


Figure 71. Athens annual lighting energy demand of WINscr and EPscr methods

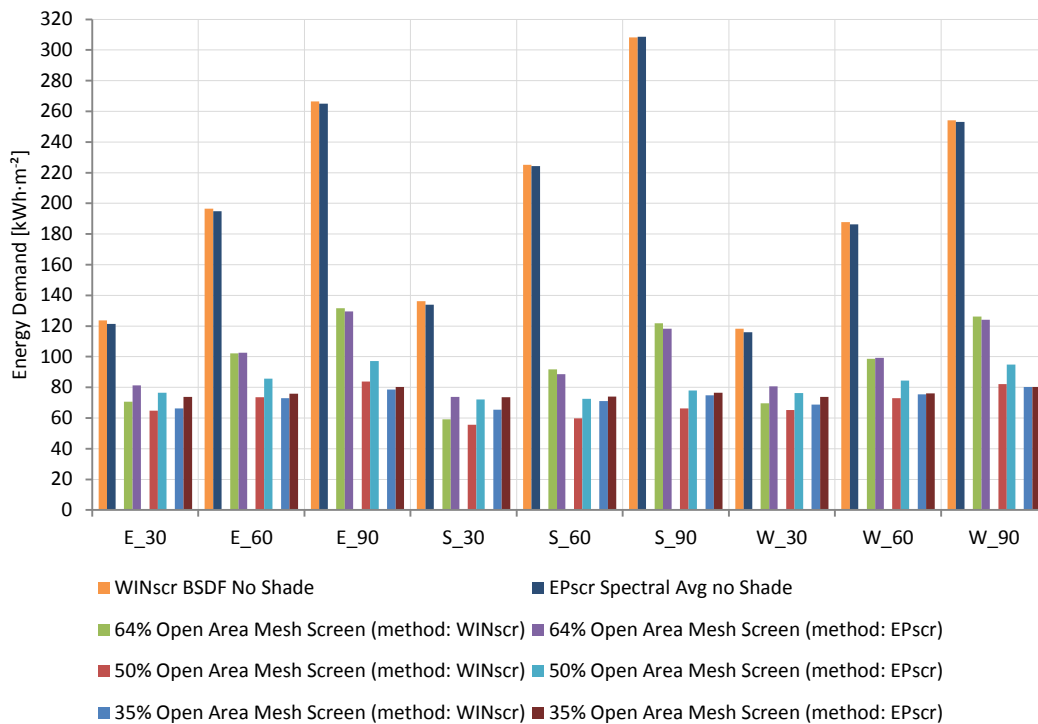


Figure 72. Athens total annual energy demand of WINscr and EPscr methods

Location Vienna

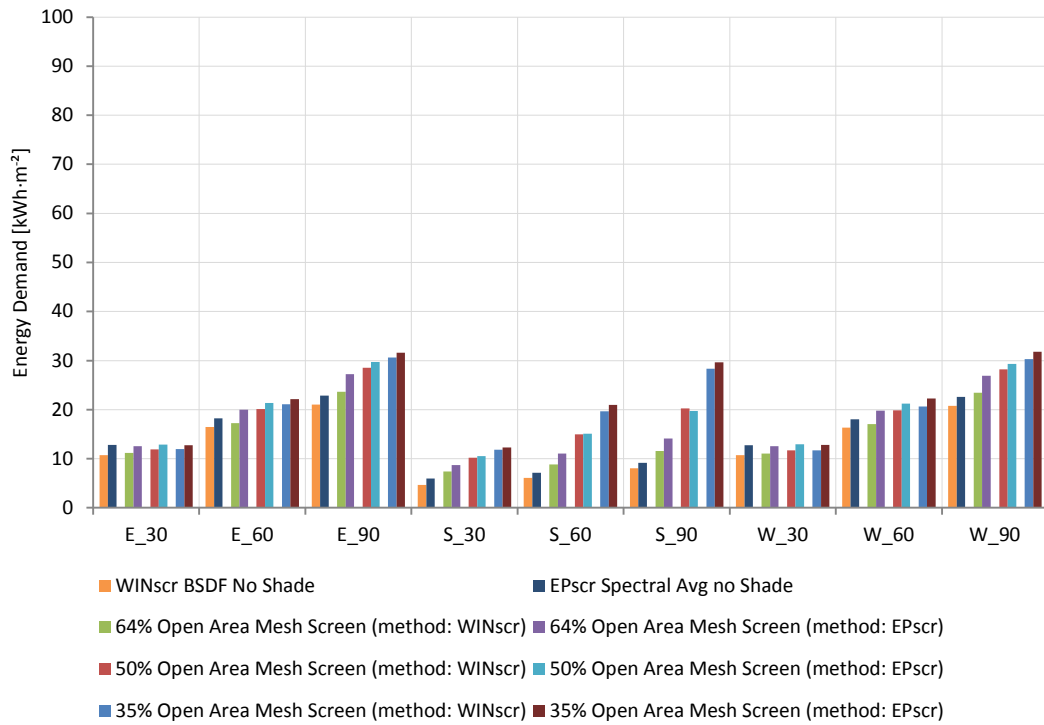


Figure 73. Vienna annual heating energy demand of WINscr and EPscr methods

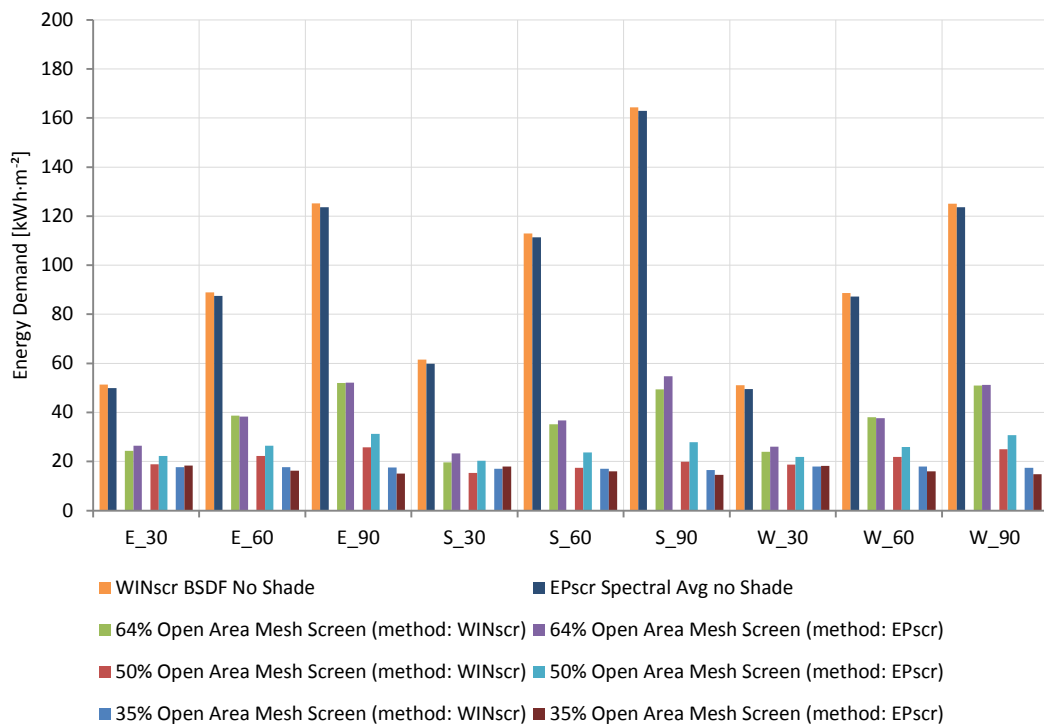


Figure 74. Vienna annual cooling energy demand of WINscr and EPscr methods



Figure 75. Vienna annual lighting energy demand of WINscr and EPscr methods

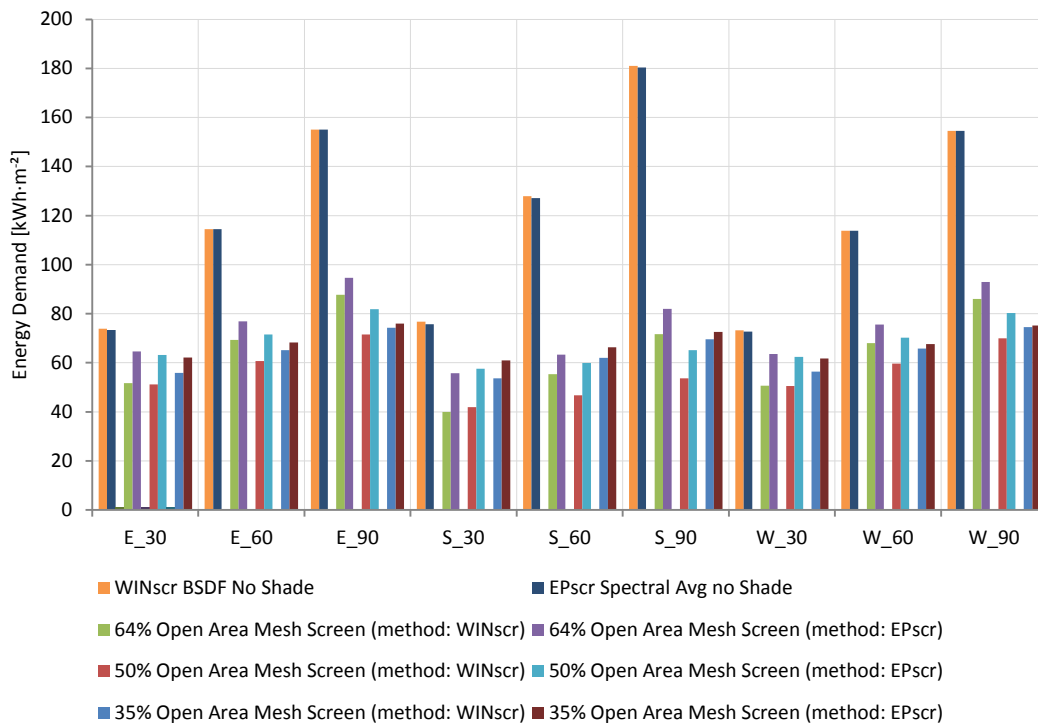


Figure 76. Vienna total annual energy demand of WINscr and EPscr methods

Location London

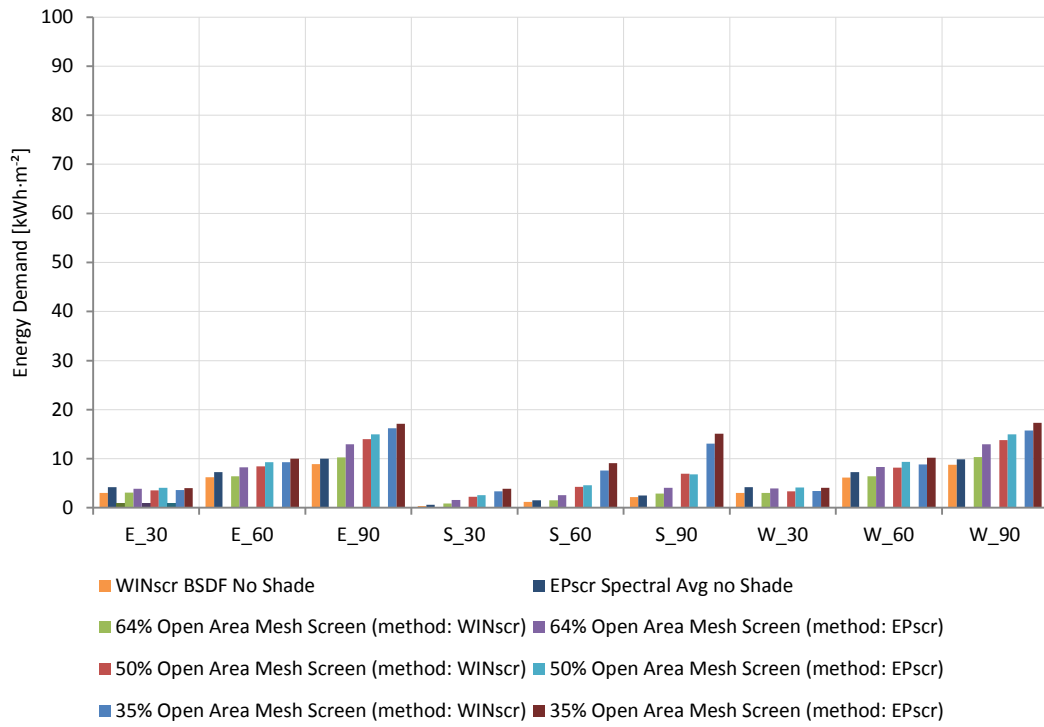


Figure 77. London annual heating energy demand of WINscr and EPscr methods

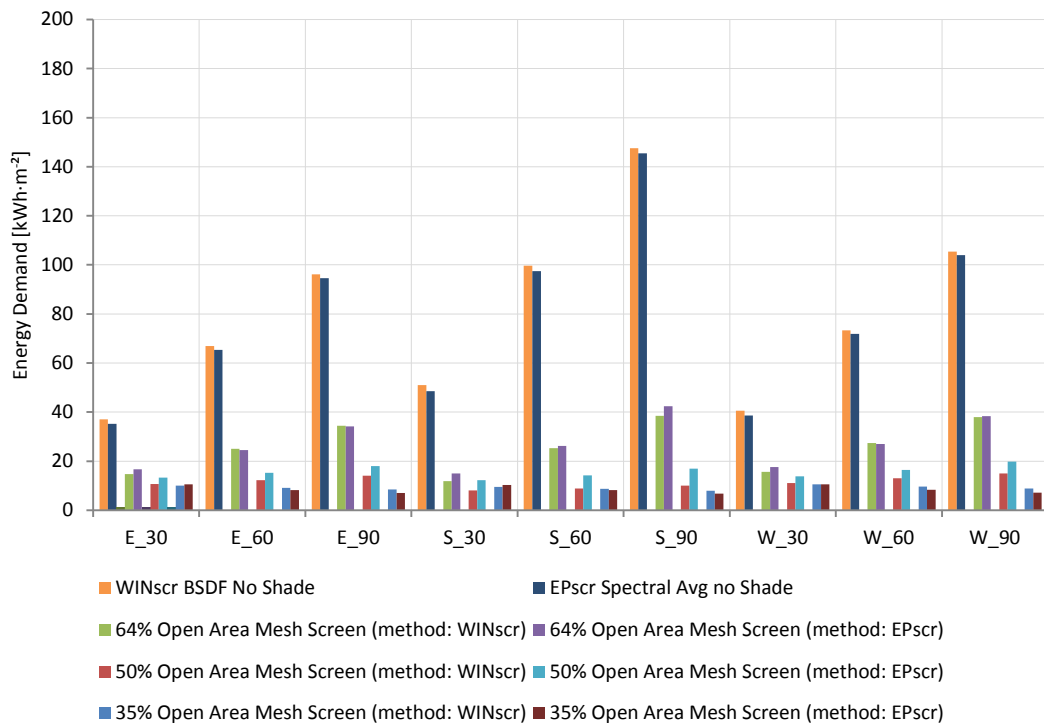


Figure 78. London annual cooling energy demand of WINscr and EPscr methods

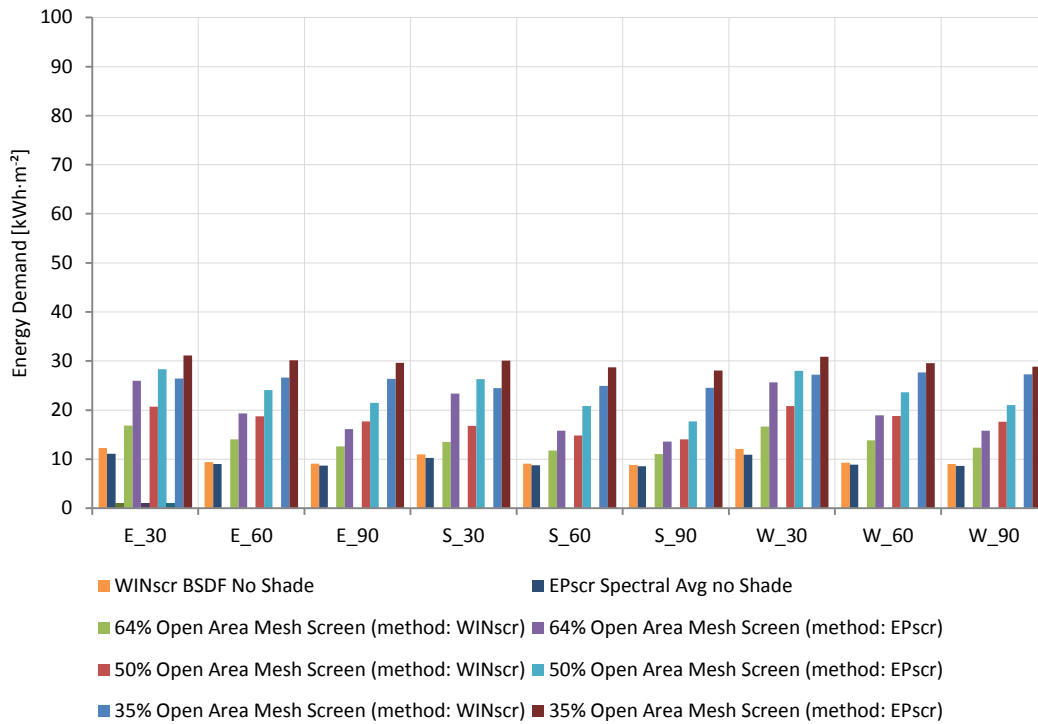


Figure 79. London annual lighting energy demand of WINscr and EPscr methods

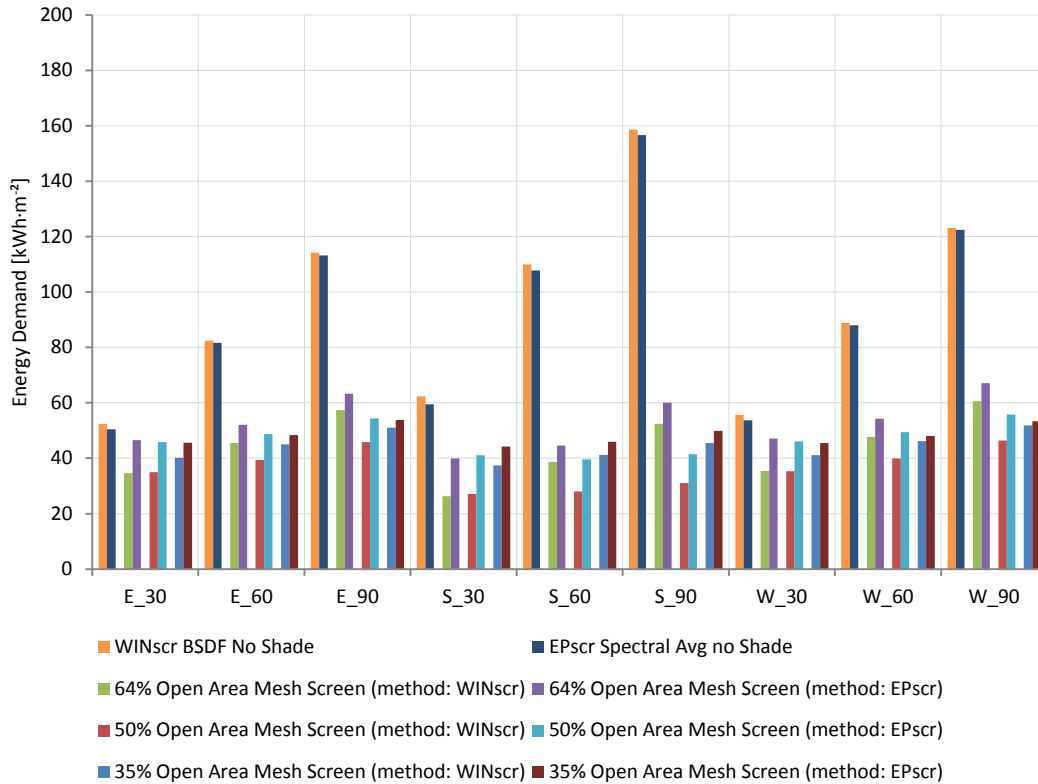


Figure 80. London total annual energy demand of WINscr and EPscr methods